Autocyclic behaviour of alluvial and deltaic systems

Maurits van Dijk

Members of the dissertation committee:

Prof. dr. P. Hoekstra
Faculty of Geosciences
Utrecht University, the Netherlands

Prof. dr. S.M. de Jong
Faculty of Geosciences
Utrecht University, the Netherlands

Prof. dr. S.B. Kroonenberg
Faculty of Civil Engineering and Geosciences
Delft University of Technology, the Netherlands

Dr. A. Moscariello
Faculty of Civil Engineering and Geosciences
Delft University of Technology, the Netherlands

Prof. dr. J. Reijmer
Faculty of Earth and Life Sciences
VU University of Amsterdam, the Netherlands

Omslag illustratie – Puinzandwaaier overgaand in een alluviale vlakte. Inzet: schaduw-relief kaart van een hoogtemodel uit één van de puinzandwaaier experimenten laat een vergelijkbare morfologie zien.

Autocyclic behaviour of alluvial and deltaic systems

Autocyclisch gedrag van alluviale en deltaische systemen

(met een samenvatting in het Nederlands)

PROEFSCHRIFT

ter verkrijging van de graad van doctor aan de Universiteit Utrecht
op gezag van de rector magnificus, prof.dr. J.C. Stoof,
ingevolge het besluit van het college voor promoties
in het openbaar te verdedigen op donderdag 14 mei 2009 des middags te 2.30 uur.

door

Maurits van Dijk

geboren op 12 oktober 1977
te Zeist

Promotor:
Prof. dr. P.L. de Boer

Co-promotoren:
Dr. G. Postma
Dr. M.G. Kleinhans

Voor Selle en Lean

Contents

Introduction, approach and outline

1.1 General

Silliciclastic sedimentary systems occur where sediments are available on the surface of the Earth. Sediments appear where rocks are eroded to smaller pieces (grains) which may subsequently be transported over thousands of kilometres before deposition. Sedimentary systems are both the conveyor and the product of sediments. The spatial extent of sedimentary systems ranges from metres (e.g. small alluvial fans and streams) to thousands of kilometres (large river systems and river deltas).

Sedimentary systems can be considered from 1) a geological, and 2) a morphodynamical perspective. The geological perspective focuses on the characteristics of the deposits of the sedimentary systems. The morphodynamic point of view emphasises the present-day physical dynamics. I combined these two worlds to enhance the comprehension of how deposits and depositional cycles are formed and which intrinsic processes are involved. The controls on the evolution, size, morphology and architecture of a sedimentary system comprise:

a) *Allogenic* controls; boundary conditions originating from outside the system:
1) supply; the mixture of water and sediment delivered to the upstream end of the system, available for transport and deposition.
2) accommodation, the space available to be filled; strongly related to sea level as it governs how far and high systems can build up.

b) *Autogenic* behaviour; internally generated processes.

The allogenic controls interact and impose boundary conditions. Within the set of boundary conditions, autogenic processes operate. For example, an instantaneous and permanent base-level drop may decrease accommodation and generate incision in an individual system. The maximum depth of the incision is then defined by the magnitude and duration of the base-level fall. However, the development of an incised valley is controlled by the frequency of occurrence of autogenic processes in the system. For example channel avulsion and channel migration may lead to narrower or wider incisions within the limits set by the erodability of the substrate, and affect the character of the corresponding deposits. When autogenic processes occur (quasi-) periodically, they are referred to as autocyclic processes.

The timescale of a system's autogenic response is scale dependent, so for large systems autogenic signals can show similar frequencies as allogenic quasi-periodic controls. In that case the two (or more) sets of signals may interact and interfere. During a sea-level rise as for example occurred during the Holocene, rivers aggraded continuously to keep up with the rising base level. Morphodynamic behaviour of the rivers was defined by the imposed base-level rise with possible autogenic variations superimposed. The distinction between autogenic and allogenic influences then may be difficult or impossible. The objectives of this thesis are to:

1) investigate autogenic and autocyclic processes in silliciclastic sedimentary systems and their importance relative to allogenic processes,
2) examine their sedimentary characteristics (signals) and compare these with those generated by allogenic processes.

1.2 Base level

Two different definitions of base level are practised: the 'geomorphic base level' and the 'stratigraphic base level' (Blum and Törnqvist, 2000). The different usage of the term base level originates from its application in different settings. The stratigraphic view is used widely in sequence stratigraphy models, derived in the last 40 years (cf. Jervey, 1988; Posamentier and Vail, 1988), and focuses on marine systems, where sea level and base level are equivalent and no deposition is possible above sea level. Geomorphic base level comes from the continental realm where the boundary condition formed by the sea determines a graded profile (Fig. 1.1A). Figure 1.1A shows typical profiles of a river with increasing discharge and associated downstream decreasing gradient. The upper limit is tied to the water level of the body into which the river flows. The lower limit is determined by the deepest scours in the river bed (Fig. 1.1A).

The 'stratigraphic base-level' in a fluvial context is not a cause but an effect (Wheeler, 1964). It is the upper limit to accommodation, which is not a force in itself but is controlled by the geomorphic base level in combination with the supply of water and sediment, where the supply determines the gradient of the surface of the system sloping to the geomorphic base level.

The surface of a fluvial system can vary between maximum and minimum possible aggradation (Fig. 1.1B, Holbrook *et al.*, 2006). Minimum aggradation occurs when delivery of sediment is lowest and water discharge is highest (most efficient configuration), maximum aggradation corresponds with highest sediment supply and lowest water discharge (least efficient configuration). Within
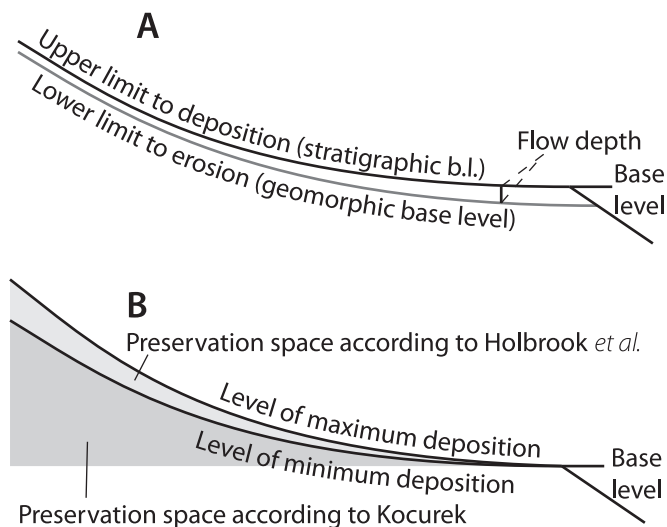

Figure 1.1 Conceptual comparison of 'stratigraphic' and 'geomorphic base level', B) variations between maximum and minimum deposition tied to the same base level.

the limits of the two profiles the surface can aggrade and degrade. The fluvial system thus can act as a buffer for storage and release of sediment. Holbrook *et al.* (2006) attribute the (laterally variable) storage and release of sediment to variability in supply (Fig. 1.1B). Kim *et al.* (2006) inferred on the basis of experiments that autogenic and autocyclic processes also can store and release sediment, and thus may be responsible for aggradation and degradation and varying surface profiles of fluvial systems.

To avoid confusion caused by the use of the same term with a different meaning in different settings, the term 'accumulation space' is adopted for accommodation in continental settings (Kocurek, 1998). 'Accumulation space' is defined as 'the volume of space that can be filled within present process-regimes, governed by the input of water and sediment and the geomorphic base level' (Kocurek and Havholm, 1993; Kocurek, 1998).

For the preservation of autogenically or autocyclically generated sedimentary successions, they have to arrive below the lowest level of erosion as defined by base level, e.g., by basin subsidence. This is expressed by the definition which Kocurek (1998) gave for 'preservation space': 'the accumulation *below* the level of minimum incision'. In contrast, Holbrook *et al.* (2006) define 'preservation space' as the space bounded by the levels of maximum and minimum aggradation (Fig. 1.1B). Holbrook *et al.*'s definition only preserves additional deposits when the boundary conditions change, while Kocurek's definition allows additional preservation of sediments during constant conditions, which is necessary to be able to compare deposits formed by autogenic or autocyclic processes to those generated by allogenic variations. The results presented in this thesis support Kocurek's definition by showing how autogenic and autocyclic successions can be preserved.

1.3 Scope

The shoreline is most commonly regarded as the base level in marine and continental systems, with sea level as the major control. Sea-level variations have occurred continuously in the geologic record, and the importance of sea-level change in the recent past is beyond doubt. Sea-level change and tectonic movements are responsible for most of the base-level variations. Here, I concentrate on the effect of base-level change (induced by basin water-level change) on the evolution of sedimentary systems. I investigate the behaviour of alluvial-fan, fan-delta, flood-tidal and ebb-tidal delta systems by means of analogue flume studies, in which boundary conditions determining the development of base level can be perfectly controlled:

1) autogenic behaviour of alluvial fans that prograde over a slightly inclined alluvial plain: the shoreline (base level) is far beyond the active progradational system and has no influence;
2) autogenic behaviour of fan deltas, a system where the feeder system of the delta is an alluvial fan, but where fan evolution is directly controlled by the shoreline;
3) autogenic behaviour of fan deltas during sea-level rise;
4) autogenic behaviour of a flood-tidal delta.

After having identified the intrinsic processes and mechanisms, I investigate the impact of base level by imposing different base-level variations on sedimentary systems in order to:

5) extend the above derived principles to systems subjected to rising and/or oscillating base level.

Finally, I demonstrate that autogenic and autocyclic processes are of considerable significance, and show that our results have implications for the morphodynamic and stratigraphic development of sedimentary systems. Carbonate systems have not been regarded in this study.

1.4 Approach: experiments

To isolate the autogenic and autocyclic processes in the sedimentary systems introduced above, I devised and carried out analogue experiments with different base-level configurations, as experiments are the only way to study the sedimentary systems under comparable controlled conditions. Studies of natural systems are problematic for the above purposes as natural systems are also influenced by allogenic changes. In addition, the morphodynamical evolution of natural sedimentary systems lasts decades up to many millennia. In the experiments, the evolution of the systems is reduced to hours or days, allowing multiple runs for each system. The temporal and spatial scale at which delta and alluvial fan systems develop, do not allow hydraulic scaling. Therefore I developed an alternative scaling strategy, based in part on the 'similarity of process'-concept of Hooke (1968), and in part on the relative depth of erosive events and preservation potentials.

Analogue experiments are but one example of the different types of experiments used to study sedimentary systems, with a varying degree of replication of the prototype characteristics (Peakall *et al.*, 1996, Fig. 1.2). On the smallest temporal and spatial scales, 1:1 replica models have been successfully used for modelling bedform generation (e.g. Baas *et al.*, 1993). Froude scale models and distorted-scale models increasingly deviate from the 1:1 ratio, but in this way larger systems can be modelled over longer timescales. Analogue models, at the other end of the spectrum, can capture
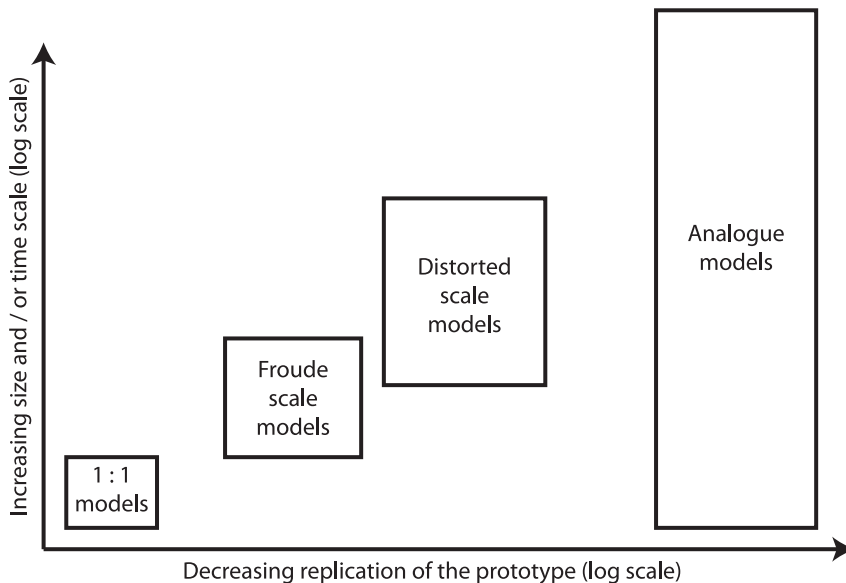

Figure 1.2 schematic view of the balance between model specificity and spatial/temporal scales for different modelling techniques (after Peakall *et al.*, 1996). The log-scale on the x-axis refers to the difference in replication of the prototype between analogue models, distorted-scale models, Froude-scale models and 1:1 models.

processes over the longest time span in the largest systems (Fig. 1.2). In order to extrapolate the experimental results to the scale of natural systems, analogue models rely on 'similarity of process', i.e., that models are landforms in their own right (Hooke, 1968).

Alluvial fans were studied experimentally by Hooke (1968), who derived his 'similarity of process' principles from observations of experiments and natural examples. Hooke and Rohrer (1979) extended Hooke's earlier studies by investigating slope-of-fan surfaces and surface sediments. Schumm *et al.* (1987) brought together morphological, sedimentological and morphodynamical data on a variety of landforms, including drainage basins, rivers, valleys and alluvial fans. Their notion of autogenic processes and accurate descriptions of system evolution make their book an inspiring piece of work.

Whipple *et al.* (1998) extended the work of Schumm *et al.* (1987) by studying alluvial-fan behaviour and slope over a wide range of transport conditions, ranging from bed-load dominated to suspended-load dominated transport. Simultaneously, Parker *et al.* (1998a) constructed a numerical model of alluvial-fan morphology in two end-member configurations, sheet flow and channelised flow, using the experiment data of Whipple *et al.* (1998). Parker *et al.* (1998b) used both numerical and physical experiments to test the behaviour of mine tailings. Clarke *et al.* (2008) continued this line of research by investigating intrinsic fan evolution on an experimental alluvial fan whose size was limited by erosion at the lower boundary. In addition, they performed numerical simulations, and showed that major incisions on alluvial fans can be generated by internal feedback mechanisms without any external trigger (Nicholas and Quine, 2007).

The last set of experiments vital for this thesis are the experiment runs of Kim and co-workers (Kim *et al.*, 2006a; Kim *et al.*, 2006b; Kim and Muto, 2007; Kim and Paola, 2007; Kim and Jerolmack, 2008). They showed that sedimentary systems can dynamically vary their slope, and thus deliver pulsating sediment fluxes to a shoreline, leading to continuously varying shoreline-migration patterns. This behaviour was studied briefly, with a non-dimensional approach under steady conditions (Kim and Jerolmack, 2008), and it persists during long-lasting (experimental) tectonics and sea-level variations (Kim *et al.*, 2006a, b; Kim and Paola, 2007).

The experiments reported here are different from those summed up above. Most of them studied processes intrinsic to the system but did not keep all boundary conditions steady during an experiment. Hence, the processes described are still the result of interaction between autogenic and allogenic processes. For example, the alluvial-fan experiments of Schumm *et al.* (1987) showed 'spontaneous' incisions, which were assigned to autogenic processes. However, the supply of sediment to the alluvial fans was generated by incision into a drainage basin, leading to a highly variable delivery of sediments. Therefore, correlating the incisions to intrinsic processes is ambiguous at the least. Other experiments involved excellent qualitative observations on the processes present in the systems. However, quantitative measurements were absent or too infrequent, making comparison with natural systems difficult.

My experiments were carried out in the Eurotank (Fig. 1.3), apart from the tidal studies, which were performed in a different flume. The Eurotank is located in Utrecht and is a large (6 m wide and 11 m long) flume facility capable of simulating tectonic uplift and subsidence, base-level variations and variations in sediment input, all over a wide range of setup dimensions, geometries and shapes. It also features measurement equipment capable of obtaining high-resolution digital surface topography. Thus large-scale landscape evolution studies can be performed, and the evolution of scaled fluviodeltaic systems, rivers, deltas and alluvial fans can be simulated with great accuracy and quantified sufficiently for detailed comparisons with each other and with

Figure 1.3 overview of the Eurotank facility. Author for scale. Image courtesy of Raymond Rutting, and the image was previously published in the Volkskrant in 2004.

natural analogues. The tidally influenced system is studied in a smaller flume, in the Earth-Science Building at the Utrecht University, specially adapted to generate bidirectional currents.

1.5 Thesis outline

In *Chapter 2* the generation of a series of fan deltas under conditions of steady sea level, discharge and supply is investigated. The development of the fan delta thus is driven by intrinsic processes. Important features include cyclically alternating sheet and channelised flow, the latter caused by deep incisions in the subaerial part of the delta. Fan-delta morphology is characterised by changes in slope and associated erosion and deposition patterns. These characteristics are explored while the fan deltas evolve, and the differences in the evolution of different fan deltas demonstrate trends in the frequency of events in relation to the alternating sheet and channelised flow.

Chapter 3 describes a series of alluvial fans prograding over an inclined alluvial plain, with base level far beyond the toe of the prograding fan. The development of alluvial fans follows similar patterns as observed in the fan deltas, although cycle frequency differs from those in the fan-delta development described in *Chapter 2*. The differences are evaluated in terms of the different base-level configurations.

Chapter 4 describes experiments in which the water level (base level) in a small crater-like basin is progressively rising. Under these conditions cyclic development of shore line terraces occurs, resulting in a morphologically characteristic feature that is also found in delta bodies in craters on

Mars. Using the shoreline terrace features and volume of the sediment bodies on Mars, estimates of the duration and total discharge of water on Mars could be made. In addition, the effects of varying input of water and sediment on delta system evolution are assessed.

Chapter 5 describes a unique flume study of the intrinsic behaviour of a flood-tidal delta system subject to high-frequency water-level oscillation in the absence of waves. The preliminary results are compared with the autogenic behaviour of fan deltas and alluvial fans described in *Chapter 2* and *3*.

The conclusions of this thesis are presented in *Chapter 6*.

CHAPTER 2

Autocyclic behaviour of fan deltas: an analogue experimental study

Authors:
Maurits van Dijk, George Postma, Maarten G. Kleinhans

Abstract

Fan deltas are excellent recorders of fan-building processes because of their high sedimentation rate, particularly in tectonically active settings. Although previous research has focused mainly on allogenic controls, there is clear evidence for autogenically produced storage and release of sediment by flume and numerical modelling that demands further definition of characteristics and significance of autogenically forced facies and stratigraphy. Analogue experiments were performed on fan deltas with constant extrinsic variables (discharge, sediment supply, sea-level and basin relief) to demonstrate that fan-delta evolution consists of prominent cyclic alternations of channelised flow and sheet flow. The channellised flow is initiated by slope-induced scouring and subsequent headward erosion to form a channel that connected with the valley, while the removed sediment is deposited in a rapidly prograding delta lobe. The resulting decrease in channel gradient causes a reduction in flow strength, mouth-bar formation, flow bifurcation and progressive backfilling of the channel. In the final stage of channel filling, sheet flow coexists for a while with channellised flow (semi-confined flow), although in cycle 1 this phase of semi-confined flow was absent. Subsequent autocyclic incisions are very similar in morphology and gradient. However, they erode deeper into the delta plain and, as a result, take more time to backfill. The duration of the semi-confined flow increases with each subsequent cycle. During the period of sheet flow, the delta plain aggrades up to the 'critical' gradient required for the initiation of autocyclic incision. This critical gradient is dependent on the sediment transport capacity, defined by the input conditions. These autogenic cycles of erosion and aggradation confirm earlier findings that storage and release of sediment and associated slope variation play an important role in fan-delta evolution. The erosional surfaces produced by the autocyclic incisions are well-preserved by the backfilling process in the deposits of the fan deltas. These erosional surfaces can easily be misinterpreted as climatically, sea-level or tectonically induced bounding surfaces.

Keywords

Analogue experiment, autocyclic behaviour, channellised flow, fan delta, sedimentary cycles, sheet flow, slope variation.

2.1 Introduction

Fan deltas are coastal prisms of sediment derived from an alluvial-fan feeder system. These deltas are deposited partly or fully subaqueously at the interface between the active fan and a standing body of water and are common along tectonically active basin margins (Nemec and Steel, 1988a). Fan deltas can preserve sensitive records of variable tectonic, climate and base-level conditions (Collinson, 1988; Nemec and Steel, 1988b; Whipple and Trayler, 1996). Variations in climate conditions are inferred to have a large impact on the gradient of the fan and on stratigraphic architecture due to changes in water and/or sediment yield (e.g. Bull, 1977; Hooke and Rohrer, 1979; DeCelles et al., 1987, 1991; Blair and McPherson, 1994; Milana and Ruzycki, 1999; Milana and Tietze, 2002; Saito and Oguchi, 2005). The effects of tectonics and base-level changes on alluvial fans and fan deltas have also been described extensively (Steel et al., 1977; Gloppen and Steel, 1981; García-Mondéjar, 1990; Gawthorpe and Collela, 1990; Fernandez et al., 1993; Nemec and Postma, 1993; Li et al., 1999; Soria et al., 2001; Harvey, 2002; Viseras et al., 2003; Garcia-Garcia et al., 2006; Pope et al., 2008).

Flume and numerical modelling of alluvial and fan delta-type systems reveal that autogenic control plays an important role in fan-delta evolution (e.g. Schumm et al., 1987; Whipple et al., 1998; Kim et al., 2006; Kim and Muto, 2007; Kim and Paola, 2007; Nicholas and Quine, 2007). However, autogenic behaviour is usually observed during allogenic variations, which makes it difficult to study its characteristics and significance. Schumm et al. (1987) modelled alluvial fans using a catchment as a sediment source which was progressively eroded by precipitation. The water and sediment were led to a basin where the fans were deposited. Those authors concluded that the frequency of fan-head entrenchment observed in analogue experiments had no relation to the changes which were measured in the unsteady sediment supply. Hence, Schumm et al. attributed the trenching to autocyclic behaviour. A closer investigation of the measurements reported by Schumm et al. (1987, fig. 9.22) shows that, in general, the frequency of entrenchment decreases with decreasing ratio of sediment to water discharge (Q_s/Q_w). However, during the experiment the frequency of entrenchment increased occasionally with decreasing Q_s/Q_w, contradicting the general trend within the same data set. The use of a catchment as a sediment source and the resulting unsteady supply make interpretation of these measurements difficult and conclusions regarding autocyclic processes ambiguous. Whipple et al. (1998) investigated quasi-steady surface aggradation of an alluvial fan in a flume under conditions of base-level rise and constant water and sediment supply. These authors observed autogenic flow variation on the fan that varied in space and time between a state of sheet flow and a state of distinctly channelised braiding. During braiding, zones of flow concentration formed, entrenched and backfilled. Building further on the experiments of Whipple et al. (1998), Clarke et al. (2008) performed a set of experiments on internal processes of alluvial fans. A specific aspect of these models was the removal of sediment at a certain radius, limiting fan growth to simulate truncation by, for instance, axial river systems. Short-term fluctuations between sheet and channelised flow were observed throughout these runs. Fan-head entrenchment dominated during the last third of these experiments which in total lasted from 5 to 13 h. Studying relative sea-level forced shoreline migration in an analogue flume experiment, Kim et al. (2006) found that significant, high-frequency autogenic slope fluctuations persisted even when the effect of channel switching was eliminated by lateral averaging of the shoreline migration rate and after accounting for the sea-level variations. The autogenic signal in the laterally averaged shoreline migration rate implied a fluvial process that caused variation in the sediment yield to the shoreline. These authors also observed sheet-like flow alternating

with phases of strongly channelised flow, suggesting that the fluvial system alternated between states of storing sediment and then releasing it by incision. The one-dimensional numerical model that Kim *et al.* (2006) derived from the analogue experiments treated the autogenic variations as a cyclic change between two extreme slopes. Hence, two potential fluvial profiles were defined, representing maximum possible aggradation or maximum possible incision. Nicholas and Quine (2007) found autogenic channelised incisions using constant sediment and water input in a three-dimensional numerical model of evolving alluvial fans. Muto *et al.* (2007) combine previously published experimental and numerical modelling results to show the non-equilibrium behaviour of fluvial systems during steady forcing. This analysis allows the detection and identification of autogenic responses and allogenic events in the stratigraphic record. Muto *et al.* show convincingly that at least part of the assumptions on which sequence stratigraphic models have been built in the late 1980s and 1990s is in need of modification to include the impact of autogenic behaviour during allogenic variations (see also Muto and Steel, 1997, 2000).

All of the above experimental studies demonstrate that autogenic incisions in the alluvial-fan apex may occur during allogenic variations; but can they occur when allogenic conditions are constant? To date, experimental studies on autogenic behaviour have never been conducted entirely without change in external forcing. Hence, the present work aimed to study the behaviour of fan-delta systems under steady conditions, in the absence of variations in tectonics, sea-level, sediment supply and water discharge, so that the resulting behaviour must then be of autogenic origin. This study contrasts with the work focussing on autostratigraphy, performed by, for example, Muto and Steel (2000), who studied delta evolution by 'steady' forcing during constant base-level rise and fall.

By repeating the same controlled experiment for different steady discharge values, insight will be gained into autogenic behaviour in relation to water discharge. As shown by Schumm *et al.* (1987), Bryant *et al.* (1995), Whipple *et al.* (1998) and Milana and Tietze (2002), different discharge conditions lead to different sediment transport capacities that have effects on the dynamics of the fan-delta plain. Therefore, it is expected that these differences in discharge will also affect the autogenic behaviour. Finally, the stratigraphic architecture of the model is evaluated to determine whether autogenic features can be preserved in real-world fan-delta deposits.

2.2 Experimental design

2.2.1 Flume set-up and materials
The experiments were conducted in the Eurotank Flume Facility at Utrecht University. Three experiments were carried out, R1, R2 and R3, each using different water discharge, but all other

Table 2.1 Input conditions and dimensions of the experimental setup

Run	R1	R2	R3
Lab name	A008	A004.1	A004.2
Sediment supply, Q_s (m^3/hr)	0.001	0.001	0.001
Water supply, Q_w (m^3/hr)	0.60	0.55	0.35
Ratio Q_s/Q_w	0.00167	0.00182	0.00286
Setup size (m)	5.4 x 3.0	2.7 x 2.7	2.7 x 2.7
Total run time (hrs)	18	44	44

Cross sectional view

Input of water and sediment

Shelf; water depth 1 cm

Basin

z-axis (mm)

0

400

Plan view

Y-axis (mm)

0   1000   2000   3000   4000   5000   6000   7000

0

Shelf; water depth 1 cm

Basin

Feeder channel

1000

2000

Input of water and sediment

3000

Impermeable walls

4000

5000

Drain

6000

X-axis (mm)
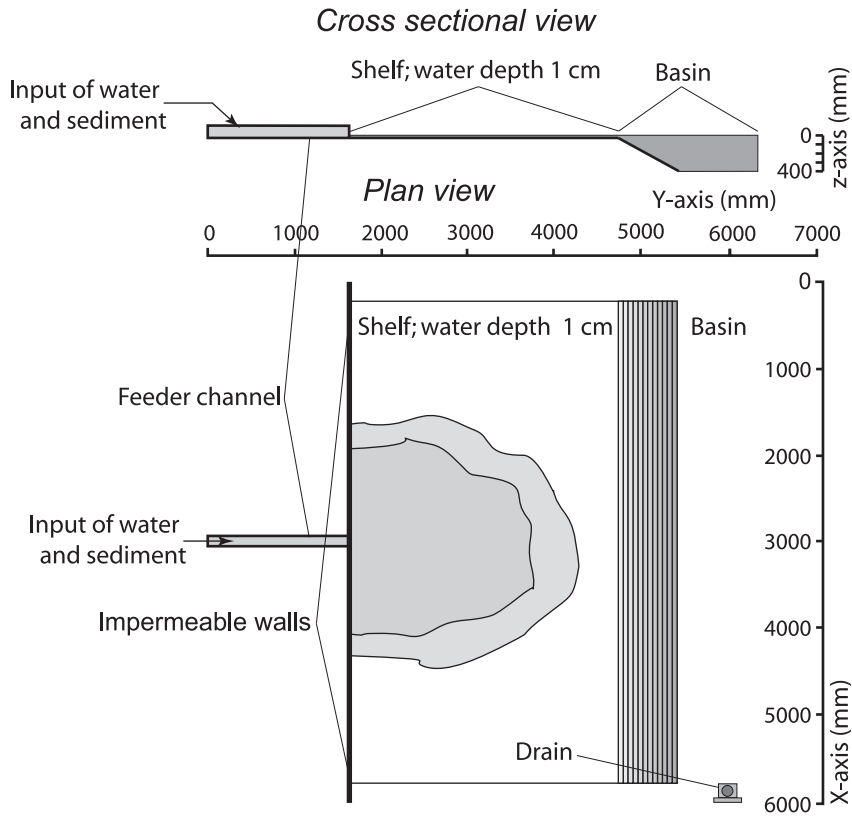
Figure 2.1 Schematic view of the set-up of experiment R1. Experiments R2 and 3 were carried out in smaller but otherwise identical setups.

input conditions extrinsic to the system were held constant (i.e. sea-level, discharge and sediment supply). The input conditions and other variables are provided in Table 2.1.

The set-up of experiment R1 (the experiment that lasted longer than the other two and which was also measured in more detail) consisted of a horizontal shelf (5.4 x 3.0 m) and duct (1.5 x 0.05 m), the latter acting as a feeder channel (Fig. 2.1). The shelf was submerged under 1 cm of water, while a drain located in the basin ensured a constant water level. The bed of both the shelf and the channel consisted of fine sand to provide a realistically rough and also erodable initial surface. The sand bed in the duct could aggrade freely to produce a sloped surface connected with the evolving fan delta. The horizontal shelf ensured progradation into a constant water depth throughout the experiment. Feeder channel dimensions allowed the flow to leave the feeder channel and enter the shelf in a steady, centred jet, located in the centre of the upstream edge of the shelf. The sediment was delivered at a constant rate from a hopper with a rotating helix and mixed with the water supply before entering the feeder channel. Deviations of the delivery by the feeder were measured to be less than 1% over 15 min. All sediment was stored in the flume.

For the smaller set-ups (R2 and R3), the size of the shelf was limited to 2.7 by 2.7 m, in order to fit two set-ups side by side for simultaneous experiments. A ditch between the two prevented the experiments from influencing each other. Both set-ups had their own separate feeder channel,

located in the centre of the upstream edge of their shelf. Apart from the smaller shelf size, all other components of the set-up were identical. Sediment input in all three experiments was identical $(1.0\,l\,h^{-1})$; water discharges were $600\,l\,h^{-1}$ (R1), $550\,l\,h^{-1}$ (R2) and $350\,l\,h^{-1}$ (R3).

To enhance visualisation of the morphological changes on the fan deltas, grey and white sand were supplied intermittently. The grey sand was also used as substrate in both the shelf and the feeder channel. Both sand types consisted of quartz, with a bulk density of 2650 kg m^{-3}, and the grain-size distributions of the two sands were very similar (Fig. 2.2).

The critical Shields parameters of the two sand types, calculated using the model of Vollmer and Kleinhans (2007) accounting for shallow flow depth, were 0.0668 and 0.0622 for the grey and white sands, respectively. It is assumed here that the small difference between the two sand types had a negligible effect on the experiments. The grain-size of the sediment used in the experiments was chosen such that sediment transport would occur as bed-load under the range of discharges used, in analogy with modern alluvial fans and fan deltas that are dominated by bed load transport. The transport capacity *h* of the channellised flow was estimated by means of Eq. 2.1:

$$\theta = \frac{\tau'}{(\rho_s - \rho_w)gD_{50}} \tag{2.1}$$

with:

$$\tau' = \rho_w g \left(\frac{u}{C'}\right)^2 \tag{2.2}$$
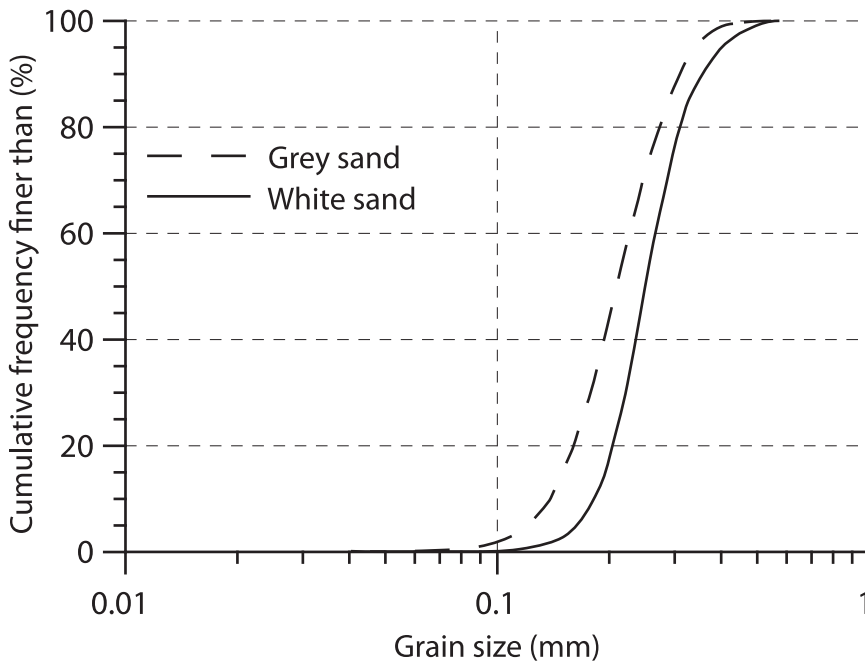

Figure 2.2 Cumulative grain-size distributions of the grey and white sand used in the experiments

and:

$$C' = 18 \, \log\left(\frac{12d}{2.5D_{50}}\right) \qquad\qquad (2.3)$$

where d is the depth (m), u is the velocity (m s^{-1}), g is the gravitational constant [9.81 m s^{-2}], C' is the Chézy constant (m sec$^{0.5}$), ρ_s is the sediment density (kg m^{-3}), ρ_w is the density of water (kg m^{-3}) and τ' is the bottom shear stress (N m^{-2}). Calculated values for h averaged 0.20 m and were never higher than 0.28 m. These values easily exceed the critical Shields parameters for the sediment used and are just above the criterion for suspended sediment transport derived by Soulsby (1997), indicating that transport as bed load will be the rule rather than the exception. The smaller flow depths of the non-channellised flows yield higher Chézy values and smaller values of h, ruling out suspended transport outside the channels.

2.2.2 Measurements

The surface topography was quantified using photogrammetry based on stereoscopy (for example, Chandler *et al.*, 2001; Brasington and Smart, 2003). In the Eurotank flume, an automated movable platform is attached to the ceiling. It contains a set of cameras, which takes four simultaneous photographs of the surface from different angles. The images are processed using software package sandphox™ (Geodelta, Delft, the Netherlands), into a Digital Elevation Model (DEM) of the sand surface. The vertical resolution of the DEMs is 250 μm and the horizontal resolution is better than 100 μm. To avoid reflections of the running water in the images, the experiment was stopped before each photogrammetry scan and the water was slowly drained to avoid compaction of the bed. The experiments R2 and R3 were halted every 4 h, while experiment R1 was stopped at uneven intervals depending on the progress of the experiment. The intervals ranged from two photogrammetry scans every hour during periods of high (autogenic) activity to a single scan every 8 h during periods of less activity.

In addition, time-lapse photography using digital video cameras recorded the entire experiment. During experiment R1, the camera was mounted directly above the fan delta for a plan view of the experiment. The images were recorded on a digital recorder, the camera taking three images every 10 min. The flow depth within confined flows was measured directly with a ruler, especially when the flow within the channels was not bankfull. When flow was bankfull, the flow depth was derived from the DEMs.

2.3 Results

The experimental fan deltas accumulated through cycles of alternating sheet and channellised flow. The fan-delta evolution of experiment R1, preceded by sheet flow building up the initial fan delta, involved five channellisation events. The initiation and backfilling of the first of the channellisation events is shown in detail in Fig. 2.3A to H. Figure 2.3I to L shows later events as the delta grows in size. The detailed development of a single cycle is demonstrated by a set of shaded relief maps (Fig. 2.4A to G) and topographical profiles (Fig. 2.5) from the first autogenic cycle of experiment R1. The duration of sheet flow and channellised flow for R1 is given in Fig. 2.6 and for experiments R2 and R3 in Fig. 2.7. Both Figs 2.6 and 2.7 also show curves for the aggradation on the apex, slope measurements and delta growth rates for given positions on the delta.
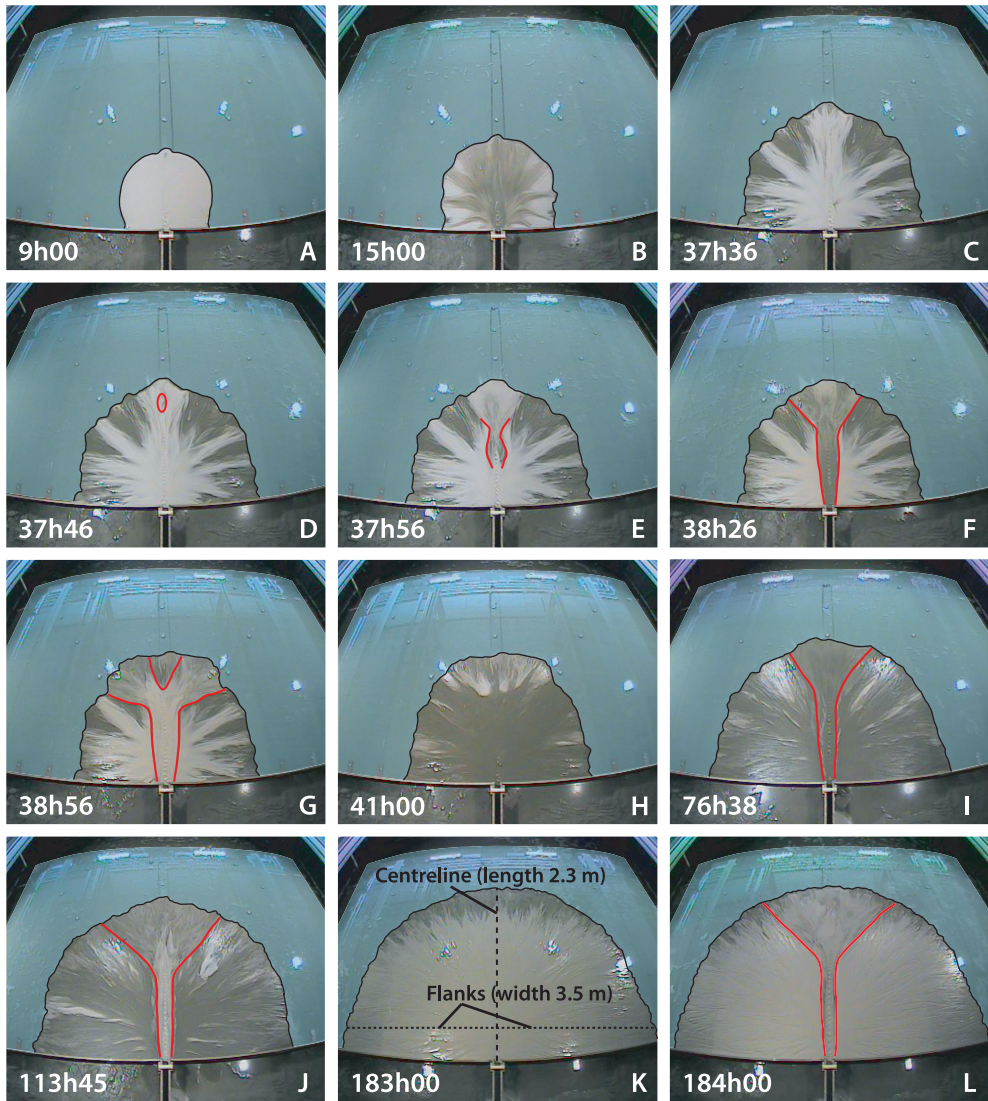
Figure 2.3 Video images of the plan view development of the alluvial fan-delta of experiment R1. Blue areas represent the standing body of water, the black lines show the shoreline of the delta, and the red lines mark the boundary of the incised channel. Run time is indicated in the lower left of each picture. The curvature of the boarding at the bottom of all the pictures is caused by the birds' eye lens used to capture the entire set-up with one camera. The inside of the feeder channel at the bottom of the figures is 5 cm wide. In Fig. 3K the width and length and the location of the profiles along the centreline and the flanks of the delta are specified. Note that the inflow in these images is from the bottom, whereas in Figures 1, 4, 5, 8, 9 and 11 flow enters from the left-hand side.

2.3.1 Fan-delta morphodynamics during an autogenic cycle

At the initiation of the experiment, the water entered the basin as a jet to produce an initial lobate-shaped, submerged delta at the outlet of the feeder channel. Within an hour, a distinct delta plain formed that was covered entirely by a single sheet flow. After 9 h, deposition shifted from the centreline to the flanks of the delta and its morphology changed from lobate to semicircular (Fig. 2.3A), while the initial jet transformed into an expanding sheet flow, which produced a smooth delta plain topography (Fig. 2.4A).
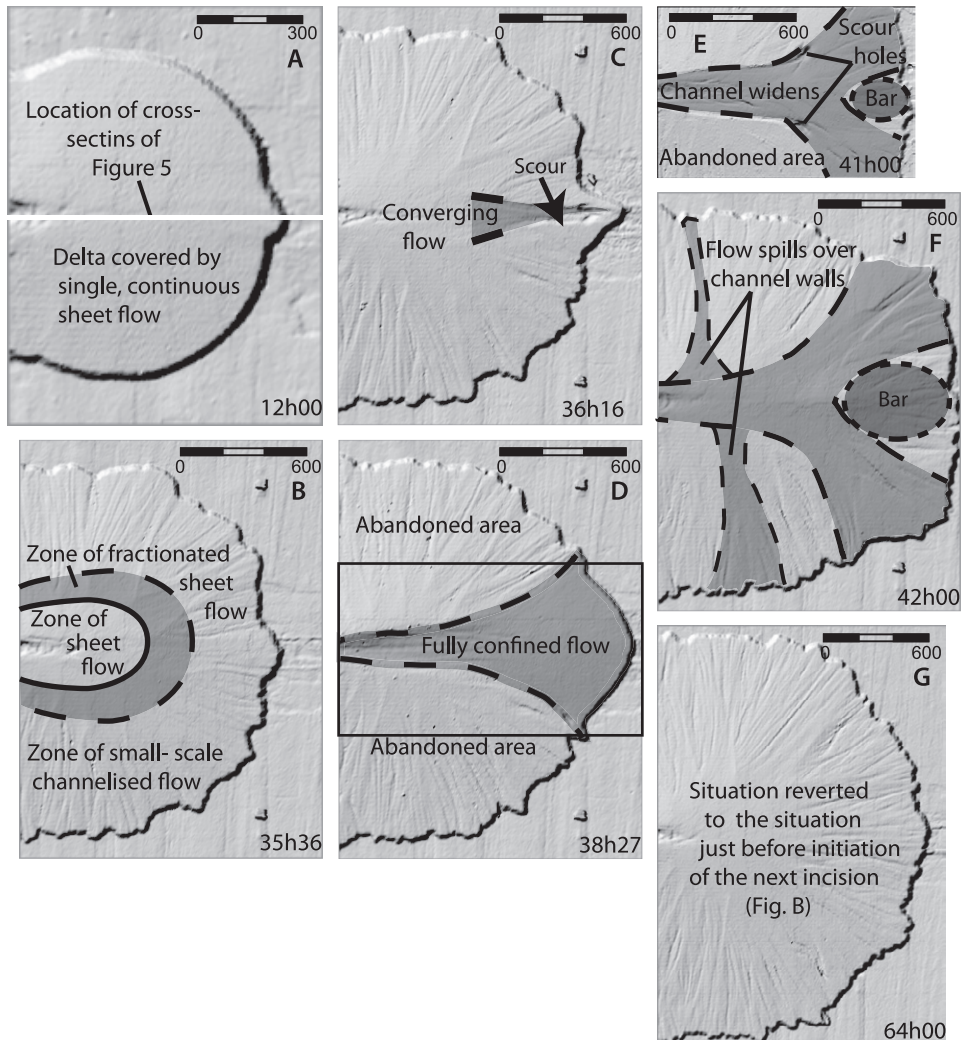
Figure 2.4 Shaded relief maps of the development of the first autogenic cycle of experiment R1. Run time is shown in the lower-right corner. The location of the cross-sections of Fig. 2.5 are indicated in Fig. 2.4A, and also the maps correspond to the labelled lines of Fig. 2.5. The scale of the plots is indicated in the upper-right corner; the position of panel (E) is given by the inset in panel (D).
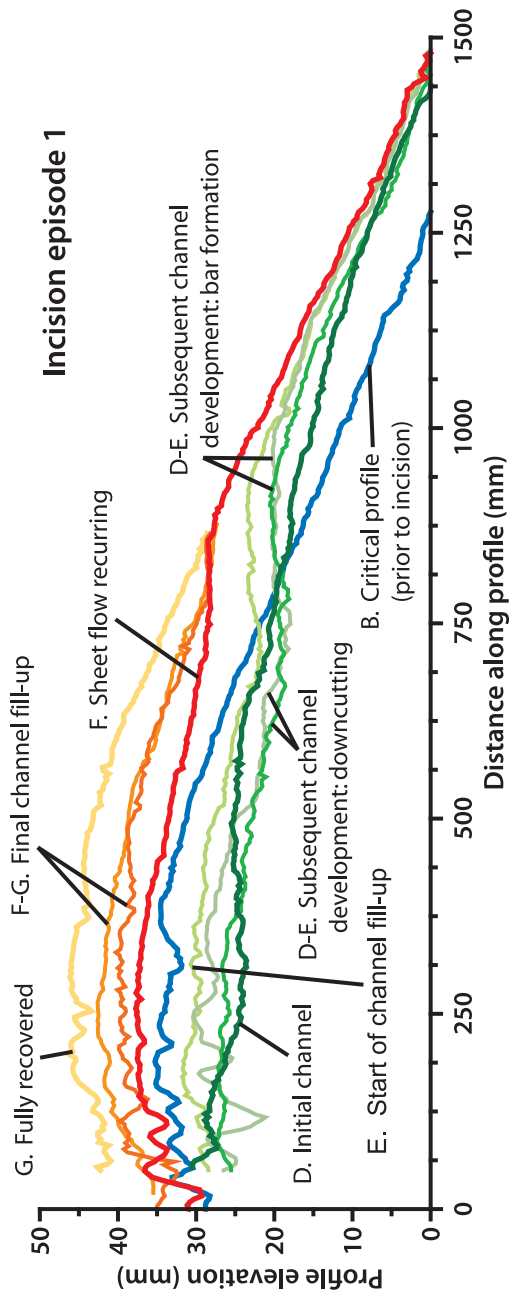
Figure 2.5 Topographic development of an autogenic cut and fill cycle. The sequence of cross-sectional lines corresponds to the shaded relief maps of Fig. 2.4. The labels marked in the figure correspond to one of the panels or to a transition between two of the panels in Fig. 2.4. The location of the transects is indicated in Fig. 2.4A.

Six hours later, the morphology of the fan delta had changed and white sediment radial 'spokes' appeared on the fan-delta surface (Fig. 2.3B and C), demonstrating that the sheet flow was only capable of sediment transport to the shoreline in distinct flow paths, leaving small segments of the delta plain inactive. Apparently, the area of the delta plain had grown too large to maintain sheet flow, which responded by breaking up into smaller sheet-flow segments separated by inactive parts. These 'fractionated' shallow sheet flows ranged in width from 5 to 50 cm. With increasing size of the delta, the fractionated flows near the delta shoreline began to concentrate, finally developing small-scale channels. Flow depths in the incipient channels increased to a maximum of 5 mm, while flow width decreased to several centimetres. As a result the small-scale channels became more pronounced and also started to form distinct 'delta lobes' at the shoreline (Fig. 2.4B). The lobes measured only a few centimetres in diameter. Usually, a single fractionated flow fed several of these small-scale nearshore channels.

At this point in time, the delta plain can be subdivided into three zones: (i) continuous sheet flow on the fan apex; (ii) fractionated sheet flow just downstream of the apex; and (iii) small-scale channellised flow near the shoreline (Fig. 2.4B). The small-scale channels shifted regularly across the delta plain in conjunction with the fractionated sheet flows, causing the delta lobes to shift laterally, thereby retaining the overall semicircular shape. The shifting occurred by both lateral channel migration and channel avulsions, all well-known processes previously described in similar physical experiments (Schumm *et al.*, 1987; Bryant *et al.*, 1995; Whipple *et al.*, 1998; Ashworth *et al.*, 2004, 2007).

After nearly 38 h, progressive aggradation at the apex increased the gradient of the delta plain up to the point when a scour hole was initiated along the centreline of the fan delta (Figs 2.3D and 2.4C). The scour hole developed quickly into a knick point that moved upstream (Fig. 2.3E) connecting the scour with the feeder channel (Figs 2.3F and 2.4D). Upon connection, the flow became fully confined to a depth of just below 1 cm, leaving a large part of the delta plain dry and inactive. The enhanced transport capacity of the channellised flow further widened and deepened the entrenchment, depositing the eroded sediment in a rapidly prograding delta lobe, followed by the development of a distinct mouth bar (Figs 2.3F and 2.4D). The bar caused the flow to bifurcate around it, leading to lateral migration of the flow away from the centreline of the fan delta (Figs 2.3G and 2.4E). Progressive deposition around the bar increased the angle of bifurcation, shifting sediment deposition and resultant delta progradation sideways. The bifurcation of the flow around the bar produced two scour holes, just upstream of the bar at the inner bends of the bifurcating flows (Fig. 2.4E) instigating erosion of the channel walls and flow widening. This effect must have decelerated the flow sufficiently for aggradation to start along the full length of the channel, as seen from the cross-sections E of Fig. 2.5 (labelled 'start of channel fill-up'). Flow widening and aggradation led to headward migration of the intersection point (at the bifurcation). The flow gradually started to exceed the confining channel walls and increasingly spilled over the margin in the course of the backfilling process (Fig. 2.4F); this progressively decreased the amount of water in the channel which is assumed to explain the increased aggradation, clearly visible in line F-G of Fig. 2.5. After 3 h, the incised channel completely backfilled from migration of the mid-channel bar, with the bar crest (visible on Fig. 2.5) shifting upstream towards the apex. When the entire channel had been filled, fractionated sheet flow and aggradation of the apex were restored (Figs 2.3H to K and 2.4G, line G in Fig. 2.5). Sheet flow persisted until the gradient had increased sufficiently to initiate another cycle of incision, progradation and backfilling (Fig. 2.3I, J and L).
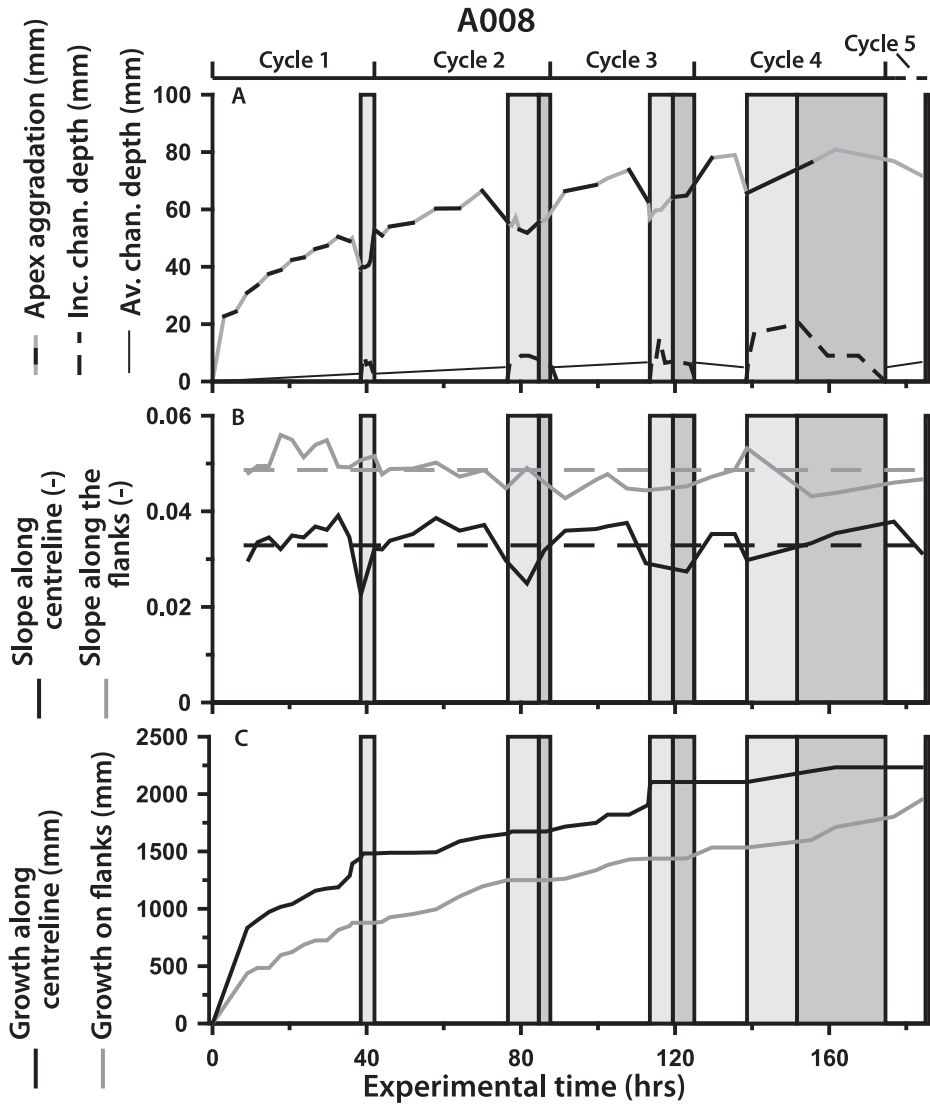
Figure 2.6 The development of the alluvial-fan feeder system during experiment R1. The light-grey areas represent periods of fully confined channelised flow, in the dark-grey areas channelised flow coexisted with sheet flow; areas without grey-shade represent sheet flow only. (A) Plot of the elevation and aggradation rate on the apex, the depth of the incised channel during phases of channelised-flow domination and the average surface-channel depth during sheet flow. The curve showing the elevation of the delta apex also designates which sand type was supplied: the black part of the curve indicates dark grey sand, the light grey part of the curve corresponds to the white sand; (B) plot of the development of the gradient of a profile along the centreline of the alluvial fan-delta and a profile along the flanks (perpendicular to the centreline); (C) plot of the growth rates of the delta in the direction along the centreline (black) and along the flanks (grey).

A summary of the development of the delta is given in Fig. 2.6. The elevation of the apex at the point of scour initiation is shown in Fig. 2.6A and the change in gradient from the apex to the shoreline along the centreline of the fan delta is shown in Fig. 2.6B. Both diagrams show a clear trend towards a maximum followed by a considerable reduction when incision occurs. Following the backfilling process, both elevation and gradient grow towards new maxima. During the period
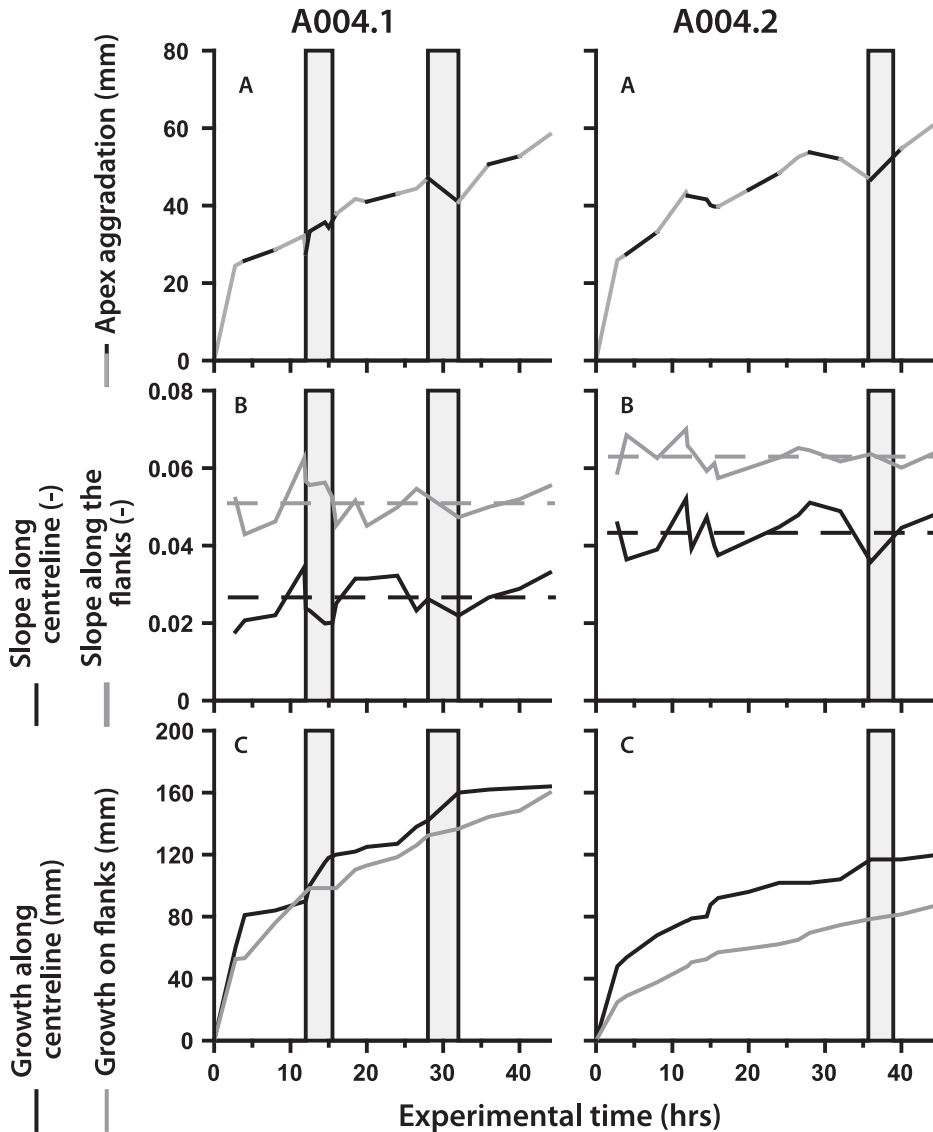
Figure 2.7 The development of the fan delta from experiment R2 and R3. Labelling and legend as in Fig. 2.6, except that data on channel depth are excluded.

of incision, the length of the delta along the centreline increases significantly (Fig. 2.6C), while the delta width remained more or less constant.

2.3.2 Slope variation

From a morphodynamical perspective, it is interesting to determine the variation of the slope as it varies around the average slope during delta evolution (see Kim *et al*., 2006). The gradients along the centreline clearly show a slope building up to a critical value, followed by a significant decrease in slope due to erosion and lengthening of the profile during channellised flow for each cycle (Figs 2.5, 2.6B and 2.7B). The variability of the slope (calculated as the standard deviation from the mean slope) is also different. The slope variability can be found in Figs 2.6B and 2.7B as the range between the maximum and minimum slope values, and differs between the locations along the flanks and 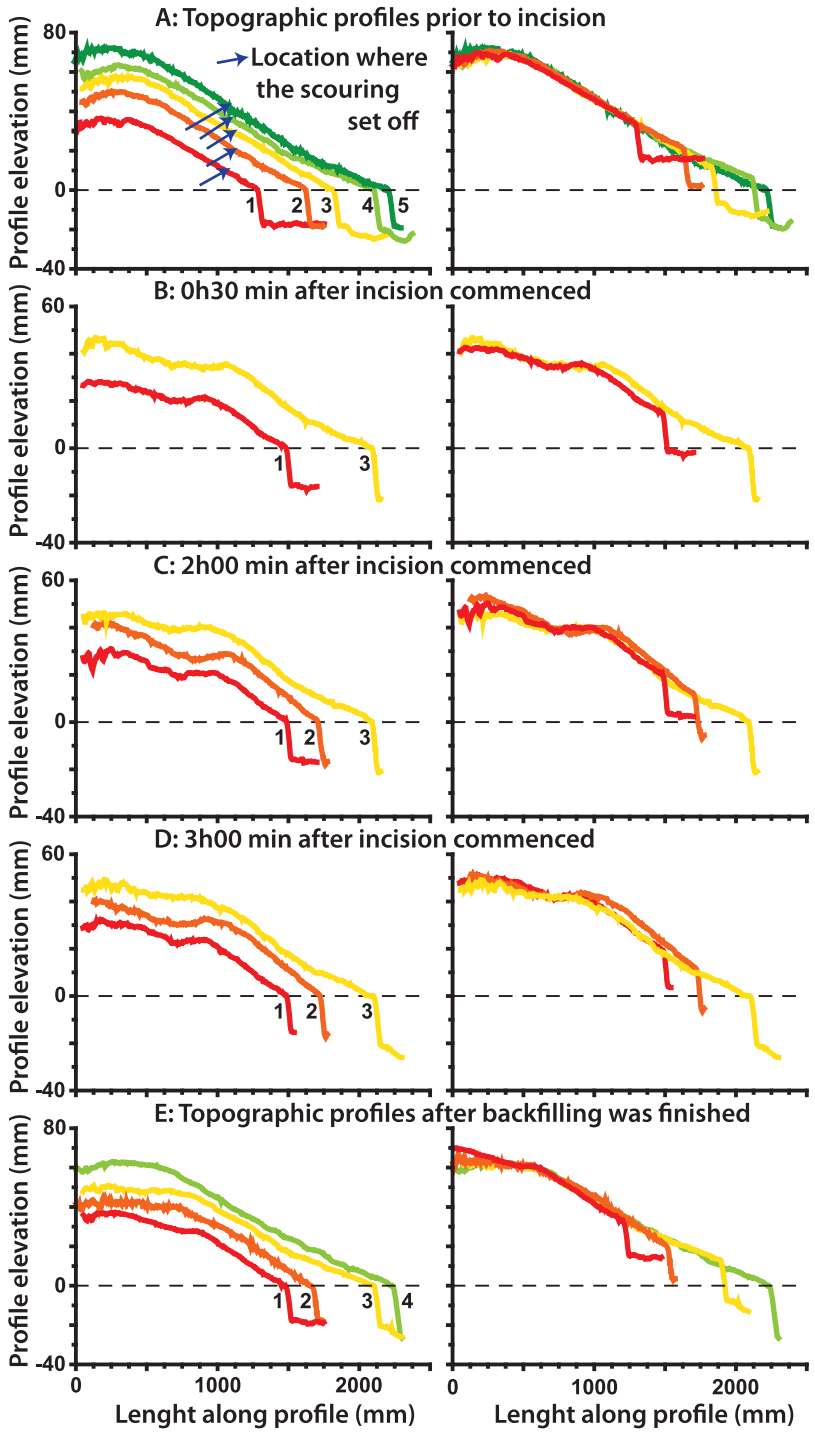the centreline and between experiments. Along the flanks (see Fig. 2.3K for locations of the profiles), the variability was 4.4%, 7.5% and 4.2% for experiments R1, R2 and R3, respectively, much smaller than the variability parallel to the jet flow, which was 8.8%, 13.6% and 9.9% for experiments R1, R2 and R3, respectively. The higher slope variability in the jet-flow direction reflects the greater variation in sediment transport due to the autogenic processes and correlates with the incision events. By contrast, the slope building on the flanks is active during the semi-confined flow stage and the sheet-flow stage, thus showing dominance of sheet-flow processes related with flow fractionation and random rill formation.

Kim *et al*. (2006) report that the autogenic slope variation decreases with (normalised) downstream system size. In the present case, Figs 2.6 and 2.7 both show that the maximum slope remains constant and that the minimum slope during incisions increases slightly, confirming the results by Kim *et al*. (2006). Unfortunately, the minimum slope is difficult to measure. The rate of slope change during active channellised flows causes very high measurement error. Therefore, the measured minimum slopes most likely are not the actual minima; the true minima probably occur just before or after the measurements. For the maximum slope measurements, this problem does not exist, as the rate of slope change becomes increasingly smaller when aggradation approaches its maximum magnitude. It is important to note that, although the minimum slope values of subsequent incisions increase during the experiments, the subsequent incisions manage to erode deeper into the delta plain.

2.3.3 Development of subsequent autogenic cycles during delta growth

Does the increasing size of the fan delta affect the autogenic behaviour of the alluvial-fan feeder system? Intuitively, it would be expected that the frequency of the autogenic behaviour would decline as the fan delta grows. The progressively larger aerial size of the delta plain needs increasingly more sediment to regain the gradient necessary for incision to commence. Hence, with sediment input being constant, it would be expected that that the time in between subsequent incisions would increase exponentially with delta growth and the related growth in sediment accumulation space (space available for backfilling). The term 'accumulation space' has been brought forward by Blum and Törnqvist (2000) following earlier studies by Kocurek and Havholm (1993) and Kocurek (1998) to avoid the confusion which would result from the use of 'accommodation' in a terrestrial context. Those authors defined accumulation space as "the volume of space that can be filled within present process regimes, and is governed fundamentally by the relationship between stream power and sediment load, and how this changes in response to geomorphic base level". Figure 2.6 shows that the time in between the incisions does not increase exponentially. Basically, the incisions occurred at regular intervals of roughly 40 h (except for the fourth cycle, which

A: Topographic profiles prior to incision

Location where the scouring set off

B: 0h30 min after incision commenced

C: 2h00 min after incision commenced

D: 3h00 min after incision commenced

E: Topographic profiles after backfilling was finished

Profile elevation (mm)

Lenght along profile (mm)

started earlier than expected). So what controls the cycle time? If it is not the size of the delta, the answer, as will be discussed below, must lie in the constant, upstream conditions.

With constant boundary conditions, similar gradients are expected throughout the evolution of the fan (e.g. Whipple *et al.*, 1998). Figure 2.8A to E left column shows topographic profiles along the centreline for each cycle (various colour tones) measured just before and after incision and during the activity of the channellised flows. To show the similarity in style of each cycle, the profiles for each cycle have been shifted vertically until they overlie each other (Fig. 2.8 right-hand column). The patterns in gradients are strikingly similar in each cycle and confirm the idea that upstream conditions play a major role in the autocyclic fan-delta evolution. The cause of subsequent channellisation is clearly over-steepening of the delta plain apex. The incision and headward erosion start just at the down-slope end of the water jet on the convex-up surface, thus always about the same distance from the valley outlet. Figure 2.8A shows the topographic profiles along the centreline just prior to incision. The blue arrows indicate where the first mark of incision (scour hole) was observed on the planview camera images. Scouring started roughly 110 cm downstream from the feeder channel in all five cases. The topographic profiles of experiments R2 and R3 are not included, but the first incision of experiment R2 started 70 cm from the feeder channel and the second one started 75 cm from the feeder channel. Experiment R3 showed only one incision, which was initiated at a distance of 70 cm from the feeder channel. The constant input of water and sediment not only leads to the same 'critical gradient' responsible for the initiation of the channellised flow, but also to the location of incision. The gradients and concave-up shape of the channel are strikingly similar, as well as the position of the mid-channel bar and the slope downstream of the bar. Moreover, the backfilling of the channels shows the same development in morphology and gradient. Hence, the increasing size of the delta had no impact on the delta plain slope which is governed primarily by water discharge and sediment yield.

Especially later on in the delta evolution, the gradients near the shoreline tended to become less steep (Fig. 2.8). After the delta had grown beyond a radius of 150 cm, the profile became slightly concave-up near the shoreline. This point remained stationary during the experiment. The concavity might be related to fractionation of the sheet flow and progressive rill formation, leading to enhanced concentration of the flow in the rills (small channels that adopt their concave profile in a way similar to the incision events on the apex). Although the present experiments are not directly scalable to natural systems, it was noticed that concave-up profiles away from the apex of fans are very common in natural alluvial fans and fan deltas. Moreover, the incised channel length (the distance from the outlet of the feeder channel to the intersection point) grew very little compared with the delta radius, although its slight lengthening appears to coincide with a reduction in its width (compare Fig. 2.3F, I, J and L). The slight growth in channel length with each cycle can be attributed to the progressive narrowing of the channel in each subsequent cycle due to progressive deepening of the subsequent incisions, enhancing the effect of the jet 'pushing' the intersection point more basinward. The jets in experiments R2 and R3 are considerably smaller in length, reflected by the fact that the scourings in R2 and R3 were initiated significantly further upstream and confirming the control of the length of the jet.

The increasing size of the delta does play a role, however, in the backfilling process. From incision cycle 2 onwards (after approximately 80 h run time), the increased duration of channellised flow was accompanied by the occurrence of a new stage in delta evolution. The channellised flow graded from fully confined (light grey in Fig. 2.6) to semi-confined, coexisting with sheet flow (dark grey in Fig. 2.6). This result contrasts with the first incision, when the transition from channellised flow to sheet flow was quite abrupt. After the occurrence of the semi-confined flow stage, backfilling of the incised channels took progressively longer. The first incision lasted 4 h, whereas the incision of cycle 4 took 18 h to fill (see Fig. 2.6). As the sediment supply is constant, it must be a reflection of the progressively larger accumulation space characterising subsequent cycles. The volume of the five incisions in experiment R1 does indeed increase (see Fig. 2.9), although the volume change is smaller than expected from the growth of the delta radius. The decreasing channel width and the increasing minimum slope probably are the limiting factors on the growth of accumulation space.

2.3.4 Varying water discharge and sediment supply

The delta growth rate associated with the incisions decreases sharply with decreasing water discharge. Experiment R1 on several occasions showed growth rates of more than 50 mm h^{-1} (Fig. 2.6), the growth rate of experiment R2 is no more than 20 mm h^{-1} and of R3 only 10 mm h^{-1} (Fig. 2.7). These growth rates vary in a non-linear way with imposed water discharge, as noted by, for example, Postma *et al.*, 2008. Yet, what are the consequences for the frequency of the autocyclicity? It can be argued that erosion and backfilling cycles will shorten in duration with increasing discharge, due to higher sediment transport rates.

Using the numerical ACRONYM 6 model of Parker *et al.* (1998) (available at *http://cee.uiuc. edu/*people/parkerg), depositional slopes were calculated for both sheet and channellised flow on the deltas (Table 2.2, Appendix) and the characteristic convexup shape for delta plain development during sheet-flow conditions and the concave-up to straight shape for channellised segments of the delta were reproduced for the three different experiments R1, R2 and R3 (Fig. 2.10A). The elevation plots in Fig. 2.10 have been normalised to the highest apex elevation obtained for sheet flow. The normalised gradients predicted by the numerical model show much similarity with
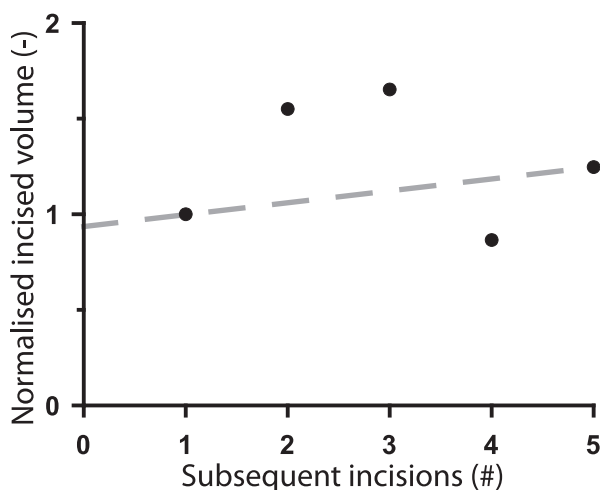

Figure 2.9 Volume of the five subsequently incised channels, normalised by the first incision.

Table 2.2 Variables used in the ACRONYM 6 modelling runs.

Variable	Physical model	Gravel fan	Sand fan	Notes
L (m)	2	10000	10000	Basin radius
θ (-)	180°	120°	120°	Fan angle
D (mm)	0.25	20	0.3	Grain size
p (-)	0.33	0	0	Exponent in resistance relation
α_r (-)	10	10	15	Coefficient in resistance equation
n (-)	1.5	1.5	2.5	Exponent in transport equation
α_{so} (-)	11.25	8	11.25	Coefficient in transport relation
α_{sa} (-)	1	3	1.5	Channel morphology coefficient
τ_c^* (-)	0.03	0.03	0	Dim.less critical shear stress
τ_a^* (-)	1.8	0.042	1.8	Dim.less chann. forming shear stress
Q_w (m^3/s)	1.67×10^{-4} (R1)	250	25	Water discharge
	1.53×10^{-4} (R2)	200	20	
	0.97×10^{-4} (R3)	150	15	
Q_{so} (m^3/s)	0.278×10^{-6}	0.1	0.04	Sediment discharge
I (-)	1	0.02	0.05	Intermittency

those obtained in the flume, and confirm that for any discharge the gradients for channellised flow are much lower than for sheet flow (Fig. 2.10A). To extrapolate these results to a wider range of conditions and natural systems, the impact of discharge variations for fans constructed of gravel-sized sediment was assessed, as performed theoretically by Parker *et al.* (1998). The same data which Parker *et al.* (1998) listed for their Sand and Gravel Fans and used to calculate the normalised gradients for discharge values were used in this study. To illustrate the effect of small deviations in discharge on the depositional profile, slopes were also calculated for discharges that are 25% lower and higher, respectively (Fig. 2.10B and C). The results show that the impact of variations in water discharge on the slopes produced by sheet-flow conditions is much greater than for channelised flow conditions (shaded areas), and also that the impact is largest for the Gravel Fan. The numerical results show that the greatest difference in gradients (and thus accumulation) between sheet flow and channellised flow occurs at low discharge, when sediment transport rates are minimal. In such conditions, accumulation space requires more time to be refilled, which increases cycle duration.

However, although relationships between autogenic cycles and delta growth rates and discharge can be inferred, the present experimental results do not show them explicitly. The erroneous cycle in experiment R2 produced an anomalous incision after roughly 13 h (Fig. 2.7), as shown by the decrease in gradient of the apex (Fig. 2.7A), yet the incision generated hardly any degradation. The other phase of incision generated during experiment R2 and also the incisions in the experiments R1 and R3 did show significant degradation prior to backfilling of the incision (Fig. 2.6A and 2.7A). The cause of the aberrant incision remains unclear.

2.4 Discussion

The present experiments show similarity of process with gravelly alluvial fans built by sheet-flow and sheet-flood processes. Hogg (1982) separates sheet flows from sheet floods based on the lesser
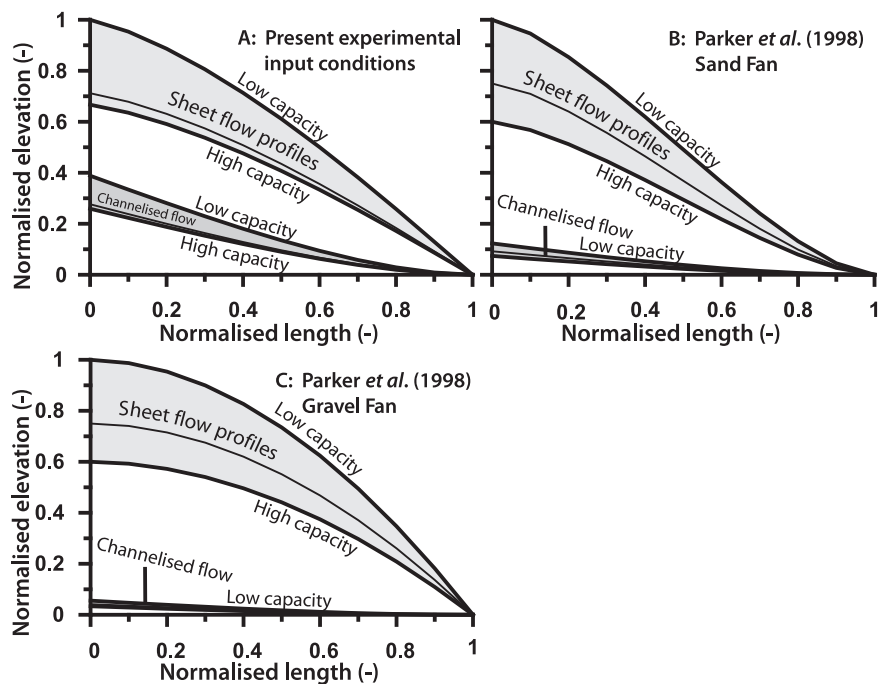
Figure 2.10 Numerical modelling results using the model 'ACRONYM 6' from Parker *et al.* (1998). Fig. A uses the input variables also used in the experiments R1, R2 and R3; Fig. B and C show data from Parker *et al.* (1998) for comparison. See the Appendix for further details.

magnitude and more frequent occurrence of sheet flows. Factors contributing to the formation of sheet flow include sufficient intensity of precipitation, lack of channellised drainage and low ground permeability (Hogg, 1982). These characteristics also emerge from the descriptions of modern, sheet-flood dominated fans in Dead Valley described by Blair (1999, 2000). The fan deposits consist mostly of flood-generated deposits, comparing well with the models described here, if they are considered to be in a continuous state of flooding (see also Paola, 2000).

In flume models not all geometric features, kinematics and dynamics governing natural systems are captured. Hooke and Rohrer (1979) suggest that observations of processes on laboratory fans and their characteristics can still provide a basis for understanding similar characteristics on natural fans (see also Hooke, 1967; Paola, 2000). Peakall *et al.* (1996) refer to such experiments as 'analogue experiments'. Whipple *et al.* (1998) question the extrapolation of fan-head trenching effects to the scale of natural systems. Reduced flow Reynolds numbers and exaggerated geometric scaling relationships may exaggerate the incision depth and suddenness of initiation of the entrenchment process. However, slopes in the present experiments are quite similar compared with gravelly alluvial fans. Blair (1999, 2000) reported slopes ranging from 0.044 to 0.087 (2.5° to 5°) which compare well with values generated in the present experiments and those of others (Whipple *et al.*, 1998; Clarke *et al.*, 2008). However, as the streams constructing these depositional slopes are much shallower than those on natural fan deltas, the authors agree with Whipple that, from a hydraulic viewpoint, the experimental processes cannot be extrapolated to the natural systems directly as the time and spatial scales simply prohibit doing so. Sediment transport rates compare

nicely with transport rates in natural systems if transport is time averaged over sufficiently long time periods (hundreds to thousands of years) to mimic sediment transport occurring mainly during catastrophic events (e.g. Sheets *et al.*, 2002). Hence, although the hydraulic processes are not scaled, the sedimentary processes responsible for creating or filling of accumulation space are (e.g. Postma *et al.* 2008). These are the processes that ultimately define depositional architecture in depositional systems and that are also captured by analogue flume models.

One important conclusion to draw from the large experiment R1 is that the autocyclic fan-delta behaviour is a product of the steady input conditions, although more long-term experiments with steady input conditions are needed to demonstrate how the magnitude and frequency of the cut and fill events are related to differences in discharge. The incisions in R1 are the result of internal feedback mechanisms at regular time intervals. The findings complement the autostratigraphy mechanism derived by Muto *et al.* (2007) which maintains that, for stationary sealevel, systems will remain aggradational and show monotonous progradation basinward at an ever-decreasing rate over longer temporal scales. The only other factor influencing this progradation rate in the autostratigraphy concepts is the shelf-platform topography (Muto *et al.*, 2007). The findings of the present study show how sedimentary systems behave when external forcing is steady, and, although overall aggradation occurs, sediment is released occasionally leading to pulsating rather than monotonous progradation. How these findings (mainly based on the extensive data base of experiment R1) relate to earlier experiments described in the literature and to natural fan-delta systems is discussed in detail below.

2.4.1 Slope variation and related sediment release

What are the consequences of the observed autocyclicity for sediment release and delta progradation rate? Firstly, the slope varies both on the flanks and along the centreline between a maximum value and a minimum value, confirming the conceptual model presented by Holbrook *et al.* (2006) where two potential (fluvial) profiles are defined, representing maximum possible aggradation and maximum possible incision. These authors proposed that the two potential profiles are determined by the variability of the upstream controls. The slope variability observed here shows that the conceptual model can be expanded for constant upstream input, which actually inhibits the dynamic storage and release effect found by Kim *et al.* (2006). The shoreline progradation in the present case is governed completely by these dynamics as the smooth horizontal shelf prevents any effects due to bottom relief changes. The standard variations of the gradient in these experiments (13.6% the highest of experiment R2) are within the range of those given by Kim *et al.* (2006) for the Mississippi, Po and Niger river deltas (up to 40%, Kim *et al.*, 2006; their fig. 13). The dynamic equilibrium slope averaged over time for several cycles is constant (Figs 2.6C and 2.7C) and can be seen as a mean slope that is related to sediment mobility (Schumm *et al.*, 1987; Whipple *et al.*, 1998).

Secondly, the slope and the delta progradation rate along the centreline are much larger than the variation at the flanks of the fan (cf. Figs 2.6C and 2.7C). Kim *et al.* (2006) and Kim and Muto (2007) averaged supply variation over the entire modeled width, which may well be justified for their rectangular model set-up that produced an almost straight (two-dimensional) prograding shoreline. However, the present experiments show that the assumption does not appear to be valid for systems that produce a semi-circular fan delta, which illustrates important autogenically controlled lateral variation in shoreline progradation. While the variation along the centreline is related clearly to the channellisation events, the slope variations along the flanks of the fan are not; their variation is more likely controlled by changes in elevation near the apex, which will

induce changes in flow fractionation and rill formation. The lateral shift in these rills must also be autogenically controlled, but that process operates on a spatial and temporal scale very different from the self-channellisation that occurs along the centreline. As a consequence of these different autogenic processes, the faster progradation rate along the centreline steepens the flanks (see also Hooke and Rohrer, 1979), and it is to be expected that the steepening will produce a major shift in deposition from the centreline to a flank position; this occurs during the semi-confined flow stage. The final shape of the delta following the backfilling process is close to semi-circular. Hence, all available accumulation space is filled at the end of the autogenic cycle.

An important implication is that the autogenic entrenchments always occur more or less along the centreline of the fan-delta plain, the location being controlled mainly by the inertia of the jet, as has also been discussed by Weaver (1984), Schumm et al. (1987) and DeCelles et al. (1991). The latter justifies the use of deterministic methods for modelling autocyclical processes in fandelta simulations (cf. Hooke and Rohrer, 1979), but only if sediment transport is averaged over a sufficiently long time and spatial scales.

2.4.2 Critical slope for autogenic entrenchment

The present experiments show that the critical slope for entrenchment is the maximum slope attained during sheet flow. Interestingly, the experiments performed by Weaver (1984), in spite of the highly variable yield at the apex of the fan, also describe a critical slope, because 'gradients exceeding 0.049 are characterised by erosion'. Weaver (1984) concludes that in these experiments the locations of entrenchment are controlled by local slope instead of average surface slope. The present experiments do similarly show a relationship between the initiation of incision and a local maximum slope which was constant for each cycle reflecting the constant sediment supply and discharge conditions. Whipple et al. (1998) also report fan-head entrenchments in experiments with rising base level, where discharge and sediment supply were held constant. The results of Whipple et al. show a critical slope for channel incision, although it is unknown to what extent the channel incisions were triggered by the changing base level itself. Base-level fall will trigger or enhance headward erosion reducing the relief and increasing the channel length by local progradation, while base-level rise reduces the channel length and potentially increases sediment storage and steepens the relief (Milana, 1998; Van Heijst and Postma, 2001; Milana and Tietze, 2002; Van den Berg van Saparoea and Postma, 2008).

As the critical slope necessary for initiating autogenic fan incision depends on the upstream conditions, a relationship between the critical slope and sediment/water ratio is expected. A plot of maximum experimental slopes versus Q_s/Q_w from this and other experimental studies (Whipple et al., 1998; Clarke et al., 2008) is given by the blue symbols in Fig. 2.11. From Whipple et al. (1998) only the data from the bed load dominated run were selected and the maximum gradient was estimated by taking the average gradient and adding twice the standard deviation. The maximum slopes for the same experimental Q_s/Q_w values were calculated using ACRONYM 6 (Parker et al., 1998) and are shown as red symbols in Fig. 2.11. The solutions (indicated by solid lines in Fig. 2.11) are also extended by doubling and quadrupling the water discharge and by dividing the water discharge by two and four. It is noted that the slopes measured in the other experiments (Whipple et al., 1998; Clarke et al., 2008) are higher than the present experimental slopes, which can partly be attributed to the fact that the fan models differed in spreading angle. In the set-up used here, the fan cone angle is 180°, while in the others it is only 90°, spreading the supply and water discharge over a much larger area. Both experimental and numerical data show a positive relationship between slope and Q_s/Q_w, but the slope trends predicted by the Parker et

al. (1998) model are much steeper than those of the experiments. It is also noted that the data by Clarke *et al.* (2008) include three experiments with the same ratio of Q_s/Q_w, but with different maximum slopes. All experiments, no doubt suffer from non-scalable hydraulic defects caused by the very limited flow depth, grain-size distributions and bed roughness, causing important non-linearity in transport rate (see Postma *et al.* 2008), which are not reproduced in the Parker *et al.* (1998) model. Moreover, the flow width may not be parameterised correctly (Nicholas and Quine, 2007). At present, there is no firm basis to justify extrapolation to natural spatial and temporal scales of either the experimental critical slopes as related to Q_s/Q_w or those obtained by the Parker *et al.* (1998) model.

2.4.3 Application of experimental results to natural systems

Before discussing how experimental results apply to natural systems, it is important to evaluate the various boundary conditions controlling fan-delta evolution. Both upstream and downstream boundary conditions appear to play an important role in the morphodynamics of the fan deltas.

The upstream boundary conditions of the fan delta include water and sediment input, type of sediment transport and width of the feeder channel outlet. The narrow outlet (5 cm width) used in the present experiments leads to narrow and deep incisions that are stable and do not migrate laterally. The only lateral process is flow widening. By contrast, the experiments of Clarke *et al.* (2008) and Whipple *et al.* (1998) were carried out with a much wider feeder channel outlet (15 cm). As a result, both sediment and water discharge at the outlet are affected by bar formation. The migration of the bars leads to pulsating rather than steady sediment transport and also to variations in flow direction on the fan apex. The autogenic incisions associated with wide feeder
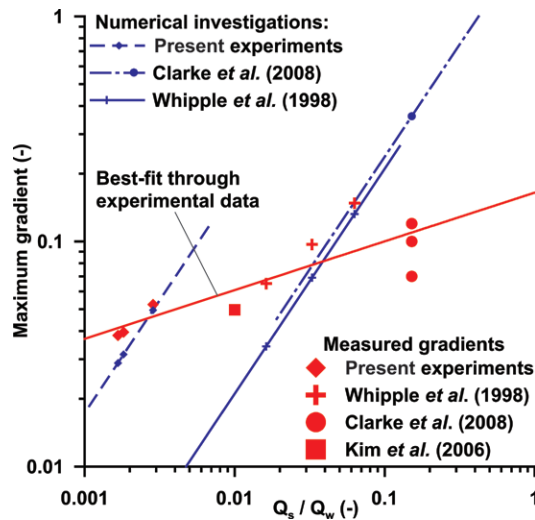
Figure 2.11 A compilation of data on maximum gradients in experiments and of numerical investigations in relation to water discharge. The blue and red lines with small symbols represent results with the numerical fan model by Parker *et al.* (1998). The symbols on those lines correspond to the numerical products using the same input conditions as the experiments. The lines show the variation in slope caused by different water discharges. The measured gradients from the experiments are shown by the solitary symbols. The dashed blue line is a regression line through the experimental data. See text for detailed explanation.

channels are less pronounced and avulsions show much more variation in direction away from the centreline. As a consequence, lateral channel migration plays a much bigger role in fans with a wide feeder channel compared with those with a narrower feeder. The experiments carried out by Clarke *et al.* (2008) show dominant channels up to 30° from the centreline. These boundary conditions (e.g. width of the feeder channel, water and sediment input) can be reconstructed by mapping the individual incised channels if the fan-delta setting is still intact (e.g. Nemec and Postma, 1993; Blair, 1999, 2000). With some notion of the dimensions of a fan body, the lateral extent of large fan-head channels and width-depth ratios can be used to estimate upstream input conditions and processes.

The downstream boundary condition for the fan delta is the shoreline. The importance of the presence of a shoreline for the development of autogenic incisions becomes clear when the present results are compared with those of Clarke *et al.* (2008). In the set-up used here, the fan delta could prograde freely in all directions and progradation was only limited by internal feedback mechanisms. The set-up used by Clarke *et al.* (2008) limited fan growth to a radius of 2.8 m. Sediment surpassing that maximum radius was removed, thereby imitating the effect of toe trimming by, for instance, axial rivers. Clarke *et al.* (2008) observed very similar autocyclic behaviour as described here until the point that the fan was trimmed. At that point in time, channel backfilling ceased as the incised channel came to grade with the new and now fixed base level. The feedback mechanism leading to flow deceleration and subsequent backfilling seen in these experiments was eliminated by limiting the fan growth through sediment removal. In summary, autogenic cycles depend on a number of boundary conditions including the width of the feeder channel and the possibility for continuous growth of the fan radius. These boundary conditions apply to both experimental and natural systems.

2.4.4 Extrapolation to natural systems and preservation potential

The autogenically triggered fan processes and resulting depositional profiles changed little during the R1 experiment. Only the duration and magnitude of the fan entrenchment increased with the size of the growing fan delta and they are likely to increase as the size of the catchment increases. The stratigraphic architecture of the successive autocyclic erosional events of experiment R1 is shown in Fig. 2.12. In the five cycles of aggradation and incision, on average 60% of the aggraded deposits were preserved (see also Fig. 2.5). In other words, the incised channel depth on average equalled 40% of the previously aggraded deposits. The exact number here depends on the experimental input conditions. However, at least some of the material deposited in between two subsequent incisions must be preserved, because on a fixed spot on the surface an incision cannot erode to the same depth as the previous one due to the progradation associated with the previous incision event.

To illustrate the significant impact that autogenic incisions would have on fan deltas in the field, the depth of incision was normalised with the average channel depth on the fan surface. This value offers an indication of the impact of autogenic incisions on natural alluvial fans. In experiment R3 the entrenchments reached depths of more than 2 cm (Fig. 2.6). The average depth of the small-scale channels covering the surface of the fan increased from 3 mm during the first cycle to 7 mm at the end of the experiment (Fig. 2.6). Throughout experiment R1, the incision was more than twice the average channel depth, with a maximum of three times the average channel depth during cycle 4. On the mid-fan and outer fan regions of natural fans comparable with these experimental fans, surface-channel depths average just under 0.5 m but occasionally reach depths of 2 m (Blair, 2000). The ratio between surface-channel depth and depth of entrenchment suggests that on natural fans autogenic incisions could easily reach a depth of 5 to 10 m, similar

to the values presented above. Assuming that in nature also 60% of the backfill is preserved (as justified above), backfill successions may be expected to range from several metres up to a few tens of metres on the apex of fan deltas with radii of a few kilometres or more.

The aggradational part of the autogenic cycles could then be estimated at 10 to 20 m on such fan deltas. Even as an extreme upper limit, at least metre-scale successions will be produced by the autocyclic behaviour and be recognisable in the field. Metre-scale incisions are also reported from alluvial fans subjected to climate change. As shown above, the downstream boundary condition affects autogenic fan-delta behaviour in a different way than alluvial fans, and it is obvious that allogenic fan-delta behaviour will also differ from that of alluvial fans.

However, it is very likely that upstream-controlled incisions will have a comparable impact on alluvial fans and fan deltas, and thus a comparison between them is justified. Climate change is the most cited cause for upstream-controlled incision on alluvial fans. Harvey (1978) found a 2 m deep incised channel on a Spanish alluvial fan, with a radius of approximately 1 km. Ritter *et al.* (1995) showed that an 11 m deep incision was controlled largely by climatic variations on a fan roughly 10 km long. Weissmann *et al.* (2002) report a 10 m deep incised valley on the Kings River alluvial fan, which measured 30 km in radius.

In summary, autocyclic incisions produce large enough changes in accumulation space to be recognisable in stratigraphic successions of alluvial fans and fan deltas if produced under conditions of fan aggradation, i.e. during periods of fan growth and limited base-level change. However, if preserved, their infill (Fig. 2.5) will be difficult to distinguish from onlap and offlap patterns produced by climate change (Milana, 1998; Milana and Ruzycki, 1999; Milana and Tietze, 2002).

Scott and Erskine (1994) report on 12 alluvial fans which show an evolution pattern that is remarkably similar to the autocyclic evolution observed in experiment R1. The fans and catchment areas involved have similar sizes and gradients and were all located in a zone which received very similar rainfall intensities. Hence, the fans were subject to similar but significant flood discharges. Of the 12 fans, seven were entrenched and five were untrenched before the storm event. The fans reacted in a different way to the storm event. Effects ranged from no change at all to trench
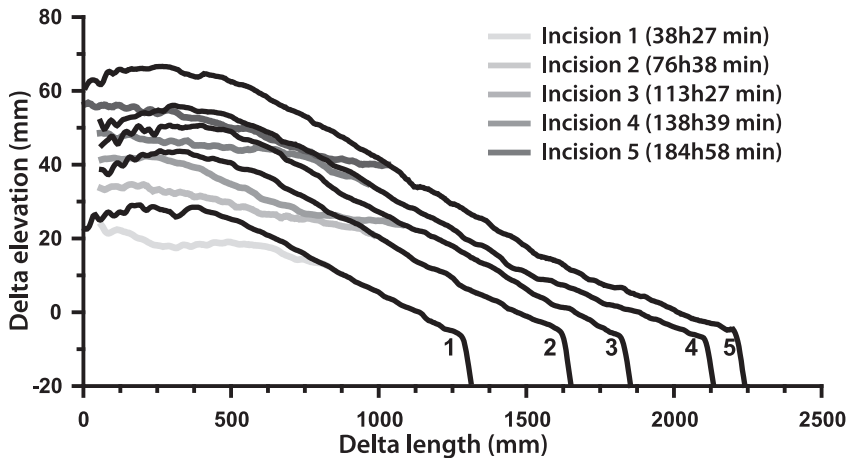

Figure 2.12 Cross-section along the centreline of experiment R1, showing its stratigraphic architecture resulting from five autocyclically generated erosion surfaces. The profiles measured just before initiation of incision that might be preserved in nature as terraces are shown as well. Timing of initiation is indicated in the legend.

incision or backfilling. Scott and Erskine (1994) propose that each fan showed a different stage of a similar autogenic cycle. The cycle consists of: (i) aggradation of the fan; (ii) the initiation of a fan-head trench due to the exceedance of a threshold slope; (iii) coalescence of scour pools to a continuous trench; and (iv) backfilling of the trench due to its widening and slope reduction.

Facies characteristics of autogenically produced channels and their fill (see Fig. 2.5) must include successions characterised by coarse channel lags (pavement and minimum gradient) at the base, covered by thick successions of longitudinal bars and subordinate stream-channel deposits which are capped by combinations of sheet-flow and shallow channellised-flow deposits. Studies from the late Palaeocene Beartooth Conglomerate reveal tens of metres-thick conglomerate cycles in alluvial fans that can be attributed to autogenic behaviour (DeCelles *et al.*, 1991). The entrenchments show typical staircase erosion surfaces (terraces) with bar flank accretions. The backfill consists of onlapping stream flow facies with gravelly longitudinal-bar and side-bar deposits and rare deposits of hyperconcentrated flows (DeCelles *et al.*, 1991). The channel-fill successions do not need to have conspicuous grain-size trends in contrast with the coarsening and fining upward alluvial successions as described by Steel *et al.* (1977) and Gloppen and Steel (1981) from the Devonian Hornelen Basin (Norway).

By definition, the erosional bounding surfaces of autogenic cycles are restricted to the fan, and cannot be traced regionally. Hence, highly synchronous entrenchments in adjacent fans rather point to a tectonic (cf. Gloppen and Steel, 1981) or climate origin (cf. Nemec and Postma, 1993; Pope *et al.*, 2008), while non-synchronous evolution might allude to autogenic origin.

2.5 Conclusions

1   Autocyclic behaviour of fan-delta systems is observed from flume experiments to consist of alternations of sheet flow and channellised flow along the central line of deposition of the fan and more rapid events related to crevassing (rapid migration) of rills along its flanks. The flanks steepen progressively, increasing the available accumulation space.

2   The cyclical alternations of sheet flow and channellised flow consist of distinct stages. (i) Channellisation commences when the fan apex reaches a critical slope value. Incipient scouring and headward erosion forms a channel that connects with the feeder channel. The now confined water flow deepens the channel and deposits the removed sediment in a rapidly prograding delta lobe. (ii) Progressive reduction in the channel gradient makes the flow decelerate, leading to deposition of a mouth bar; this causes widening of the flow upstream of the bar and the beginning of backfilling of the channel. (iii) Progressive backfilling causes the water to leave its channel confinement at some point in time resulting in the coexistence of both channellised and sheet flows filling the available accumulation space at the flanks. (iv) When the channel is filled completely, sheet flow resumes again over the entire fan until the critical slope is attained and the channellisation process begins once again. This critical slope for entrenchment to start is constant for a given discharge and sediment supply.

3   The slope of alluvial-fan feeder systems cyclically varies around a mean value and the latter is defined by the imposed constant water and sediment discharge. The autogenic cycles produce variations around the equilibrium slope of the fan leading to autogenically forced dynamic storage and release of sediment, corroborating the findings of Kim *et al.* (2006).

4   At least 60% of the total thickness of the autocyclic incisions and their channel fills were preserved in these experiments that were run under constant boundary conditions. This observation makes it very likely that similar autogenically forced successions are recorded in natural fan-delta stratigraphy. In studies that focus on one single fan-delta system, such incisions could easily be confused with successions of similar size that are produced by allogenic forcing. However, if compared with contemporaneous and adjacent systems, they are likely to be revealed by characteristic, non-synchronous timing of the incision events. Moreover, the depths of the autocyclic incisions were two to three times deeper than the average channel depth on the delta plain; this provides an application of the experimental results to the field scale and interpretation of fan-delta surface dynamics.

5   Autogenic fan morphodynamics, particularly the tendency to entrench either cyclically or permanently, depends on both the width-depth ratio of the upstream feeder channel and the presence of downstream boundary conditions such as toe trimming or limits to the lateral growth of the fan.

2.6 Acknowledgements

2.7 Appendix

The numerical modelling runs were performed using the model developed by Parker *et al.* (1998), ACRONYM 6, available on *http://vtchl.uiuc*.edu/people/parkerg. The plots showing the Sand fan and Gravel fan were produced using the identical variables as reported by Parker *et al.* (1998, their table 1). The deviating examples were produced by varying the reported water discharges by 25% (Table 1). For the sand fan (Q_w = 20 m^3 s^{-1}) three runs were performed using a Q_w of 15, 20 and 25 m^3 s^{-1}, and for the Gravel fan (Q_w = 200 m^3 s^{-1}) the deviations measured 150, 200 and 250 m^3 s^{-1}. The plots of Fig. 2.10 were calculated using the values of R1, with a Q_w of 0.97 x 10^{-4} m^3 s^{-1} (R3) and 1.67 x 10^{-4} m^3 s^{-1} (R1), Q_s was 0.278 x10^{-6} m3 s^{-1} and the same in all runs. All other model inputs are identical (see Parker *et al.*, 1998; Table 2.1), except for fan angle, which was set to 180°, fan length to 2 m and the grain-size to 0.25 mm to better match the flume experiments for the present study (Table 2.1). Intermittency, a variable included in the model to incorporate the effect of fan activity, was set to 1. In contrast to most natural fans which are active only part-time, these flume experiments were active all the time. Some 'auxiliary' input was also modified to better represent the bed load transport in the flume experiments: the coefficient of adjustment in sediment transport relation to channel morphology (*asa*) was set to 1, as the flume experiments lacked braiding or meandering. The dimensionless exponent in the sediment transport equation (*n*) was set to 1.5 reflecting the lack of suspended transport. The dimensionless exponent in the resistance equation (*p*) was set to 0.33 instead of 0 to account for the increased roughness of the present flume experiments compared with the numerical model.

CHAPTER 3

Autocyclic behaviour of alluvial fans and their distinction from fan deltas

Authors:
Maurits van Dijk, George Postma, Erin R. Kraal, Maarten G. Kleinhans

Abstract

Alluvial fans accumulating on the same piedmont and subjected to similar flooding conditions can show dissimilar responses in sheet-flow deposition, channel incision and filling. It has been proposed that these fans must each have been in a different phase of their autogenically controlled development. This is supported by new flume studies of the autogenic evolution of alluvial fans. In the experiments, alluvial fans were allowed to grow on an inclined fluvial plain without variation in external forcing. Alluvial-fan evolution proceed by cyclic alternations of sheet and channelised flow that followed fan incision by headward erosion. Mid-channel bar formation, flow bifurcation and semi-confined flow lead to progressive backfilling of the channel. Subsequent autogenic incisions are very similar in morphology and gradient, although in later cycles re-incisions occurred before sheet flow had restarted completely, here contrasting with autocyclic behaviour found in modelled fan deltas. Hence, alluvial fans are more often in a state of channelised flow than fan deltas because their sheet-flow stages are much shorter. Further comparison of alluvial-fan and fan-delta evolution shows that the variation in slope produced by the alternating sheet flow and channelised flow conditions is much less on alluvial fans than on fan deltas, so that the frequency of the autogenic cycles is much higher for alluvial fans. Hence, a distinct difference in evolution of alluvial fan and fan deltas exists, which must be caused by the lower boundary condition, the shoreline. It is further argued in this chapter that the control of the lower boundary condition is the amount of accumulation space and if sediment is bypassing this space. The amount of bypass, which itself is determined by the degree the system is off grade, determines the accumulation and progradation rate of the system. During the start-up stage the accumulation rate maximises with no flux bypassing the system, during the fill-up stage increasingly more sediment is bypassing the system and aggradation rate is decreasing steadily up to about 10% of the rate during the start-up stage, while in the keep-up stage the system is close to dynamic equilibrium (grade) with little aggradation and erosion. The different evolution of fan deltas and alluvial fans dictated by the lower boundary condition reflects the different infill-stage they are in. This behaviour can be translated to characteristics used in models of fluvial stratigraphy, and has consequences for the way avulsion frequency is parameterised.

Keywords

Alluvial fans, fan deltas, analogue experiments, autogenic behaviour, incisions, downstream boundary condition, channelised flow, sheet flow, accumulation space.

3.1 Introduction

Alluvial fans are depositional systems developing where sediment-carrying flows emerge from relatively steep source areas onto gentler sloped piedmont topography. Commonly, alluvial-fan surfaces form a cone radiating downslope from its source (Bull, 1977). They are most widespread in (semi-)arid environments, but also occur in humid regions (Bull, 1977; Saito and Oguchi, 2005). Alluvial fans have diverse sizes, slopes, types of deposits and source-area characteristics, caused by the wide range of conditions associated with alluvial-fan formation. They can be formed by debris-flow processes or by fluvial-flow processes (e.g. Hooke, 1967; Bull, 1977; Nemec and Postma, 1993; Blair and McPherson, 1994; Blair, 1999; Moscariello, 2005).

Alluvial-fan development is subject to climate changes, tectonic activity and base-level variations. Tectonics and base-level changes directly affect the downstream edge of fan systems, the effects of which can potentially reach up to the fan apex (Bull, 1977; Stokes and Mather, 2000; Harvey *et al.*, 2003; Viseras *et al.*, 2003; Blair and McPherson, 2008). Climate changes affect the upstream input conditions, leading to aggradation or degradation on the fan (Bull, 1977; Dorn *et al.*, 1987; Wells *et al.*, 1987; Ritter *et al.*, 1995). However, alluvial-fan evolution also comprises autogenic alterations of unconfined sheet flow and channelisation. Scott and Erskine (1994) studied twelve similarly sized Australian alluvial fans, that all were subjected to the same catastrophic flood. The fans responded in various ways, which was surprising as both the fans and the flooding conditions on each fan were quite similar. To explain the observations, Scott and Erskine (1994) propose that the fans must each have been in a different phase of their autogenically controlled development. Although the cycle characteristics are not precisely known, cut and fill events were inferred to play a major role. This is but one example showing why it is imperative to understand the autogenic behaviour before assessing allogenic forcing.

Unlike in nature, allogenic and autogenic factors can be isolated in experiments. Experimental studies revealed similar autogenic behaviour in alluvial fans (e.g. Schumm *et al.*, 1987; Bryant *et al.*, 1995; Whipple *et al.*, 1998; Nicholas and Quine, 2007; Clarke *et al.*, 2008). Schumm *et al.* (1987) modelled alluvial fans using a catchment progressively eroded by steady precipitation, building an alluvial fan by sheet and channelised flow from unsteady water and sediment fluxes. Interestingly, the observed frequency of fan-head entrenchment had no relation to the changes measured in the sediment supply to the fan apex. Hence, they attributed the trenching to an autogenic origin. A closer investigation of the measurements by Schumm *et al.* (1987, fig. 9.22) suggests that the frequency of entrenchment generally decreased with decreasing ratio of sediment to water discharge (Q_s/Q_w), while occasionally the frequency of entrenchment increased with decreasing Q_s/Q_w. The use of a catchment as a sediment source and the resulting unsteady supply make interpretation of their measurements difficult and conclusions regarding autocyclic processes ambiguous. Whipple *et al.* (1998) investigated quasi-steady surface aggradation of an alluvial fan in a flume under conditions of base-level rise and constant water and sediment supply. They observed autogenic alternations between a state of sheet flow and a state of distinctly channelised braiding. During braiding, zones of flow concentration formed, entrenched and backfilled. In similar flume

experiments, Clarke *et al.* (2008) removed sediment at a certain radius, mimicking an axial river system to limit fan growth and simulate truncation. Here, again short-term fluctuations between sheet and channelised flow were observed throughout their runs. However, fan-head entrenchment dominated during the last third of their experiments lasting from 5 to 13 hours in total, suggested that the downstream boundary affected channel backfilling. This behaviour was also reproduced in a diffusion-based 3D numerical model (Nicholas and Quine, 2007).

Comparing fans to fan deltas permits direct assessment of the effect of the downstream boundary condition conditions on internal fan processes. Autogenic cycles in experimental fan deltas (*Chapter 2*) are similar to those on alluvial fans. Analogue experimental fan-delta evolution show prominent cyclic alternation between channelised flow and sheet flow on the delta apex with similarities in morphology and gradient. The duration of the semi-confined flow increased with each subsequent cycle. The key difference between deltas and fans is that though the upstream boundary conditions for experimental alluvial fans and fan deltas are the same, the downstream boundary condition is not (Fig. 3.1). On fan deltas, streams debouch into a standing body of water, causing abrupt deceleration of the water flow. The point to which deceleration is hydraulically 'felt' upstream, a phenomenon called the backwater effect, is approximate by equation (1). The distance L upstream of the shoreline at which the backwater has adapted to 67% of its upstream normal flow depth is estimated for subcritical flow by:

$$L = \frac{h}{3s} \tag{3.1}$$

with h = flow depth [m] and s = channel slope [-]. For example, the Yallahs fan delta on Jamaica, described by Wescott and Ethridge (1980), has a relief of 0.015. For measured flood-water flow depth of less than 2 m, the backwater effect is not more than 45 m on a fan radius of at least several km. For the experimental fan deltas reported in *Chapter 2*, the backwater effect is only about 10% of the channel length and does not approach the apex, so the backwater effect cannot be the cause of the cyclic alternations found in the fan deltas (Fig. 3.1A).

Postma *et al.* (2008) suggested an effect of the downstream boundary condition on fluvial systems. They studied the evolution of a fluvial system to grade, with 'grade' defined as 'carefully adjusted to be able to transport downstream all the sediment supplied to its upstream end' (Mackin, 1948), in other words: total sediment bypass. Postma *et al.* (2008) recognised three stages in the evolution of a fluvial system to grade: 1) start-up stage, in which the system progrades towards base level, 2) fill-up stage, where the system both aggradation (steepening of the depositional slope) and sediment bypass occurs, and 3) keep-up stage, in which only 10% of the sediment input is used for aggradation, the rest is bypassed. These stages are illustrated in the two panels of Figure 3.1B. The upper panel shows the fluvial stratigraphy of the evolving system, the lower panel expresses the development of the output yield of the system. During the start-up stage, as the fluvial system still grows to base level, no output yield is generated either. When the system reaches base level, signalling the start of the fill-up stage, bypass of sediment starts as well, expressed as increasing output yield (lower panel of Fig. 3.1B). The keep-up stage is the final and longest stage of the evolution of the fluvial system. It is defined to begin when (less then) 10% of the supplied material is used for aggradation, but at this point the rate aggradation decreased considerably and the fluvial system takes a long time to get from 90% bypass to 100% bypass (Fig. 3.1B).

Applying these concepts to the fan deltas and alluvial fans we compare to assess the effect of base level, we demonstrate that they reside in a different infill-stage. The fan delta prograds into water and therefore has reached base level by definition. As the delta grows, its base level (the
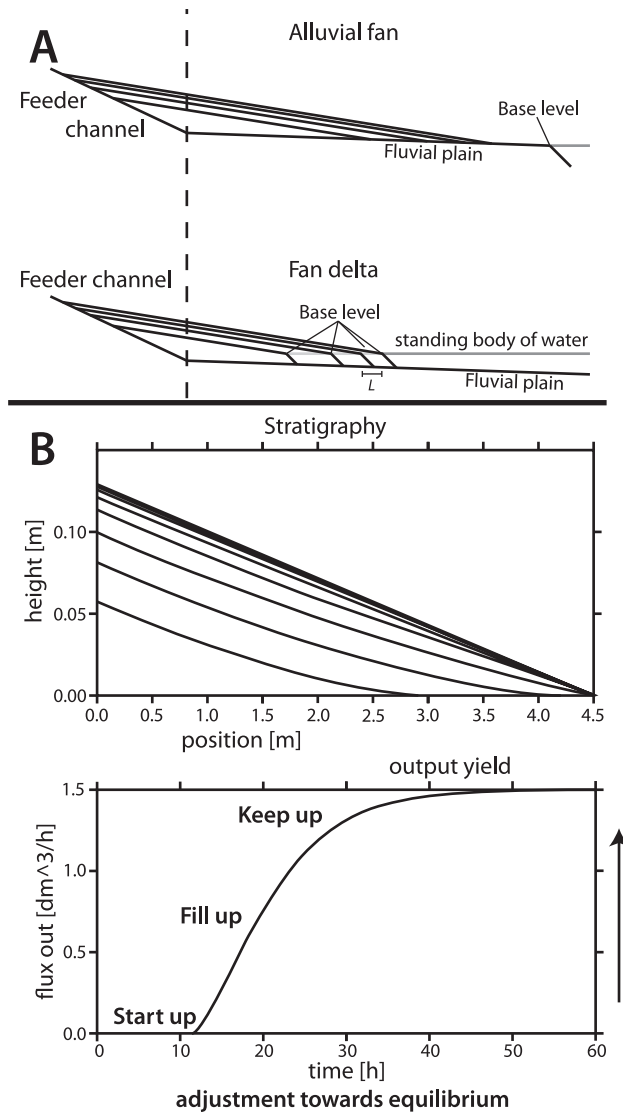
Figure 3.1 A) Schematic illustration of the conceptual difference between alluvial fans (upper panel) and fan deltas (lower panel). The length over which the backwater effect potentially affects fan-delta behaviour (*L*) is indicated in the upper panel, B) illustration of the fluvial stratigraphy (upper panel) and the output yield (lower panel) during the evolution of a fluvial system.

shoreline) migrates basinward, placing it in Postma *et al.*'s fill-up stage. The alluvial fan, on the other hand, has not yet arrived at the base level and still lingers in the start-up stage.

We also expect the behaviour of the systems in the different states to reflect the different sedimentation rates associated with absence or presence of sediment bypassing. Quantitative models of alluvial stratigraphy aim to understand and predict the relative occurrence of channel-belts within overbank deposits. A widely used example of these models is the 2D LAB model,

developed over the course of the 70s, 80s and 90s by M.R. Leeder, J.R.L. Allen and J.S. Bridge (e.g. Allen, 1978; Leeder, 1978; Allen, 1979; Bridge and Leeder, 1979; Alexander and Leeder, 1987; Mackey and Bridge, 1995). The 3D channel- belt architecture, the distribution of the channel belts within the basin, is determined by channel-belt width, floodplain width, bankfull channel depth, channel-belt and overbank sedimentation rates, avulsion location and period, compaction and tectonism (Mackey and Bridge, 1995). Within these controls, avulsion dynamics remains one of the least constrained (Paola, 2000; Slingerland and Smith, 2004). The LAB model predicts that with constant avulsion frequency, channel-belt density should be inversely related with sedimentation rate. Bryant *et al.* (1995) questioned the assumption of constant avulsion frequency, and presented experimental data on alluvial fans suggesting that avulsion frequency strongly increased with sedimentation rate. In contrast, Ashworth *et al.* (2004; 2007) infer from their braided-river experiments that avulsion frequency increases slower than sedimentation rate. Could these differences in avulsion frequency reported by Bryant *et al.* (1995) and Ashworth *et al.* (2004, 2007) be explained by differences in the evolutionary state of the modelled systems?

This paper investigates the control of the downstream boundary condition on alluvial-fan evolution through autogenic alterations of channelised and sheet flow phases using experiments of alluvial fans prograding over a fluvial plain with variable discharge and fluvial-plain slope. To facilitate comparison with the fan-delta experiments, the experimental setup is very similar to those of earlier fan delta experiments, and similarly no external variations were imposed on the experiments (*Chapter 2*). After the autogenic development of the alluvial fans is determined, the effect of the downstream boundary condition is investigated by comparing the alluvial-fan and fan-delta experiments. We also explain the different results on avulsion frequency and sedimentation rate, and explore the implementation of our model results on alluvial stratigraphy. Finally, the implications for natural alluvial fans and fan deltas are explored.

3.2 Experimental setup

3.2.1 Flume setup and materials

A set of 5 Runs A1 to A5 was performed in the Eurotank Flume Facility at Utrecht University (Table 3.1). During each experiment, the conditions extrinsic to the systems were held constant (i.e. base level, discharge, sediment supply). All runs were done in pairs (except for Run A1, which means that two alluvial fans were formed side by side in the Eurotank (Fig. 3.2). To avoid ponding of water, a sloping substrate (flat sand bed) was chosen with a gradient that was much less than the gradient of the prograding fan surface (Table 3.1).

In all cases the bed was 2.7 m wide while the downslope length varied from 2.5 m for Run A1 – 3 to 5 m for A4 and A5. A ditch between the two prevented the Runs from influencing each other. The downslope end of the bed was a fixed base level formed by a shoreline that separated the bed from a 25° inclined subaqueous slope (Fig. 3.2). The sediment grain size of the bed and the sediment feed was the same and held constant during the Runs. Each setup had its own feeder channel, located in the centre of the upstream edge of sloping bed. The duct was positioned horizontally, and its width of 5 cm was chosen carefully to ensure that no alternating bars would occur in the duct at the range of discharges used to avoid flow variations at the outlet of the duct. The sediment was mixed with the water flow by means of a sediment feeder. The sediment feeder delivered a constant sediment volume by means of a worm gear. Deviations of the delivery by the feeder were measured to be less than 1% over 15 minutes.
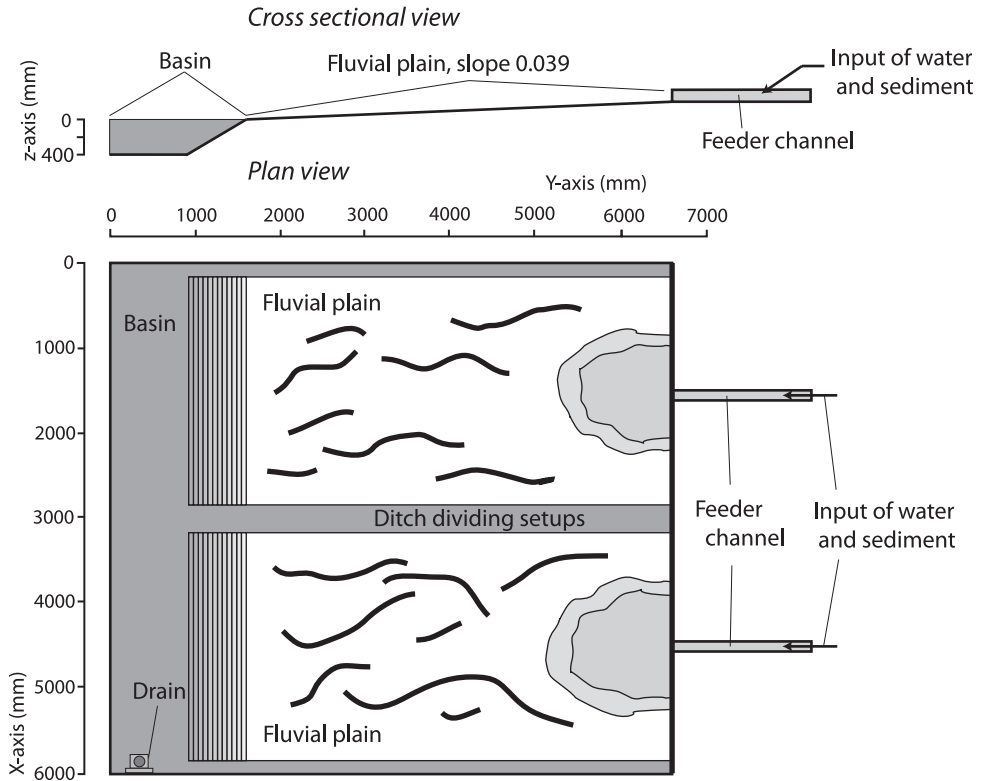
Figure 3.2 Schematic view of the set up of experiment A4 and A5. Differences between this set up and the set ups of the other alluvial-fan experiments are listed in Table 3.1. They are limited to differences in setup length and fluvial-plain slope.

Alternating feeds of grey and white sand facilitated process visualisation. Both sands consisted of quartz with a bulk density of 2650 kg m^{-3}. The grey sand was used as substrate of the erodable fluvial plain (as described above) and the feeder channels. Grain-size distributions are shown in Figure 3.3. Median grain size of the grey sand was 230 μm corresponding with a critical Shields parameter of 0.0688, whereas the white sand had a median grain size of 240 μm with a critical Shields parameter 0.0622 using the model of Vollmer and Kleinhans (2007) accounting for shallow flow depth. We assume that the difference had a negligible effect on the experiments.

In analogy with modern bed-load dominated alluvial fans, our selected grain sizes and settings of water discharge and sediment supply ensures that bed-load transport was the dominant sediment transport mechanism. The sediment transport capacity θ of the water flow over the alluvial-fan was estimated by:

$$\theta = \frac{\tau'}{(\rho_s - \rho_w)gD_{50}} \tag{3.2}$$

with

$$\tau' = \rho_w g \left(\frac{u}{C'}\right)^2 \tag{3.3}$$

and

$$C' = 18 \log_{10}\left(\frac{12d}{2.5D_{50}}\right) \tag{3.4}$$

using d = depth [m], u = velocity [m s^1], g = gravity constant [9.81 m s^{-2}], C' = Chézy coefficient related to skin friction [m s$^{0.5}$], ρ_s = sediment density [kg m^{-3}], ρ_w = water density [kg m^{-3}] and τ = bed shear stress related to grains [N m^{-2}]. Calculated values for θ averaged 0.20 and were never higher than 0.28. These values clearly exceed the critical Shields parameters for the sediment used, and are only just above the criterion for suspended sediment transport derived by Soulsby (1997) indicating bed-load. The smaller flow depths of the non-channelised flows yield higher Chézy values and smaller values of θ, ruling out suspended transport beyond the channels as well.

3.2.2 Measurements

The surface topography was quantified using photogrammetry based on stereoscopy (Chandler *et al.*, 2001; e.g. Brasington and Smart, 2003). In the Eurotank flume, an automated movable platform is attached to the ceiling. It contains a set of cameras, which takes four simultaneous photographs of the surface from different angles. The images are processed using software package SANDPHOX™, into a Digital Elevation Model (DEM) of the sand surface. The vertical resolution of the DEMs is 250 μm and the horizontal resolution is better than 100 μm. To avoid reflections of the running water in the images, the experiment was stopped before each photogrammetry scan and the water slowly drained to avoid compaction of the bed. Runs A1 and A2 were halted every four hours, while experiments A3, A4 and A5 were stopped at uneven intervals depending on the progress of the experiment. The intervals ranged from two photogrammetry scans every 15 minutes during periods of high (autogenic) activity to a single scan every eight hours during periods of less activity. Apex elevations were obtained from the topographic scans; alluvial-fan progradation data were calculated by averaging the progradation of the fan edge along 5 transects, which run from the apex along the centreline and were directed 27° and 63° away from the centreline on both sides.

Time-lapse photography (one image per 10 minutes) using digital video cameras recorded all Runs. To view the entire upper part of the fluvial plain including the fan apex the cameras were mounted obliquely. When required, a normal digital camera was used to take close-range and overview images from alluvial-fan processes that were poorly visible on the time lapse video images.

3.3 Results

A set of 5 Runs (listed in Table 3.1) was performed with constant input conditions throughout each run. Between Runs A1-3, water discharge was varied using the same fluvial-plain gradient, while runs A4 and A5 shared identical input of water and sediment but had different fluvial-plain gradients. All Runs showed alluvial-fan accumulation by similar autocyclic alternations of sheet and channelised flow following an initial phase of unfractionated deposition from the jet.

Table 3.1 Input conditions and set up characteristics of the alluvial-fan experiments. The fan-delta experiment from Chapter 2 is included as well.

	Alluvial fan					Fan delta
Run nr (this chapter)	A1	A3	A3	A4	A5	R1
Eurotank File name	A006.2	A006.1	A005.1	MA1	MB2	A008
Set up length (m)	2.5	2.5	2.5	5.0	5.0	4.0
Set up slope (-)	0.025	0.025	0.025	0.031	0.039	0.0
Sediment input Q_s (m³/hr)	0.001	0.001	0.001	0.001	0.001	0.001
Water discharge Q_w (m³/hr)	0.30	0.45	0.55	0.35	0.35	0.60
Ratio Q_s/Q_w	0.00333	0.00222	0.00182	0.00286	0.00286	0.00167
Total run time (hrs)	32.0	32.0	68.5	85.3	85.3	183

Simultaneously, a channel network was generated on the fluvial plain downstream of the fan. Apex incision and subsequent channelisation were initiated by scour holes that migrate upstream, followed by channel back-filling and return to sheet flow.

First, the detailed alluvial-fan morphodynamics and autogenic behaviour are described for Run A4, which provided the most extensive dataset. The behaviour of Run A4 is demonstrated using photographs (Fig. 3.4), a diagram summarising topographic data (Fig. 3.5), shaded-relief maps (Fig. 3.6), and topographic transects (Fig. 3.9). Next, the effect of varying fluvial plain is assessed by comparing Runs A4 and A5, and the impact of the sediment/water flux ratio is assessed by comparing Runs A1 to 3 (Fig. 3.7). Finally, differences between alluvial-fan and fan-delta development are pointed out and explained by comparing the occurrence of channelised flow and the slope variability (Fig. 3.7 and 3.8). The diagrams showing Runs A1-3, A5 and R2 and 3 are shown in the Appendix.
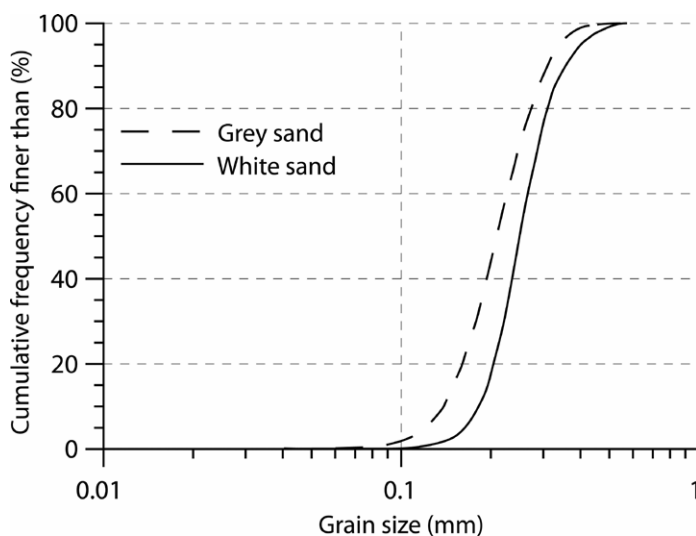

Figure 3.3 Cumulative grain-size distributions of the grey and white sands used in the experiments.

3.3.1 Autogenic behaviour of alluvial fans (Run A4)

Initially, the jet emerging from the feeder deposited a small elongated lobe in front of the feeder channel. Downstream of the lobe, the water spread out forming a sheet flow of shallow depth (Fig. 3.4A). Within 10 minutes, rills appeared on the sand bed and 5 minutes later the lobe at the feeder-channel outlet had widened and became fan-shaped (Fig. 3.4B). Over the course of the first hour, the rills in the sheet flow on the fluvial plain gradually transformed into a braided-channel network that extended from the fan apex downstream to the shoreline (Figs. 3.4A and B).

The sheet flow on the fan began to fractionate once more channels had appeared along its flanks (Fig. 3.4C). Particularly in the mid-fan region, small bars emerged between channels of about 2-3 cm width and 0.5 cm flow depth that migrated across the entire fan surface. Along the centreline of the fan, these channel-bar networks developed much further downslope giving the fan a typical irregular, elongated morphology (Fig. 3.4C). After the initial 2.5 hours in which the fan-shape was established, aggradation and progradation started, as shown by the plots of 'averaged progradation' in Fig. 3.5A and 'apex elevation' in Fig. 3.5B, leading to significant steepening of the slope along the centreline (Fig. 3.5A).

A much larger channel was generated by headward erosion after 11½ hours. It was initiated by a scour that emerged on the fan apex (Fig. 3.4D) and soon attracted more water. When the upstream migrating scour reached the feeder channel, it connected the newly formed channel directly with the outlet. As a result, the entire water flow became confined leaving part of the upper and middle fan inactive, while deepening and also extending the channel further down the fan (Fig. 3.4E). The removal of sediment at the apex was also apparent in Fig. 3.5A and B; fan progradation accelerated, apex elevation declined and the slope decreased.

A bar formed within the channel a metre downstream from the feeder channel, causing the channel to widen and bifurcate around the bar. In both bifurcated channel branches, new scours were formed which migrated sideways (perpendicular to the direction of the inflowing water) to the flanks of the fan (Fig. 3.4F). This further enhanced widening and shallowing of the bifurcated channel branches (Figs. 3.4G and H). Subsequently, the trunk channel backfilled, leading to progressive flooding of the banks while channelised flow persisted (semi-confined flow, indicated by dark-grey bands in Fig. 3.5). During the first cycle, semi-confined flow occurred briefly, after which the trunk channel was filled completely and the entire alluvial fan was covered again by sheet flow (Fig. 3.4I and 3.4J). Aggradation on the apex continued for 10 more hours, until a second cycle of incision was initiated by a scour on the centre of the fan (Figs 3.4K- P).

Three complete cycles of sheet flow and channelised flow occurred in A5. The experiment was terminated after channelised-flow initiation but before completion of cycle four (Fig. 3.5). The spatially averaged progradation rate decreased steadily whilst the fan body increased in size. The apex aggraded progressively, interrupted by degradation during channelisation, and the slope along the centreline increased during the sheet-flow phases, and decreased whilst flow was channelised. The second and third cycles evolved very similar to the first one, although the cycle duration progressively increased as incisions lasted longer. The increase in cycle duration was accompanied by longer phases of semi-confined flow. Also, the second and third incision showed re-incisions, temporarily halting backfilling and generating additional degradation (Fig. 3.5B). The re-incisions were in both cases triggered by a new scour that formed along the fan axis in between the two bifurcated channels and downstream of the two secondary scours. Headward erosion led to upstream migration of this new scour into the trunk channel (see also Fig. 3.4O).

Morphodynamics of the re-incision event in cycle three is illustrated by shaded-relief maps (Fig. 3.6). Following sheet flow, incision occurred on the fan surface leading to fully confined flow

(Fig. 3.6A and B). The incised channel bifurcates in two channel branches, with a scour hole in each bifurcated branch (Fig. 3.6B). As the two scours in the bifurcated channel branches migrated sideways, the bifurcation angle widened (Fig. 3.6B and C). The local in-channel slope decreased, which is illustrated by the gradients pointed out in the channel branches in Fig. 3.6C and D. At the same time, the cross-sectional area of the branches decreased as well, which can be seen in the cross-channel transects shown at the bottom of Figure 3.6 (A-A', B-B', C-C' and D-D'). In Figure 3.6D, re-incision had commenced, across a part of the alluvial-fan surface which prior to re-incision had much steeper gradients than the gradients of the two branches (Fig. 3.6C). The degradation associated with re-incision was less substantial than the incision occurring at the beginning of channelised flow, and so re-incision events did not last very long (Fig. 3.5 and 3.6). Following re-incision, semi-confined flow quickly reappeared and backfilling was completed.

3.3.2 Role of slope and aggradation rate in alluvial-fan evolution (Run A4)

Slope changes played a major role in the development of the alluvial fan. For instance, during periods of sheet flow, the slope along the centreline steadily increased as the fan was building up, but steepening of the fan surface halted abruptly when incisions formed (Fig. 3.5A). The maximum slope appeared very similar throughout the run, measuring around 0.05. That value can be regarded as a 'critical' gradient necessary for the initiation of autogenic incision. The minimum slope values, measured during phases of channelised flow, showed a slight increase during the run, although it was very hard to capture the minimum slope due to the rate of slope change during channelised flow. Even if the slope minimum occurred just before or after the measurement was taken, the measured value may deviate from the actual minimum.

The slope along the flanks of the fan body showed a much wider range compared to the slope along the centreline. Its development showed an inconsistent response to both sheet and channelised flow. For example, the slope decreased during the sheet-flow stage of cycle 1, the slope increased during the same part of cycle 3, and remained steady during cycle 4 (Fig. 3.5A). The slope variations along the alluvial-fan flanks showed little relation to the autogenic incisions and were dominated by smaller-scale sheet-flow related processes such as rill formation and migration.

The aggradation rate on the apex reflected its ability to store or bypass sediment and oscillated around a value just above zero (Fig. 3.5B). Excursions from this trend corresponded to increased aggradation and degradation associated with formation and back-filling of autogenic incisions and decreased in magnitude as fan evolution progressed. However, filling the re-incisions of cycle two and three involved much higher aggradation rates than filling the initial incisions (Fig. 3.5B). During the final 20 hours of the Run, aggradation-rate excursions diminished, matching the steady apex elevation and reflecting sediment bypass. The alluvial-fan slope, apex elevation and aggradation rate on the apex all reflected the impact of the autogenic incisions on the evolution of the alluvial fan.

3.3.3 Impact of fluvial-plain gradient and discharge variation on aggradation rate

The ratio of sediment and water input determines the depositional gradient of an alluvial fan as it grows and thus affects the potential volume available for deposition. In marine systems, this volume is referred to as accommodation. To avoid confusion with this term with its relation to sea-level variations, we use the term accumulation space, introduced for use in the fluvial realm (Kocurek, 1998; Blum and Törnqvist, 2000). They defined accumulation space as 'the volume of space that can be filled by sediment within the present process regime, and is fundamentally governed by the relationship between stream power and sediment load' (Kocurek, 1998). For alluvial fans, the

accumulation space is thus the space between the depositional slope projected in the base level point and the slope of the fluvial plain over which the alluvial fan grows. It will be argued below that the way the alluvial fan grows changes with the infill of the accumulation space.

Both fluvial-plain slope and the ratio Q_s/Q_w show a positive relation with aggradation rate (Figs. 3.7A and B, and note that the y-axis is kept identical to show the different impacts). Averaged aggradation rate here means the rate of deposition on the apex divided by the time over which deposition occurred, excluding degradation. This indicates that the effect of varying discharge affects accumulation space more than the variation in fluvial-plain slope does. The varying aggradation rates related to fluvial-plain slope and discharge presented above (Figs. 3.7A and B) were combined in Figure 3.7C, which shows the channel activity versus the aggradation rate. Channel activity is defined as "the percentage of time that autogenic channelised flow is active on the apex", and it is a reflection of the autogenic activity of a system. The alluvial-fan data is shown in black, representing Runs A1-A5. The fan deltas are shown in grey (R1-R3), and are acquired from previously performed runs reported in *Chapter 2*. The added trend line for the alluvial-fan series is an exponential fit (R^2 = 0.99), the added trend line for the fan-delta series is a linear regression line (R^2 = 0.78). Figure 3.7C clearly shows that increasing aggradation rates correspond with decreasing channel activity. In other words, the autogenic activity of a system varies with aggradation rate.

3.3.4 Comparing autogenic cycles

The alternations between sheet and channelised flow on the alluvial fan model described here are similar to those in the fan-delta models described earlier (*Chapter 2*). Yet, there also are considerable differences, in particular in the slope variability and in the channel activity. First, we point out the similarities and differences between alluvial fans and fan deltas to investigate the effect of the presence or absence of a shoreline on the autogenic cycles. Second, we will show that alluvial fans and fan deltas considered here are in a different stage of filling in their accumulation space.

The first obvious difference is that the fan delta progrades into a standing body of water, whereas the alluvial fan progrades over an inclined fluvial plain. As a result, the base level of the fan delta lies at the shoreline, but the base level of the alluvial fan lies beyond the alluvial-fan limit, at the end of the fluvial plain. Hence, the alluvial fan is in the start-up stage of the model of Postma *et al.* (2008) and not directly influenced by base level, whereas the fan delta is in the fill-up stage and shows a major control by base level.

Similarities

Both systems have identical feeder conditions; a steady input of water and sediment passing through a 4.5 cm wide feeder channel. The constant input generates a steady jet flow from the feeder channel, ensuring that the magnitude of the critical slope necessary for initiation remains constant in both systems (see Figs. 3.5 and 3.8). Also, the position where scour initiation occurs remains constant throughout the runs (see Fig. 3.4D, K and O and *Chapter 2*). Increasing feeder-channel width has a considerable impact on fan-delta evolution (*Chapter 2*). Wider feeder channels allow the direction of the jet flowing out of the feeder channel to vary due to the formation and downstream migration of alternating bars in and near the outlet of the feeder channel. Hence, wider feeder channels promote lateral channel migration once autogenic incisions are initiated, while narrow feeder channels lead to stable channel configurations. A stable incision promotes the formation of an elongated depositional system, dominated by progradation, whereas lateral
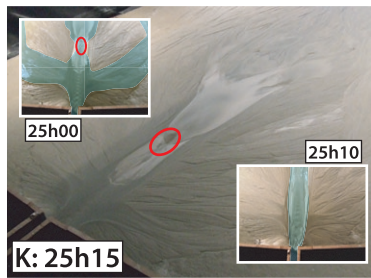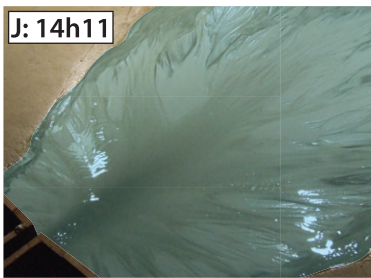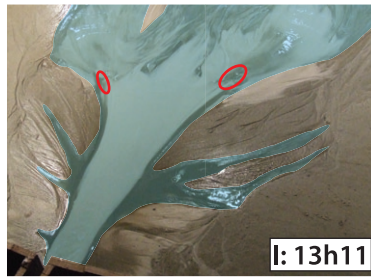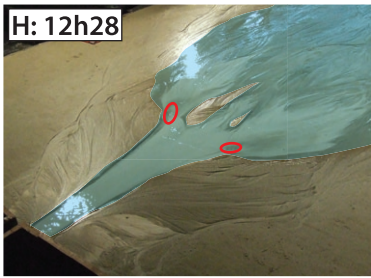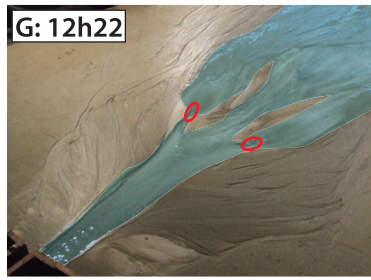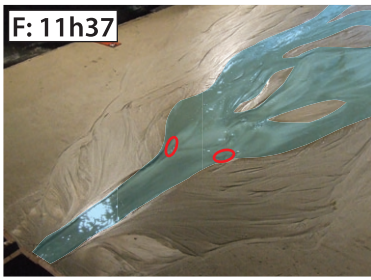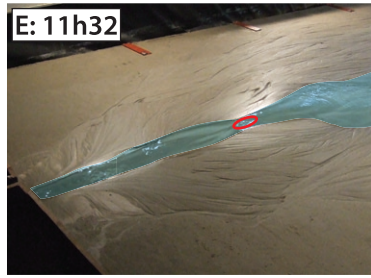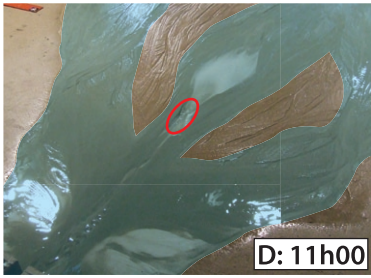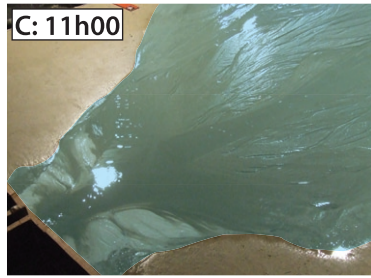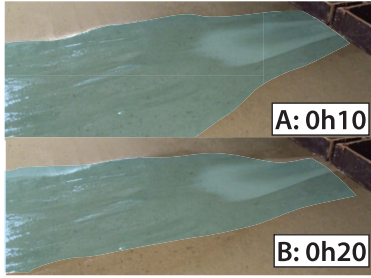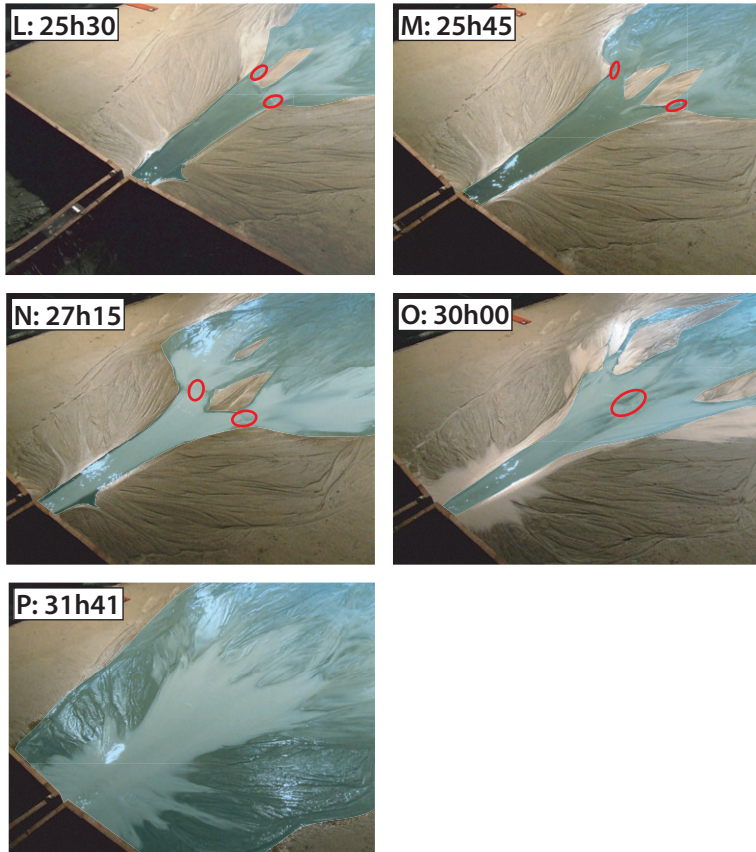
Figure 3.4 (continuing from previous page) Oblique photographs from the development of run A4. Flow is from right to left in panel A and B, and from the lower left to the upper right in the other panels. Run time is indicated in the individual panels. Blue areas are covered by water, and the red circles surround scour holes. Width of the inflow channel (clearly visible in e.g. panel L) is 5 cm.

channel migration enhances radial redistribution of the sediment leading to semi-circular fan-shaped depositional systems.

Differences

The differences between autogenic cycles of the alluvial-fan and fan-delta runs are the timing and duration of the autogenic cycles (Figs. 3.5 and 3.8). The main morphological difference lies in the slope variability (Fig. 3.7D). Could these two entities be related somehow?

The slope variability is calculated by:

$$S_{var} = \frac{(S_{max} - S_{min})}{S_{ave}} \tag{3.5}$$
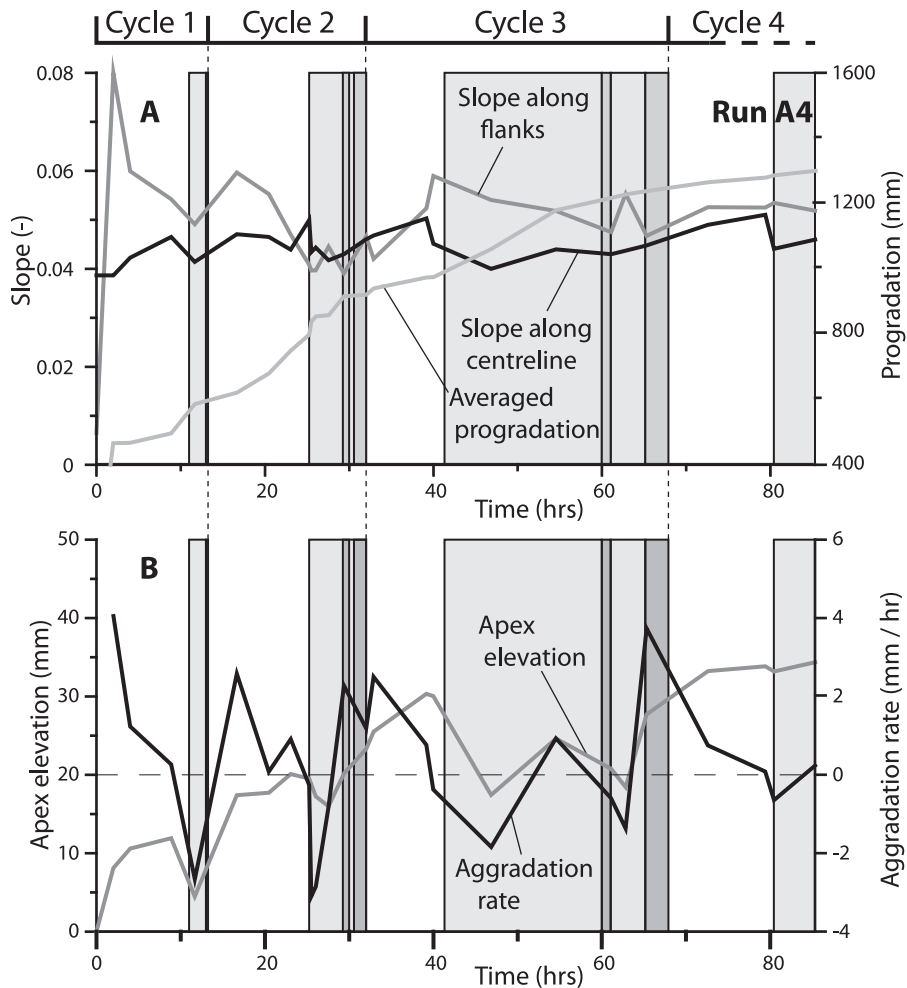
Figure 3.5 Schematic representation of the development of the alluvial fan of experiment A4. Light-grey areas represent periods of fully confined flow. In the dark-grey areas channelised flow coexisted with sheet flow; areas without grey-shade represent sheet flow. Cycle number is indicated at the top. (A) Plot of the gradient development along the centreline in black and along the flanks in dark grey (angling 63° away from the centreline), the averaged progradation of the alluvial-fan edge is indicated in light-grey. (B) Plot of the elevation (grey) and the aggradation rate at the apex (black). The dashed line indicates zero aggradation, and the timescale (the x-axis) is identical to the fan-delta evolution shown in Figure 3.7

using S_{var} = slope variability [-], S_{max}, S_{min} and S_{ave} = maximum, minimum and average slope respectively [-]. Slope variability calculated from the subsequent autogenic incisions is roughly twice as large for fan deltas compared to alluvial fans (Fig. 3.7D). The alluvial fans, still prograding towards base level, are still in the start-up stage of their development, while the fan deltas already reached base level and moved into the fill-up stage. The differences in slope variability are caused by the different infill-stages in which the two systems reside. The aggradation occurring during the fill-up and keep-up stages increases the depositional slope until it approaches the equilibrium slope.
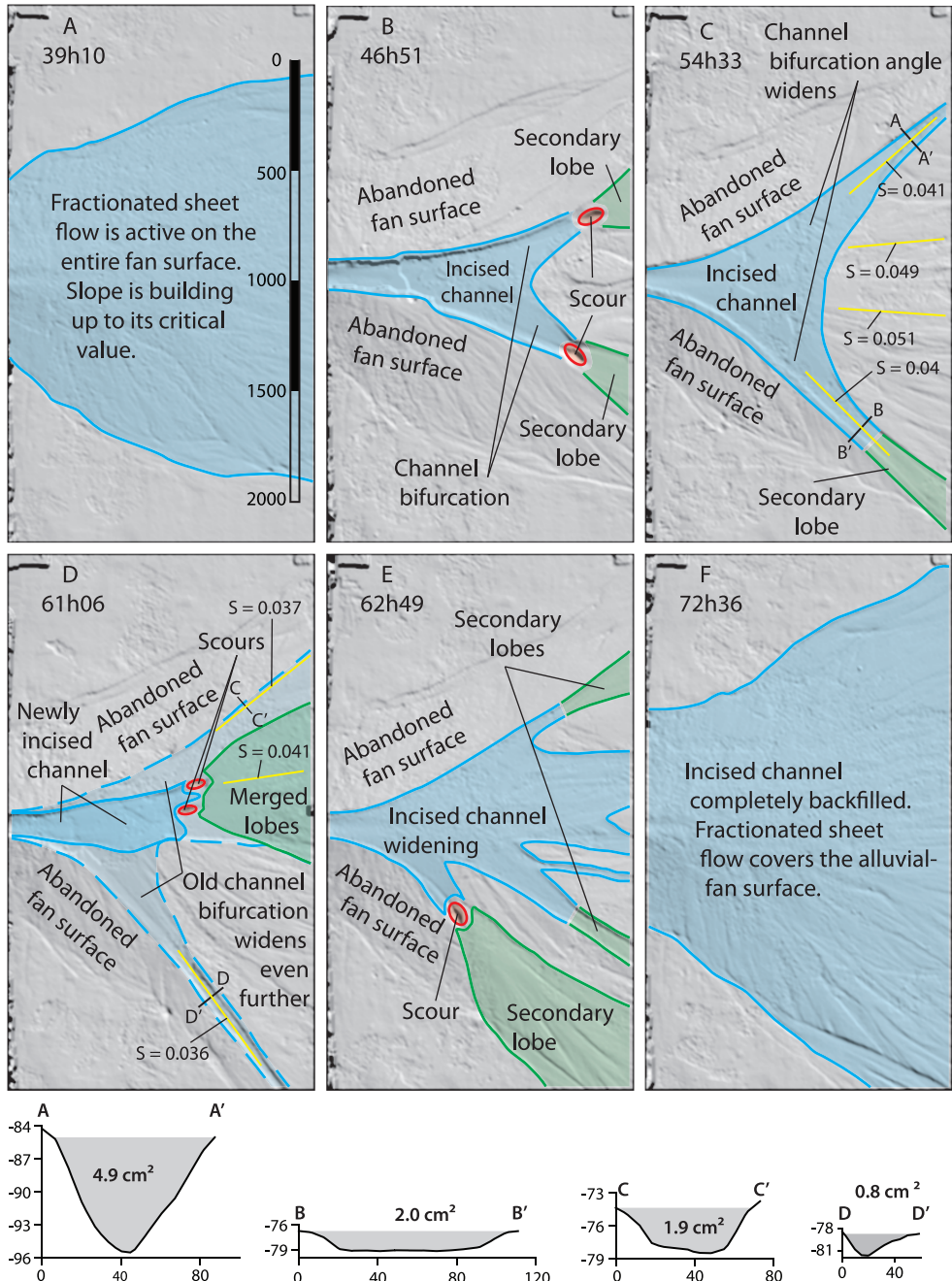
Figure 3.6 Shaded relief maps of the re-incision event observed during cycle 3. Runtime is indicated in the upper right of each panel; scale is the same for each panel and indicated in panel A. Backfilling continued in spite of new incision most likely because the fan gradient had not yet built up to its critical slope (see Fig. 3.4). Cross sections A-A', B-B', C-C' and D-D' show the decrease in cross-sectional area of the side channels, locations are indicated in panel C and D.

The rate of slope change will be largest right after the fill-up stage is reached and then decline as progressively more sediment is bypassed. In other words, under similar conditions systems in the fill-up stage are expected to show slightly higher slopes to systems still in the start-up stage (see for example Fig. 3 of Postma *et al.*, 2008 and Fig. 3.1).

The differences in slope variability observed in the fan-delta and alluvial-fan flume models neatly back up these expected differences in slope. The higher variability for the fan deltas is attributed to higher maximum slopes rather than lower minimum slopes. As reasoned in *Chapter 2*, the minimum slope, occurring during channelised flow, shows less variation in slope due to increased flow depths. In contrast, the maximum slope is affected more drastically due to the low flow depths present in the sheet flow. Hence, the increased slope variability is a manifestation of the higher maximum slopes on fan deltas, signalling that the deltas passed into the fill-up stage.

The higher slope variability on fan deltas generates much deeper autogenic incisions. Deeper incisions need more time to be filled by steady input, which explains the longer cycles occurring on fan deltas. The lower slope variability on alluvial fans excavates shallower incisions, needing less time to be filled, leading to smaller cycle lengths. On the fan deltas, the volume of the incisions increases due to lengthening and deepening of the incisions (*Chapter 2*). On the alluvial fans only lengthening of the incisions occurs. The fact that channelised-flow duration towards the end of Run A4 approximate cycle lengths of the fan delta can be assigned to the occurrence of re-incisions. Without them, the incisions would have been filled quicker and the cycles would have come up shorter.

Larger autogenic incisions produce more sediment to be redeposited downstream, and subsequently fan deltas generate larger bars then alluvial fans. Furthermore, the fan-delta bar is deposited at or close to the shoreline. The standing body of water decelerates the flows carrying the eroded material, leading to formation of a mouth bar as a pronounced feature in front of the incised channel. On the alluvial fan, less sediment is available for redeposition downstream of the incision, and the flows carrying the sediments are not decelerated by the presence of a standing body of water, and therefore produce elongated, less pronounced mid-channel bars. Sometimes the prominence of the mid-channel bar is decreased further by partial removal (Fig. 3.9). Topographic transects of a fan-delta bar can be found in *Chapter 2* and Figure 3.5.

In summary, different slope variability of fan deltas and alluvial fans is caused by different degree of development to equilibrium, and explains the differences in frequency and magnitude of the autogenic incisions, and the durations of the phases of channelised flow. Furthermore, representing the variability as a quantity normalised by average slope, we already rule out any discrepancies driven by discharge variations. The resulting quantity is independent on the input conditions (Q_s/Q_w), and enables comparison of runs with varying discharge, increasing the amount of appropriate data and the confidence for using it (*Kim et al*, 2006a).

3.3.5 Sediment bypass and channel activity

To further explore the analogy between the alluvial-fan and fan-delta experiments and the principles of infill of accumulation space derived by Postma *et al.* (2008), we will address sediment bypass and aggradation rates, which are both intimately related to the evolution of an alluvial system from its start-up stage to grade. During the start-up phase, no sediment is bypassed, so all of the supply is stored within the system by aggradation and progradation. Just after the fill-up stage is entered, much aggradation is accompanied by little sediment bypass. When equilibrium is approached, most of the sediment supplied to the system is bypassed and little is stored by aggradation (Fig. 3.1B). If the studied alluvial fans are still in the start-up stage and the studied
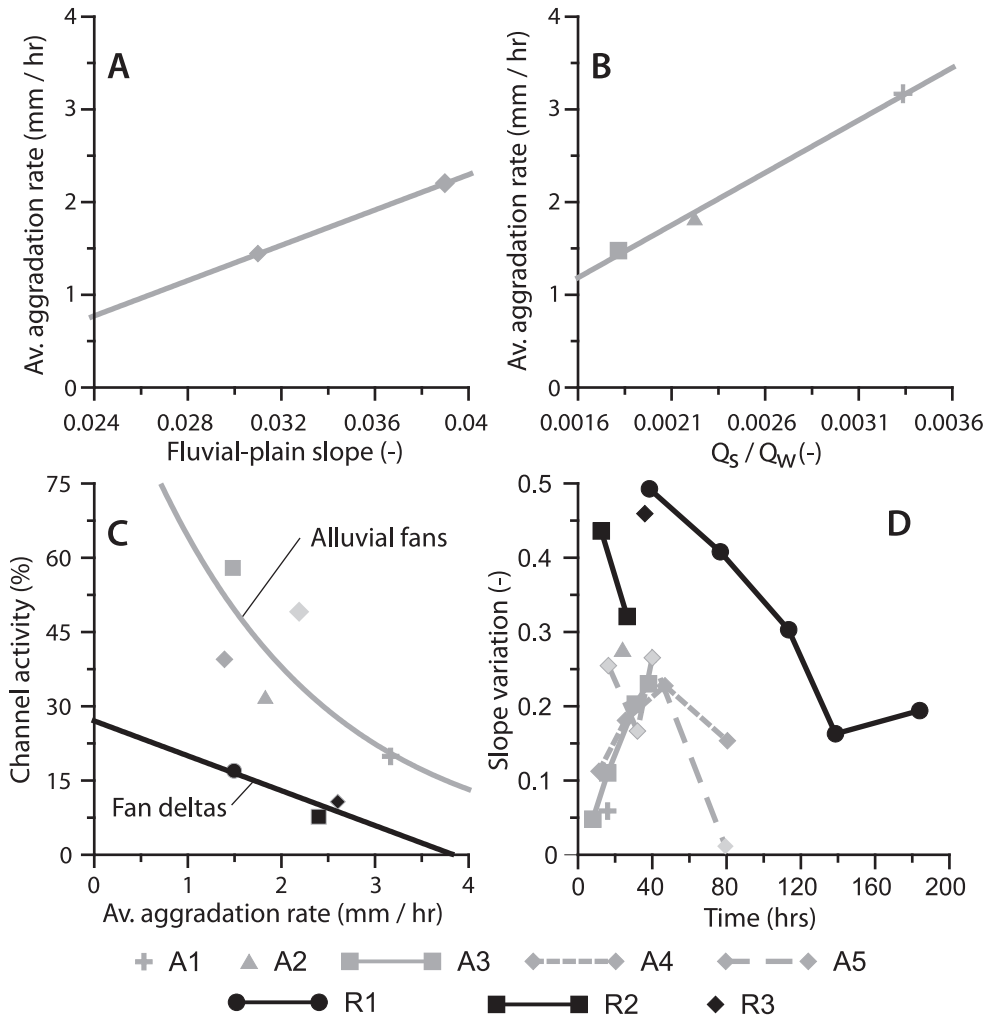
Figure 3.7 A) Impact of fluvial-plain slope on the aggradation rate (fit is a linear regression line), B) impact of discharge on aggradation rate (fit is a linear regression line), C) plot of channel activity versus aggradation rate, alluvial-fan fit is an exponential one, the delta fit is a linear regression line, and D) Slope variability of the runs through time, with the alluvial fans in grey and the fan deltas in black. Note the higher values for the fan deltas and the decreasing trends visible for both alluvial fans and fan deltas.

fan deltas already way up in the fill-up stage, how is that reflected in their evolution history? Figure 3.7D shows that under similar sediment input and discharge conditions, alluvial fans demonstrate significantly higher channel activity (higher incision frequency) than fan deltas. Thus the channel activity correlates positively with aggradation rate. Allowance needs to made for the 3D geometry of the fan, which also depends on the infill of the accumulation space. Since the system may have reached the infill stage along in the centreline, it flanks may still be in the start up stage. When all accumulation space eventually is filled, the amount of bypass will rapidly increase and the alluvial
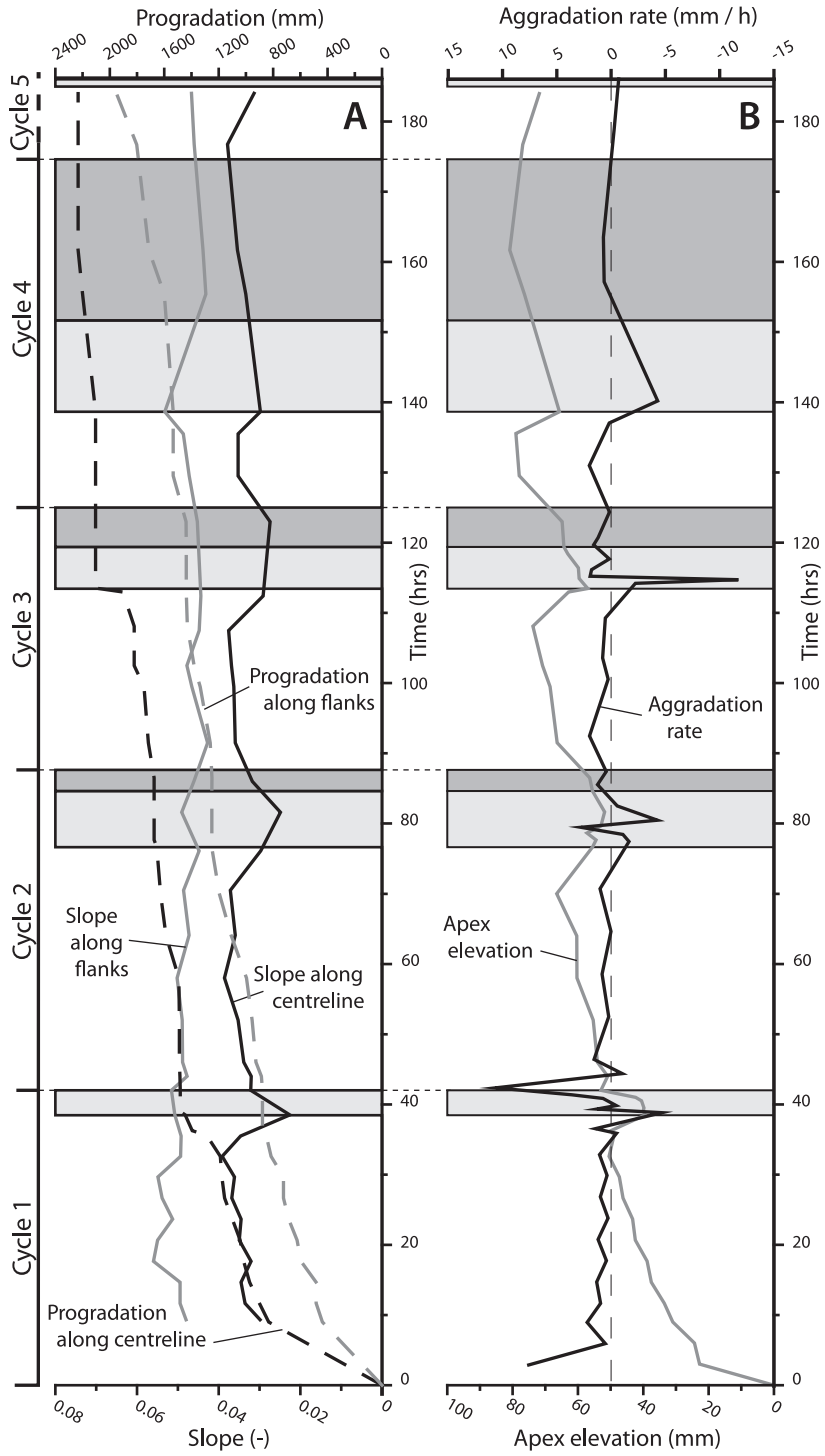
← *Figure 3.8* Schematic representation of the evolution of experiment R1. Labels are identical as those of Figure 3.4, except that the measurements along the flanks were directed perpendicular to the centreline instead of the smaller angle of experiment A4. The timescale (the x-axis) is identical to the alluvial-fan evolution shown in Figure 3.4. Note the impact of the progressively longer channelised events on the slope, apex elevation and aggradation rate, and the constant cycle length.
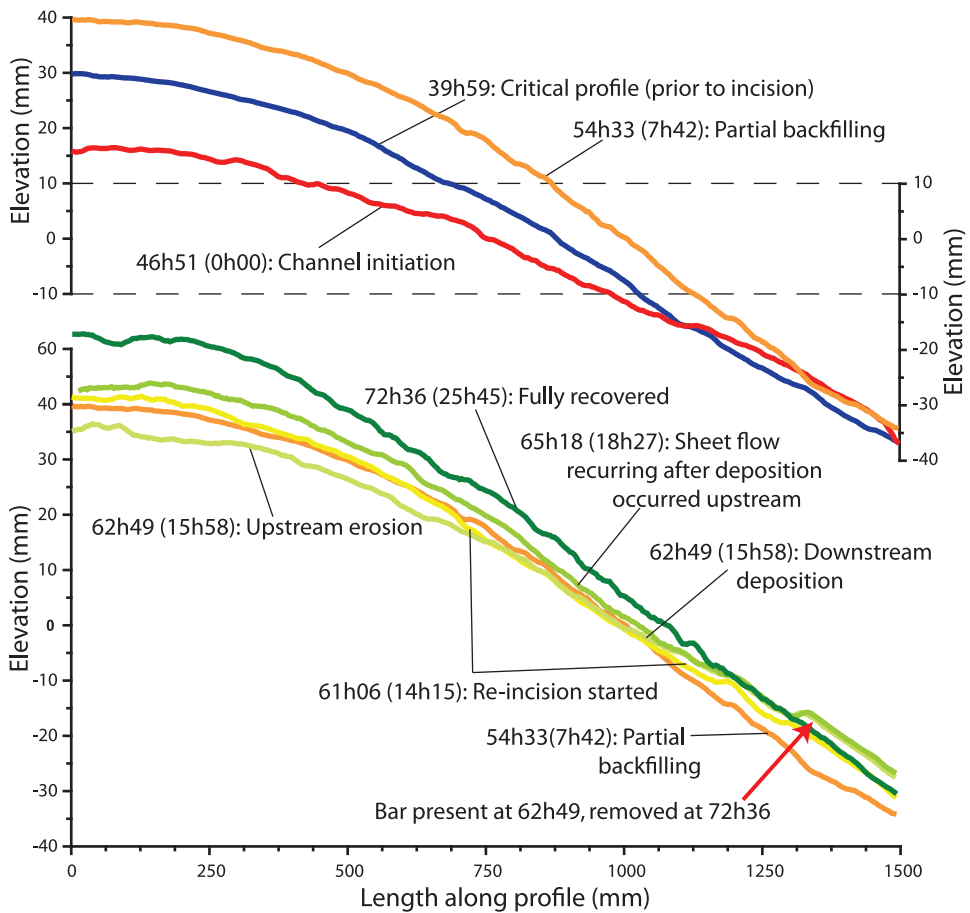
Figure 3.9 Diagram showing topographic transects along the centreline during the re-incision event of cycle 2 (run A4). Upper panel shows the profiles prior to incision of cycle 2; the lower panel shows the degradation caused by re-incision and development since 54h33. Note that the orange line (last profile prior to re-incision) linking the two panels. Note the relatively low bar formed at 62h49, which is eroded again at 72h36 (red arrow in lower panel). See text for more details.

fan will behave much more like the fan deltas: low channel activity, meaning infrequent incisions generating more accumulation space by progradation, in need of sediment to fill.

How is the sediment distributed to the available accumulation space on the alluvial fans? We have observed that the surface irregularities (lobes, channels and bars, Fig. 3.6) are likely causes to generate the re-incisions, so providing pathways (sediment routes) to the lower fan sections with unfilled accumulation space. Redistribution in the fan-delta models is described extensively by *Chapter 2*. Following autogenic incision and associated delta-lobe formation, bar formation in the incised channel leads to channel bifurcation. The two bifurcated channel branches form additional delta lobes, positioned on both flanks of the initial delta lobe. Delta-lobe formation shifts further away from the centreline of the fan delta (see Figure 2.3 of *Chapter 2*), until the entire shoreline had migrated outward and the entire fan-delta segment adjusted to the new base-level position.

3.4 Discussion

Now that the different development of alluvial fans and fan deltas have been explained conceptually by the different stages in which they reside, we will deal with the implications of these findings to natural alluvial fans and fan deltas. We will then follow up on that by estimating the preservation potential of the incisive events of the alluvial-fan models, finally, we will explore the effect of our results on stratigraphic models and assess the preservation potential of the autogenic evolution.

3.4.1 Implications of different infill-stages for alluvial fans and fan deltas

The different infill stages are responsible for characteristic architectural features such as depth of channel incisions and such as the vertical and lateral spacing of channels. Both have been argued above to be different for alluvial fans and fan deltas. So could these features tell us something about the stage of development of natural alluvial fan and fan delta systems? A large portion of natural alluvial fans seem to be entrenched, which is often attributed to Holocene climate change. The stratigraphy of an alluvial fan evolving through start-up stage will show an increase in the domination of incised channel fills. The dominancy might even be used as a tool to infer the extent of development towards fill-up stage.

Hooke and Rohrer (1979) show how the slope of alluvial fans varies from flank to centreline in experiments and field examples. These variations are attributed to the composition of the surface material (cohesiveness) and the importance of peak flood discharge. Alluvial fans with cohesive surface material will promote redistribution of sediment over the fan surface due to higher curvatures of the flows. Non-cohesive surface material will tend to flow down the centreline. If peak discharge is considerably larger than the average discharge, the variation in slope between the flanks and the centreline will be enhanced, as the higher discharges are less likely to go down the flanks. As the filling of alluvial-fan accumulation space part depends on distribution of water and sediment to the flanks of the fan, material cohesiveness and peak discharge directly affect the infill-stages.

3.4.2 Implications for models of alluvial stratigraphy

Models of alluvial stratigraphy describe the architecture of channel belts within floodplain deposits (Bridge and Leeder, 1979; Alexander and Leeder, 1979; Mackey and Bridge, 1993; 1995 and other studies commonly referred to as the LAB models). In these models, the relation between avulsion frequency and sedimentation rate is fundamental for predicting the distribution of channel belts. Experiments on avulsions on alluvial fan show a strong correlation between avulsion frequency and sedimentation rate (Bryant *et al.*, 1995), but braided-river experiments show a weaker trend

(Ashworth *et al.*, 2004, 2007). We can explain the different avulsion frequencies by using our results. The alluvial fans modeled by Bryant *et al.* (1995) are similar to our alluvial fans in the sense that they are in the start-up stage; they are filling the available accommodation until they reached the imposed downstream boundary condition. In the braided-river models of Ashworth *et al.* (2004, 2007), sedimentation on the braid plain was imposed by raising the feeder channel relative to the braid plain accompanied by supplying enough sediment to fill the thus created accumulation space. As a result, the braided channels were constantly adapting to the renewing conditions. Still, the braid plain adapted rapidly enough to these to be able to transport sediment out of the system. Ashworth *et al.* (2004) report that between 62 and 72% of the supplied sediment was trapped in the aggrading braid plain, so up to 38% of the supply was bypassed and only 15% is attributed to suspended transport. These percentages are averages over runs lasting 28 to 208 hours, comprising 56 to 112 uplift events, so at the end of single uplift events, bypass must have been even larger. Using Postma *et al.*'s criteria, the braid plains are in a start-up state immediately following feeder-channel rise and aggrade quite far into the fill-up stage. Considering the different state in which the two systems reside, and taking our experimental results in consideration, it is hardly surprising that they show different avulsion frequencies. If a system evolves to equilibrium, sedimentation rates and avulsion frequency (channel activity) decrease and sediment bypass increases even without any externally imposed change in conditions change. Hence, it is wrong to assume constant avulsion frequencies or sedimentation rates during a fan system's development.

3.4.3 Preservation potential and scaling of autocyclic incisions

What is the stratigraphic signal of the autocyclic behaviour in the alluvial-fan runs? First we will discuss the presence of the deep scours on the alluvial-fan Runs. Then we will address the preservation potential of the autogenic processes as it is very relevant for extrapolating these events to the level of natural systems, and we will use our earlier findings to do some testable predictions on natural alluvial fans.

The deep scours that occurred locally during the alluvial-fan Runs are attributed to flow boundary conditions. Flow depth reached 5 mm at most during sheet- flow conditions and transitions from rough to smooth flow might have generated locally high erosive power leading to the deep scours. On natural fans that experience sheet flows these transitions play a marginal role, so that the role of the scour pools as seen here is in the experiments is probably insignificant. Other factors that influence the occurrence of the re-incisions, such as local shallow incisions, mid-channel bars and decreasing channel slopes in the migrating bifurcated channel branches are present in both the model and the real world and are comparable. The presence of the short-lived deep scours in the experiment likely shortened the periods in between the autogenic (re-)incisions somewhat as the presence of the scours quickened initiation of the incisions. Yet, their effect is constant in view of the constant input conditions.

Will the alluvial fans show the same architecture as fan deltas? *Chapter 2* shows that the autocyclic incisions on the fan deltas will extrapolate to at least metre-scale incised channels on natural fan deltas. The erosional surfaces generated by the incisions will be preserved in the stratigraphy of the fan deltas, and may easily be mistaken for e.g. climate-change signals. On alluvial fans, the thickness of backfill successions enveloped by the erosive boundaries of the autocyclic generated incisions is less compared to fan deltas, because the variation in slope ('slope variability') between incision and sheet flow stages is less for alluvial fans. In addition, the thickness of the backfill successions of the alluvial-fan runs shows a much larger range around the average value compared to the fan-delta runs. The pattern of erosional surfaces produced by fan deltas

is more uniform, a reflection of the relatively uniform frequency of incisional events on the fan deltas. The frequency of incision on the alluvial fans is much higher but not uniform, and have been related to the lower slope variability on alluvial fans (see Figs. 3.5, 3.7D and 3.8).

The significance of the autogenic incisions is assessed by comparing the depth of the incisions to the average depth of the channels on the surface formed by fractionated sheet flow processes.. In run A4 the surface-channel depth averaged 4 mm, while the incised channels eroded to 7, 5 and 12 mm in the first, second and third cycle respectively. As the maximum depth of the incisions is difficult to establish (see the discussion on minimum slope earlier on), these values may be even larger. As it is, the incised channels are roughly 2 times deeper than the surface channels. On natural alluvial fans, the autogenically driven incisions can be expected to be deeper relative to surface channels formed by sheet flow.

3.5 Conclusions

1. Autogenic behaviour of alluvial fans is observed from flume experiments to consist of alternations of sheet flow and channelised flow and is similar to the autogenic behaviour of fan delta (*as Chapter 2*).

2. Since initiation of autogenic incisions is shown to be identical for both the modelled alluvial fans and fan deltas being governed by a slope maximum that triggers headward erosion, it must reflect the strong control of upstream input conditions on this initiation of incision.

3. Alluvial fans show much lower slope variability than the modelled fan deltas. Hence, alluvial fans display shallower incised channels and less distinct bars downstream of the incisions than fan deltas. The shallower incisions and lower bars enable the alluvial fans to fill the incisions much quicker than fan deltas.

4. Differences in evolution of alluvial fan and fan deltas reflect the importance of their infill stage in the infilling of their available accumulation space: fan deltas are invariably in their fill-up stage, while alluvial fans as modelled here are in their start-up stage (terminology and concept from Postma *et al.*, 2008). As a result, the alluvial fans exhibit incisions of variable depth, whereas the influence of the downstream boundary condition (base level) leads to similar depths of the autocyclic incisions in fan deltas.

5. Different slope variability between fan deltas and alluvial fans is caused by different degree of development to equilibriumthe different infill stage they are in.It explains the differences in frequency and magnitude of the autogenic incisions, and the durations of the phases of channelised flow. Furthermore, representing the variability as a quantity normalised by average slope, we already rule out any discrepancies driven by discharge variations. The resulting quantity is independent on the input conditions (Q_s/Q_w), and enables comparison of runs with varying discharge, increasing the amount of appropriate data and the confidence for using it (Kim *et al.*, 2006).

6. Increasing aggradation rates correspond with decreasing channel activity. In other words, the autogenic activity of a system varies with aggradation rate.

3.6 Acknowledgements

3.7 Appendix

Figure 3.A1 Schematic representation of the autogenic evolution of the fan-delta runs R2 and R3. All labels and scales are identical to the Figures 4 and 8, except the right-hand y-axis of panel B.

Figure 3.A2 Schematic representation of the autogenic evolution of the alluvial-fan Run A1 and A2. All labels and scales are identical to the Figures 4 and 8, except the right-hand y-axis of panel B.
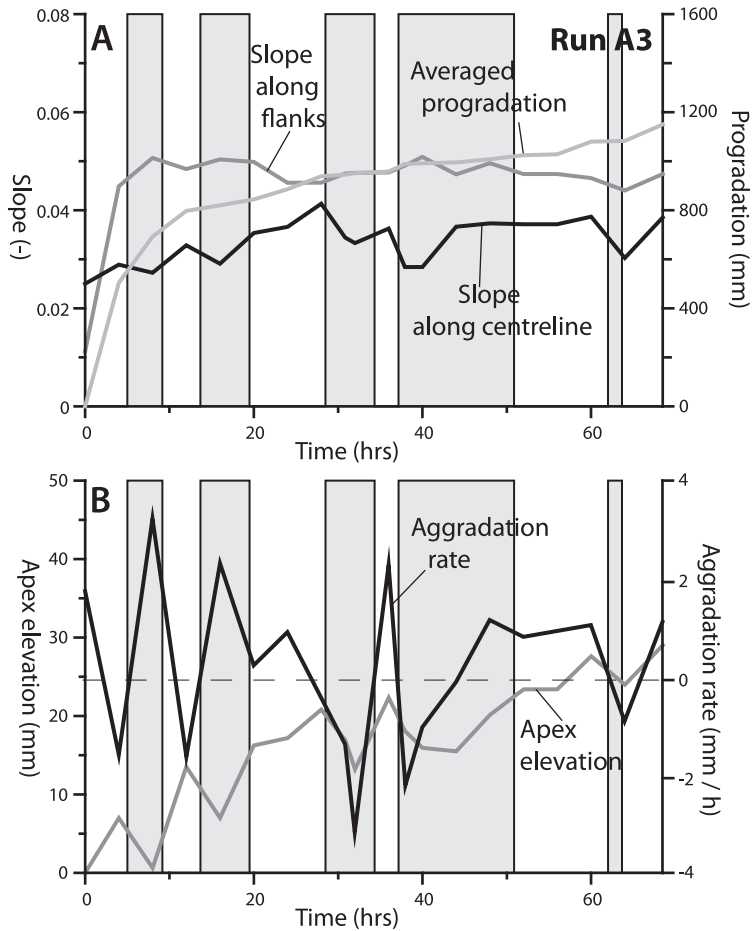
Figure 3.A3 Schematic representation of the autogenic evolution of the alluvial-fan Runs A3. All labels and scales are identical to the Figures 4 and 8, except the right-hand y-axis of panel B.

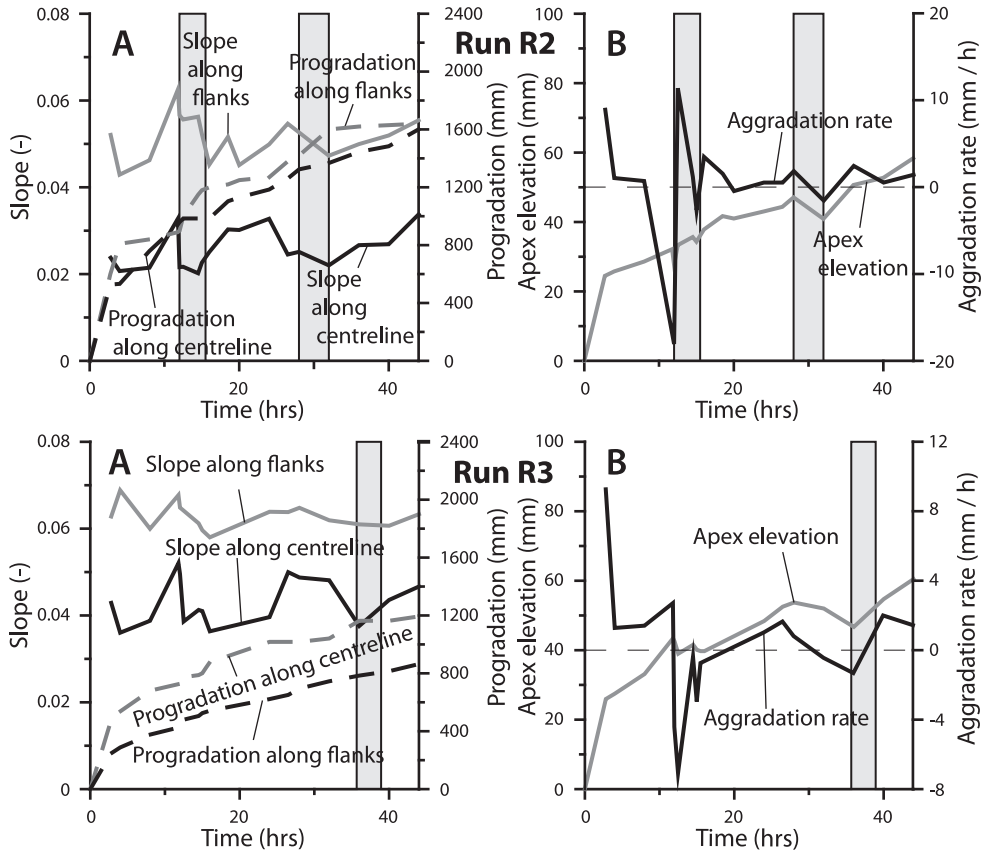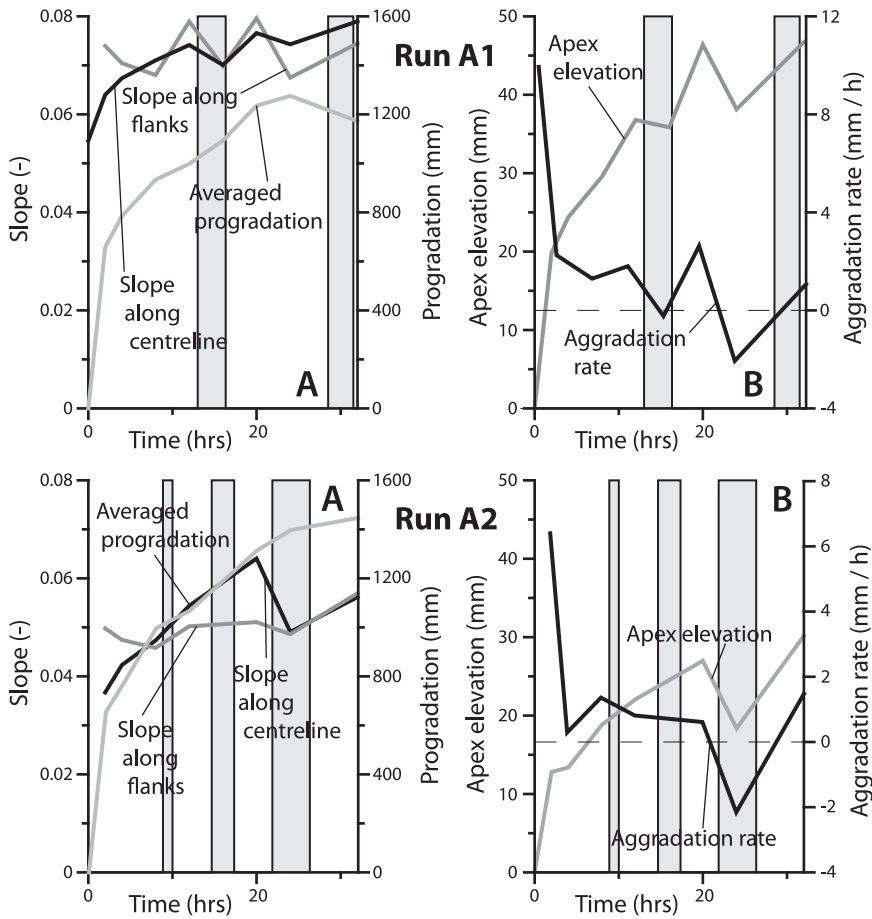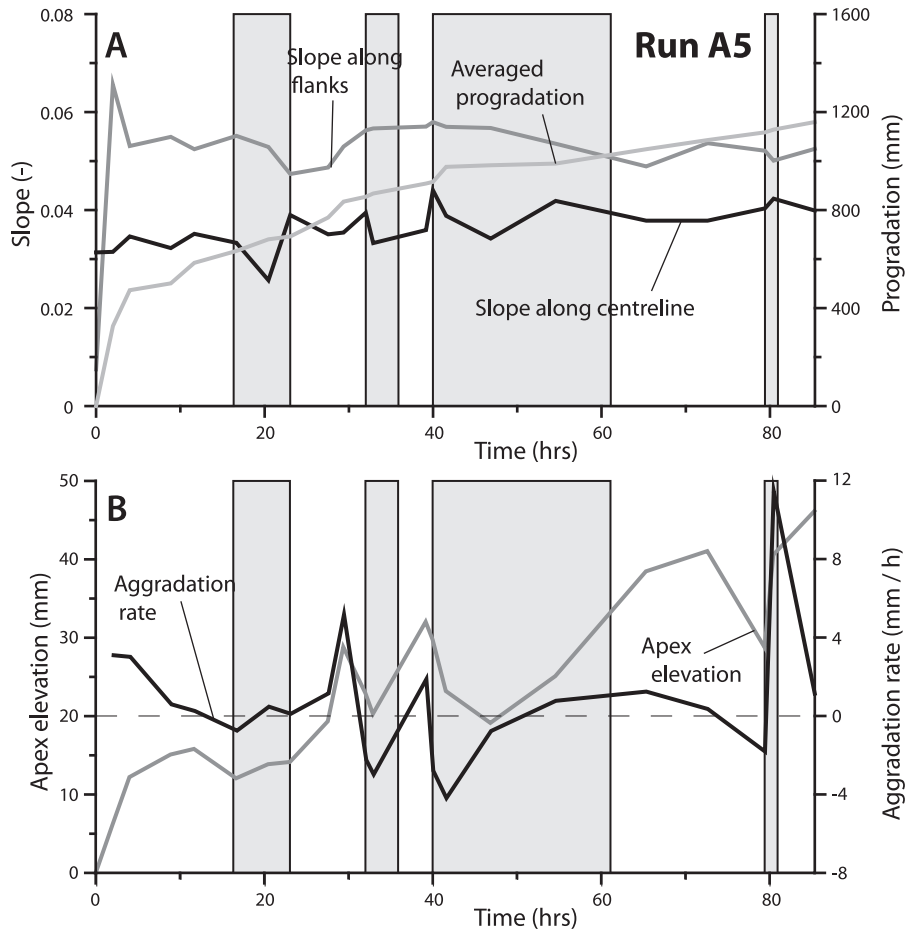*Figure 3.A4* Schematic representation of the autogenic evolution of the alluvial-fan Run A5. All labels and scales are identical to the Figures 4 and 8, except the right-hand y-axis of panel B.

Martian stepped-delta formation by rapid water release

Authors:

Erin R. Kraal, Maurits van Dijk, George Postma and Maarten G. Kleinhans

Abstract

Deltas and alluvial fans preserved on the surface of Mars provide an important record of surface water flow (Malin and Edgett, 2003; Moore and Howard, 2005; Williams *et al.*, 2006). Understanding how surface water flow could have produced the observed morphology is fundamental to understanding the history of water on Mars. To date, morphological studies have provided only minimum time estimates for the longevity of martian hydrologic events, which range from decades to millions of years (Moore *et al.*, 2003; Jerolmack *et al.*, 2004; Bhattacharya *et al.*, 2005; Irwin *et al.*, 2005). Here we use sand flume studies to show that the distinct morphology of martian stepped (terraced) deltas could only have originated from a single basin-filling event on a timescale of tens of years. Stepped deltas therefore provide a minimum and maximum constraint on the duration and magnitude of some surface flows on Mars. We estimate that the amount of water required to fill the basin and deposit the delta is comparable to the amount of water discharged by large terrestrial rivers, such as the Mississippi. The massive discharge, short timescale, and the associated short canyon lengths favour the hypothesis that stepped fans are terraced delta deposits draped over an alluvial fan and formed by water released suddenly from subsurface storage.

4.1 Introduction

Some martian fans have a distinctive 'stair step' topography (Fig. 4.1; Ori *et al.*, 2000; Irwin *et al.*, 2005; Di Achille *et al.*, 2006; Dobrea *et al.*, 2006) that might have formed by volcanic flows (Dobrea *et al.*, 2006), erosive wave action (Ori *et al.*, 2000; Weitz *et al.*, 2006), repeated alluvial fan deposition (Di Achille *et al.*, 2006), or mass wasting (Williams *et al.*, 2006).

In a permeable sediment flume, large, short-duration flows build fans draped with stepped delta deposits in a mock crater filling with water (Fig. 4.2). We use observed martian morphology combined with physical modelling to constrain the maximum and minimum duration of the martian hydrologic events on the basis of sediment transport.

To scale sediment mobility, we use the carrying capacity of the water flow (discharge and depth, Hunt *et al.*, 2006) to compare across the large spatial and temporal differences between Mars and a flume; maintaining similar Shields particle mobility number and a Froude number close to unity (Peakall *et al.*, 1996) ensures a similarity of process during the formation of the large-scale morphological features.
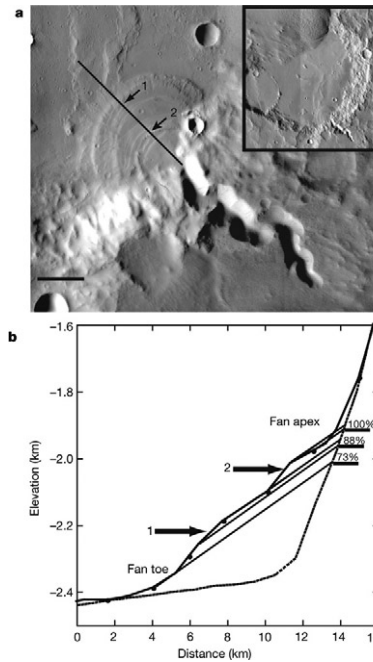
Figure 4.1 Example of a stepped delta in a martian crater at 8 S, 200 E. A, Mosaic of Thermal Emission Imaging System (THEMIS) images (resolution 18 m per pixel). Scale bar, 2.5 km. Arrows indicate the two most distinct steps of the terraces; solid line shows the transect modelled in B. First-order channel is 20 km with no developed drainage network. Inset, regional setting. B, Topographic results. Solid line, slope of delta; dashed line, average rim slope (from three profiles). Arrows indicate steps 1 and 2. The volume of the fan through time (as 73%, 88% and 100%) is estimated from the alluvial surface covered by the lobe deposits.

4.2 Methods

The experiments were performed in the Eurotank at Utrecht University, a 6 m x 11 m flume filled with sand to a depth of ~1 m. The water table in the flume is controlled using a series of inflow/outflow pumps and overflow valves. Sediment discharge is controlled using a precise worm screw sediment feeder (variations of less than 1% over 15 min). Water is discharged through a calibrated pump system. The sediment and water mix together before entry in the feeder channel (4.5 cm wide x 1.5 m long). Sand in the flume has a median grain size of 270 μm with a range of 40-500 μm; the grey and white sand used to enhance visualization of features have nearly identical grain sizes to each other.

A mock crater measuring 2.1 m x 1.6 m x 0.1 m was constructed on a 2.7 m x 5 m sand covered surface sloping 0.03 (Fig. 4.2). The crater wall was partially lined with plastic on the down-slope side to encourage the water to pond on experimental timescales. An initial shallow and small relief channel (1.5 m x ~0.02 m) routed the water flow into the crater at the start of the experiment. Water (400 l h^{-1}) and sediment (2.5 l h^{-1}) were constantly discharged into the feeder channel. The sediment constantly discharged into the feeder did not reach the fan and served only to prevent

scouring as the water transitioned from the feeder channel to the experimental set-up. However, the natural processes of infiltration, canyon widening, and incision drove fan formation. The initial regional water table (within the flume) was just below the bottom of the crater floor.

We conducted three experimental runs in the same experimental set-up with the same driving conditions. All of the experiments formed stepped morphology by the processes described above. The only differences were due to small variations in the height of the regional water (causing relatively more or less infiltration). Following the experimental runs, the regional water table was dropped and the water drained by seepage.

Digital Terrain Models (DTMs) of the surface are made using four stereo pair photographs on a 15 cm x 15 cm grid of the surface taken from an automated platform suspended above the flume. Vertical accuracy of the photogrammetry of the system is better than 250 μm (horizontal) and 100 μm (vertical). All stereo photography was completed from a dry surface to minimize reflections and errors. DTMs were calculated using SandPhox software and processed in the commercial program Surfer. The DTMs required minimal processing (approximately 1 in 1,000 points was in error due to reflection from the surface and, therefore, removed from the data sets). In addition, constant video photography (see Appendix) as well as still photography recorded the processes.
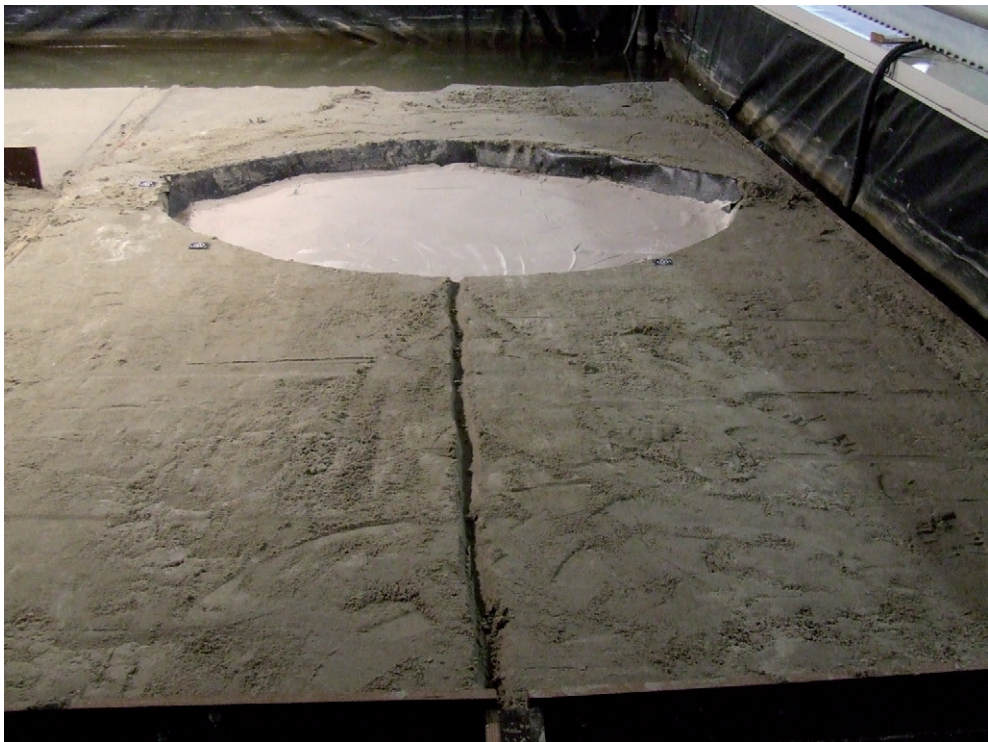
Figure 4.2 The initial set up of the Eurotank used in the formation of stepped fans. Water and sediment input is at the top of the channel and followed the molded channel, depositing a fan into the pre-existing crater. Crater is 2.1 m x 1.6 m x 0.1m.

4.3 Results and discussion

The experimental stepped deltas are produced in 24 min in three separate stages that depend on rising water level and on fluctuating discharge of sediment and water, despite constant experimental conditions (Fig. 4.3). As can be seen in the movie (see Appendix), initially water infiltrated into the channel walls and surrounding sediment, saturating the sediment and raising the local water table.

Water within the crater itself also infiltrated, but after 8 min the infiltration rate decreased below the inflow rate and the crater began to fill. Initial erosion of the steep crater lip by small, high-concentration, debris-like flows formed a cone-shaped alluvial fan (Fig. 4.3d). As canyon slope decreased, subaerial sheet-flows (Blair and McPerson, 1994a) buried the initial fan under a broader fan that contained the bulk of the sediment volume (Fig. 4.3e). Sedimentation changed to deltaic deposition only when a decrease in infiltration resulted in a rise of the water table above the crater floor (Fig. 4.3c, at 8 min). As the basin filled, infiltration significantly decreased and water discharge became steady, even though the sediment discharge feeding the fan varied according the channel processes, and experienced large fluctuations. The movie shows channel migration, bank erosion, and upstream knickpoint migration, all of which contributed to large pulses in sediment discharge. Thus, distinctive topographic steps formed at the intersection of the shoreline and the fan apron, similar to other experiments (Muto and Steel, 2001).

These experiments and two other aspects of the martian fan morphology tightly constrain the formation of stepped topography. First, the delta apex is not incised, so the feeder canyon must have ceased supplying water before the basin began draining. Second, sedimentation must have ceased rapidly to prevent long-term deposition from prograding over the stepped topography. Thus the unique driving conditions (single event, no long-term deposition), combined with morphological analysis and sediment transport modelling, permit calculation of the formation time for the martian fan (Fig. 4.1), which is the ratio of water (or sediment) volume to the transport rate.
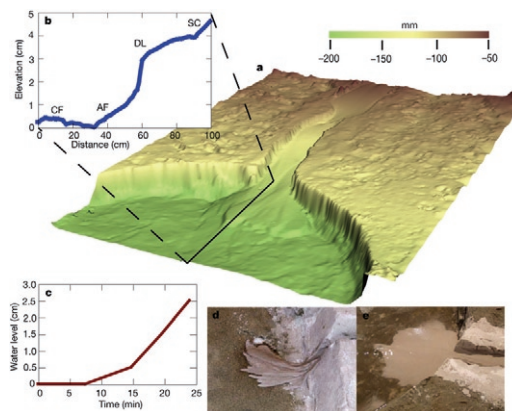
Figure 4.3 Experimental delta deposited into a crater. The colour-coded digital terrain model (a; colour bar shows mm below measuring surface) and fan profile (b) clearly show the transition from the crater floor (CF) into an alluvial fan (AF) with a prominent delta lobe (DL) transitioning to the feeding stream canyon (SC). High infiltration rates caused a slow rise in water level followed by an abrupt increase following local saturation (c). Initially, sediment was transported in concentrated flows (d) then, as stream power decreased, the fan transitioned to sheet flow deposition (e).

Using standard water discharge and bedload equations (Kleinhans, 2005), we estimate the martian and experimental sediment and water timescales by calculating the time to deposit the fan sediment or fill the basin with water. In the experiment, water discharge predicts a formation time of 12 min; sediment discharge predicts a formation time of 118 min. The experimental formation time was 24 min; therefore, the discharge estimate is 50% less than the actual time – a reflection of unaccounted infiltration losses. The bedload transport estimate overpredicts the timescale by 5 times – a reflection of the importance of *en masse* sediment transport observed early in the experiment. Indeed, in sheet flows on steep, terrestrial fans, it is observed that much of the coarse sediment is suspended in dense, *en masse*-moving slurries (Blair and McPerson, 1994b; Pierson and Scott, 1985), which decrease the net transport time significantly.

We estimate the minimum amount of water required to fill the martian crater at 6.4×10^3 km^3, based on an assumed radius of 64 km given erosion of the northern rim. We use minimum and maximum estimates for channel width, depth and slope, because discharge equations are most sensitive to channel dimensions, which are uncertain for Mars. For the maximum flow estimate (minimum time), we assume the current canyon is nearly full (1,200 m wide by 60 m deep) and the current canyon slope (0.044). The maximum assumed water discharge is 8.1×10^5 m^3 a^{-1}, 5 times the discharge of the Amazon River (1.5×10^5 m^3 s^{-1}, Milliman and Syvitski, 1992). Assuming this high, constant flow was responsible for filling the basin and depositing the delta, the formation time ranges from 0.2 yr from water discharge and 1.0 yr from sediment discharge (Table 4.1).

For the minimum flow estimate (maximum time), we assume a smaller active channel in the canyon; we take values in agreement with gravel-transporting rivers on Earth (for example, the Wairoa and Rakaia rivers in New Zealand, Milliman and Syvitski, 1992) and estimate the channel dimensions to be 100 m wide by 5 m deep. The consequent water discharge of 2.2×10^3 m^3 s^{-1} corresponds to a delta formation timescale of ~90 yr (equations used for the calculations and scaling are written down in the Appendix), as estimated from both water and sediment volume (Table 4.1). Smaller water discharges (up to the point that transport halts) have correspondingly longer timescales, and cause an unrealistic mismatch between water and sediment transport rates.

We can develop a depositional history for the delta body (Table 4.1, Figs 4.1b, 4.4) because the steps record distinct moments when the shoreline and sediment transport intersect and the surfaces of the experimental stepped terraces have the same slope as the original, underlying alluvial fan (Fig. 4.3b). The volume of the delta segments (Fig. 4.1b) lies above the relict depositional surface

Table 4.1 Estimated feature formation times

	Feature formation time (yr)	
	Maximum	Minimum
Sediment: deposit fan	90	1.0
Sediment: erode canyon	130	1.4
Water: fill basin	93	0.20
Alluvial fan: sediment	66	0.74
Alluvial fan: water	18	0.04
Step 1:sediment	14	0.16
Step 1: water	39	0.08
Step 2: sediment	10	0.11
Step 2: water	54	0.11
Data are for stepped fan sections.		

produced by projecting the alluvial fan slope headward (Fig. 4.1b). In the martian example, we use the average slope deduced from the entire population of large martian alluvial fans (0.04, Moore and Howard, 2005) because the surface area is too small for accurate slope measurements from spacecraft data. In the experimental case, we use direct measurements of the exposed alluvial surface. We assume fan thickness to be approximately uniform along any cross-section from the apex to the toe. Given the challenges of calculating the three-dimensional volume of an alluvial fan (Nanninga and Wasson, 1985) and the uncertainty of the pre-existing topography (in the martian case), the fan is approximated in only two dimensions. In both the martian and the experimental cases, most of the sediment was deposited before the intersection of the water level and fan apron. In the martian case, 73% of the sediment volume of the stepped delta body was deposited before step formation while the remainder was deposited in lobes as the shoreline prograded up the apron (Figs 4.1b, 4.4). This parallels the experimental deltas where the small sediment volume deposited during terrace formation dominates the morphology (Figs 4.3, 4.4).

For the martian maximum discharge estimate, the time required to deposit the alluvial fan segment (0.74 yr) is 19 times longer than the time required to fill the basin with water to that elevation (0.04 yr). This agrees with our experimental observation – the assumption of bedload transport in the sediment discharge calculation is not appropriate early in the depositional history of the stepped delta when high-concentration mass flows are likely. However, bedload transport is a good assumption during step deposition where the sediment discharge timescale (0.1 yr, step 2) agrees with the water discharge timescale (0.1 yr, step 2). (Steps 1 and 2 are shown in Fig. 4.1.) Assuming the low-discharge (maximum time) case, the sediment discharge timescale for alluvial fan formation (66 yr) is also higher than the water discharge timescale of formation (18 yr) but only by 4 times (Table 4.1). Whereas the timescales for the formation of the total delta by bedload transport begin to merge at lower water discharge values, the timescales for deposition of the terraces become unrealistically long: for instance, for step 2, the estimate is ~19 yr (sediment) and ~53 yr (water). This implies that there would be some 30 yr of sediment starved flow where the water would entrain bedload causing incision into the sediments, which is not observed.
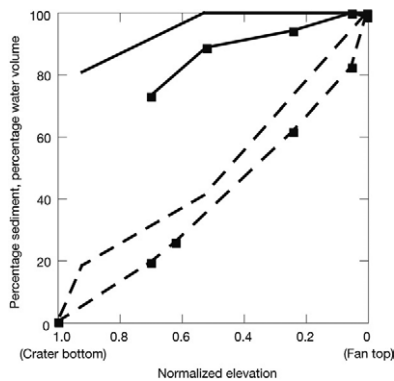
Figure 4.4 The depositional history for experimental and martian stepped fans. The normalised elevation of the delta in the crater is plotted against the percentage of water (solid lines) and sediment (dashed lines) for the martian example (filled squares; *Fig. 4.1*) and the experimental (no symbols) fans. In both cases, the majority of the sediment was deposited before the intersection of the water and the fan apron, and the sediment volume contained in the lobes is minimal compared to that of the alluvial fan.

One could argue that the discharge had been shut down and restarted after some time. But leakage through the crater floor would then cause a fall of the water level and subsequent incision, channelization and related delta lobe formation Van Heijst *et al.*, 2001). Although shallow incisions may not be visible in current imagery, the much larger size of protruding, 'telescoping' delta lobes that would form at the outlet of incised channels would be easily detected on the available imagery. Any undetected and, thus, relatively small incisions would not significantly change the formation time we calculate here. Similarly, healing of former larger channel incisions during a fall-rise cycle is, in theory, possible, but should also be detectable on the basis of the delta lobes on the terraces. In a completely sealed basin with no atmospheric loss, it would be possible to cease water flow, pause sediment deposition, and restart flow without changing the stepped morphology as we describe above. Determining the rate of water loss is virtually impossible; permeability of the martian soil is unknown but is probably very high, especially in highly fractured impact basins (Melosh, 1996; Sears and Chittenden, 2005). Evaporation rates vary from 33 m yr^{-1} to 0.16 m yr^{-1}, depending on temperature, air pressure and wind speed (Hecht, 2002; Sears and Chittenden, 2005), all of which are unknown for the time the delta formed. We know experimentally that the stepped morphology requires that the water level never dropped or stabilized for a significant period of time. Therefore, we assume a 50% discharge loss rate as an upper limit; this results in a total water loss per metre squared of $2{,}000 - 30$ m yr^{-1} to evaporation and infiltration combined. Under these conditions, the maximum formation time doubles but the ratios of sediment to water discharge remain reasonable, maintaining realistic sediment transport conditions and, therefore, the stepped morphology.

4.4 Conclusions

Stepped deltas formed during a single hydrologic event of short duration, and provide unique insight into a two-sided constraint on water discharge and formation time. The estimated water volumes and timescales indicate water discharges on a par with some of the largest terrestrial fluvial systems. For example, to fill the entire crater basin in Fig. 4.1 (6,500 km^3 of water) requires a decadal timescale with a discharge between that of the Rhine River (70 km^3 per decade; 93 yr filling timescale) and the Mississippi River (5,000 km^3 per decade; 13 yr filling timescale, Milliman and Syvitski, 1992). These discharge estimates must be reconciled with a martian canyon length hundreds of times smaller than comparable terrestrial rivers, as well as a lack of a developed drainage network. Thus, the stepped morphology and our modelling of a large, rapid, single event argue against surface precipitation and favour a hypothesis of release from subsurface water storage. These results must be integrated with other sedimentary bodies on Mars (especially fans that appear to have formed from surface precipitation) as well as with the interior processes required to store and release large quantities of water.

4.5 Acknowledgements

Autocyclic behaviour of an experimental flood-tidal delta

Abstract

Many tidal-inlet systems exhibit cyclical behaviour. In sedimentary systems such as alluvial fans and fan deltas cyclical processes may occur with constant boundary conditions, i.e., without variations of external controls. We performed an analogue experiment with steady boundary conditions to study the evolution of a flood-tidal delta, and to detect possible autogenic cyclical components. The setup consisted of a tidal inlet connecting a basin (lagoon) with 2 barrels generating bidirectional currents. In the lagoon a flood-tidal delta evolved, increased in size and height until emerging above the low-water level. Like in natural systems, the currents followed distinct flow paths. During ebb, the currents were restricted to two distinct channels, adjacent to the sand body and joined close to the tidal inlet. During flood, initially the channels were used, but towards high tide the sand body became submerged, and water and sediment covered the entire flood-tidal delta. Eventually channel migration started and showed a cyclical pattern, the morphodynamical changes occurring during rising tide. One of the two channels became dominant over the other and captured increasingly more discharge. The dominant channel widened and expanded towards the centre of the delta, and a new marginal bar formed. The channelised flow traversed an increasingly broader and more central part of the delta, increasing channel length because the length of the delta exceeds its width. The longer flow path restricted its efficiency, and the channel was ultimately filled and abandoned. Following the abandonment of the channel, the delta reverted to the initial state with two equally dominant channels. Three complete cycles were recorded, similar in duration. Cyclical processes in the experimental flood-tidal-delta thus may occur without variation of either the position of the inlet or other external boundary conditions. As processes on ebb- and flood-tidal deltas are intimately linked, internally generated cyclic processes on the flood-tidal delta may affect the entire tidal-inlet system.

Keywords

Tides, Tidal inlets, barrier islands, flood-tidal deltas, tidal channels, cyclic behaviour, autogenic behaviour

5.1 Introduction

Twelve percent of the world's present-day coastlines are characterised by tidal-inlet systems; barrier islands separated by tidal inlets. Flood- and ebb-tidal deltas form at the landward and seaward sides of tidal inlets, where tidal jets enter and leave the back-barrier basin and sands

A: Elements of tidal environments

	River deltas	Barrier islands	Tidal deltas	Linear sand ridges	Inlets	Tidal flats	Salt marshes	
6								macrotidal
4								
								mesotidal
2								
								microtidal
0								
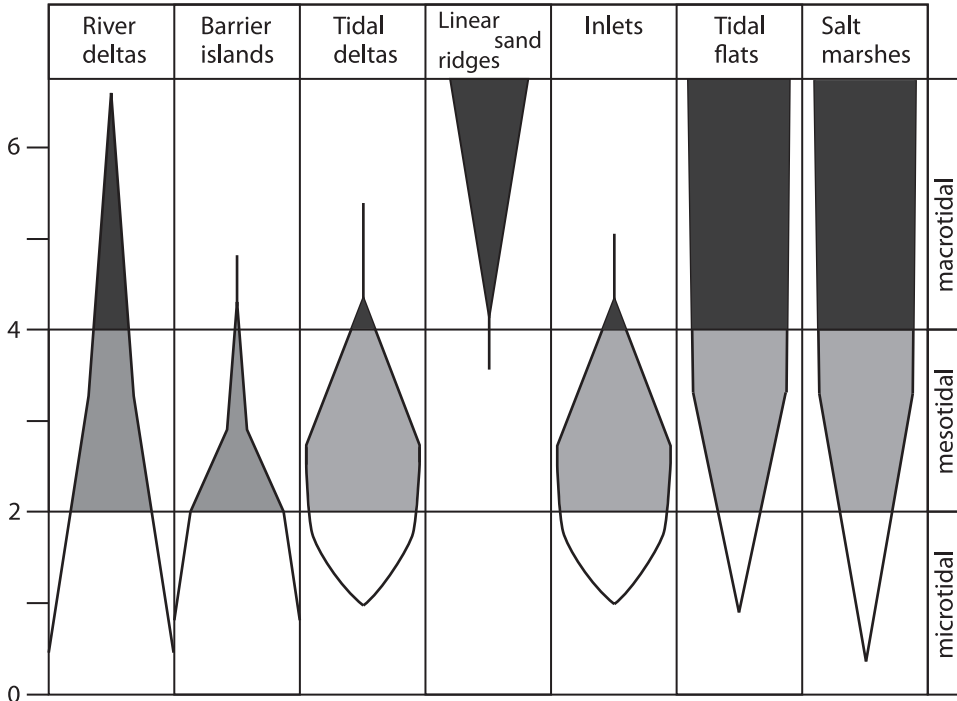
B: Elements of tidal inlet systems
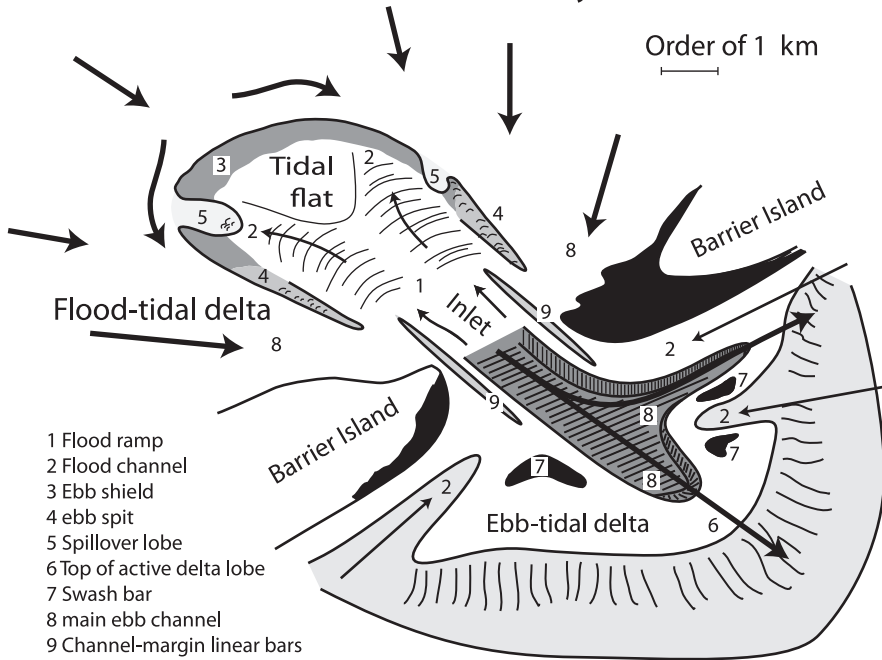
Order of 1 km

Tidal flat

Flood-tidal delta

Barrier Island

Inlet

Barrier Island

Ebb-tidal delta

1 Flood ramp
2 Flood channel
3 Ebb shield
4 ebb spit
5 Spillover lobe
6 Top of active delta lobe
7 Swash bar
8 main ebb channel
9 Channel-margin linear bars

are deposited in a delta-like fashion (Price, 1963). The ratio and interaction of tides and waves, expressed by (amongst others) tidal prism, tidal range and wave height and length, define the size and morphology of ebb-tidal deltas. In the back-barrier basin, waves are less important and the flood-tidal delta is principally defined by the tide, tidal prism, availability of sand and the back-barrier morphology and bathymetry.

Based on studies of North-American tidal systems, Hayes (1980) gave a general characterisation of tidal-inlet systems, and distinguished the tidal inlet, ebb-tidal delta, flood-tidal delta, and barrier island as the principal morphological elements. Figure 5.1A shows the significance of these elements with varying tidal range. Oost and de Boer (1994) showed that tidal prism is a better reflection of the tidal energy of a particular inlet, as the widely varying size of back-barrier basins also affects the amount of water passing an inlet. In the flood- and ebb-tidal deltas flanking the inlets, bars and channels are the most important components for transport and storage of sediments. Figure 5.1B shows the general morphology of flood- and ebb-tidal deltas.

Cyclical behaviour in tidal deltas has been observed at many places (Robinson, 1975; Oertel, 1977; Hanisch, 1981; Nummedal and Penland, 1981; Fitzgerald *et al.*, 1984; Sha, 1989a; Sha and De Boer, 1991; Oost and De Boer, 1994; Oost, 1995; Elias *et al.*, 2006; Elias and van der Spek, 2006). For instance, the ebb-tidal delta of Tybee Inlet (Georgia, USA) alternates between a stage with all discharge passing through a single large channel and a stage with numerous spill-over channels diverting part of the flood flow at the expense of the main channel (Oertel, 1977). These alternations occur at a frequency of a few years. Teignmouth Harbour Inlet in England shows a very similar cycle of roughly equal duration (Robinson, 1975). Pinkegat Inlet in the Dutch Wadden Sea alternates between a single and a multiple inlet-channel configuration, associated with clockwise channel rotation (Oost, 1994). Along the Dutch and German Wadden Sea the longshore current transports sand from west to east. While bypassing the inlets, sand is incorporated in the ebb-tidal delta swash bars (Hanisch, 1981; Elias et al., 2006; and references therein). Swash bars rotate along the perimeter of the ebb-tidal delta in conjunction with clockwise rotating tidal channels. Sand migrating along the ebb delta is temporarily stored in the bars. During migration of the tidal channel from the updrift to the downdrift side of the ebb-tidal delta, the channels show variable flow dominance. In the beginning when located adjacent to the updrift barrier island, they are flood-dominated. They change to ebb dominance when they are perpendicular to the coast, and revert to flood dominance when the channel approaches the downdrift barrier island (Sha, 1989a; Sha and De Boer, 1991; Hanisch, 1981, Nummedal and Penland, 1981, Fitzgerald *et al.*, 1984, Elias *et al.*, 2006).

Elias *et al.* (2003) stated that ebb-tidal-delta behaviour is (partly) governed by changes in the back barrier. When the back-barrier basin is filled, flood-tidal deltas can participate in the process of sediment bypassing, as Nummedal and Penland (1981) show for Norderney Inlet in the German part of the Wadden Sea. Part of the sand is transported into the back-barrier basin through flood-dominated channels, temporarily stored in the flood-tidal delta, and eroded and returned by ebb currents to the swash bars on the ebb-tidal delta. Hence, flood-tidal deltas within the back-barrier basin and ebb-tidal deltas on the seaward side of the inlet are intimately connected in their

morphodynamical behaviour. Changes in one of the two inevitably results in variations in the other (Oost and de Boer, 1994).

Migration of bars and channels on the ebb-tidal delta also affects barrier-island morphology. Attachment of ebb-tidal swash bars to the downdrift island contributes to the drumstick-morphology of the island (Fitzgerald *et al.*, 1984). The location of bar attachment is controlled by the size and orientation of the ebb-tidal delta.

Chapter 2 and *3* of this thesis address autogenic and autocyclic behaviour of alluvial fans and fan deltas. Here we test if autogenic processes can generate cyclicity in flood-tidal deltas. We focus on flood-tidal deltas as they are sheltered from wave action, which could disrupt or obliterate autogenic cyclical behaviour. Analogue experiments were conducted to study the formation of flood-tidal deltas and their evolution towards equilibrium, and to find out if such equilibrium configuration has cyclical components.

5.2 Experimental design

5.2.1 Setup and materials
The experiments were conducted in a flume capable of sustaining bidirectional flow (Fig. 5.2). The setup comprises a tidal inlet and a lagoon measuring 4 x 4 m. Bidirectional flow was produced by pumping and extracting water from Barrel 1 into Barrel 2 by two centrifugal pumps, thus producing variations in the water level in Barrel 2 (Fig. 5.2C). Highest water-level in Barrel 2 was 0.50 metre above the average water level in the lagoon, generating a pressure gradient between Barrel 2 and the lagoon so that water flowed into the lagoon. Minimum water level in Barrel 2 was 0.10 m below the lagoonal water level, reversing the gradient and directing the flow back into Barrel 2 (Fig. 5.2C). The pumps were switched on and off by water-level-sensitive sensors in Barrel 1.

The channel representing the inlet had a length of 80 cm, a width of 4 cm and an initial water depth of 20 cm at mean tide. The bottom of the channel was covered with sand which was quickly eroded by the ebb flow. The back-barrier basin initially had a flat bottom with the same water depth as the inlet channel at mean tide. It was covered with sand to give the back-barrier area a realistic bed roughness. The channel entered the back-barrier area in the middle of the flume. On both sides of the channel a board closed of the back-barrier basin, mimicking the effect of barrier islands in natural systems (Fig. 5.2). A sediment feeder with a cork screw (Fig. 5.2) was activated by the water-level-sensitive sensor in Barrel 1, and during the flood sediment was added to the flow with a precision of a few percent over an hour. The ebb flow was not strong enough to carry sediment back through the inlet.

The sand used as bed material was non-cohesive and unimodal with a median grain size of 250 μm giving the bed a realistically rough and erodable surface. The material (glass beads) fed initially to the inward-directed flow (flood) had a median grain size of 70 μm (Fig. 5.3) and was supplied at a constant rate. After 194 hours in the experiment natural quartz sand was used with a median grain size of 105 μm and a wider distribution (Fig. 5.3). The only observed effect was that the coarser sand created a slightly steeper avalanche slope, while the morphology and behaviour of the sand body did not change.

5.2.2 Measurements
The entire experiment was monitored by a camera positioned above the delta, attached to the ceiling 2 m above the high-water level and 50 cm seaward of the inlet. A birds-eye lens enabled
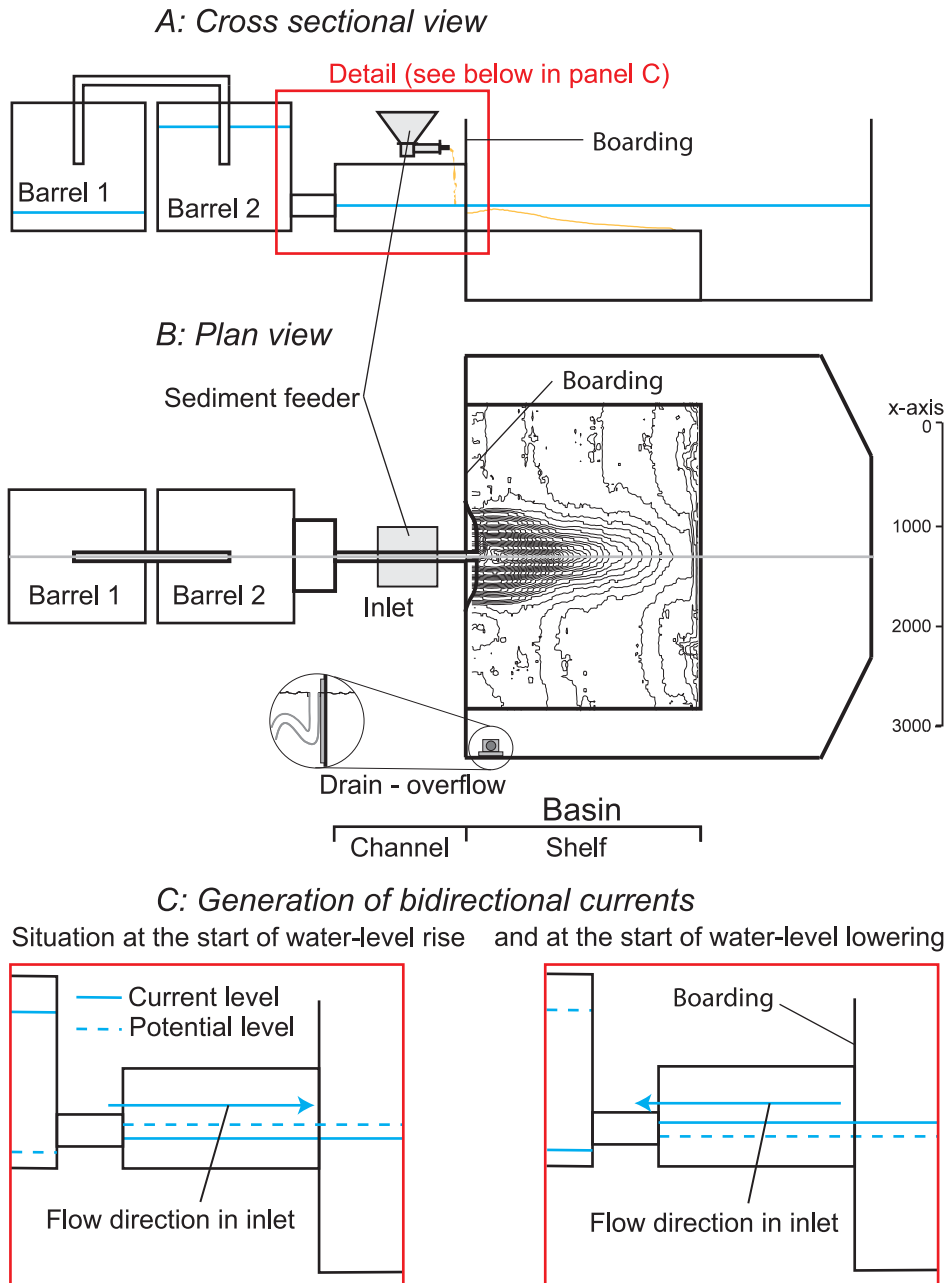
Figure 5.2 Schematic illustration of the experimental setup used in the experiment in: A) cross-sectional view, B) plan view. C) close-up of the inlet showing the situation at the start of rising and falling water level. The lagoonal (back-barrier) area measured 3 by 2.5 m.
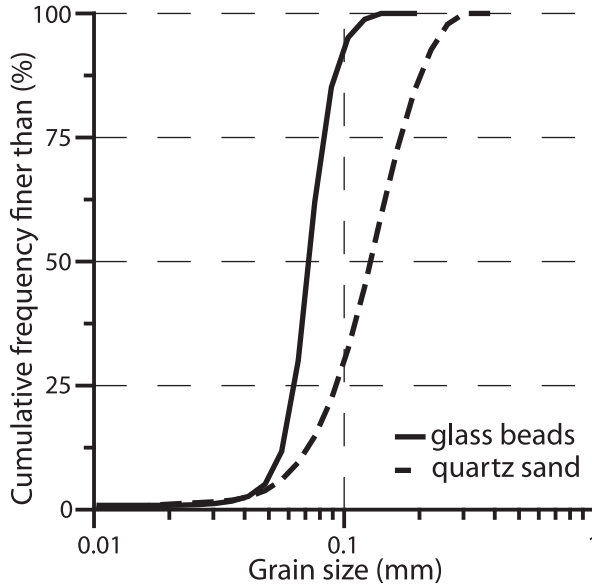
Figure 5.3 Cumulative grain-size distribution of the two types of sediment supplied to the system.

a detailed view of the central part of the delta where the principal processes occurred, while the less active perimeter of the system was monitored in less detail. In addition, the morphology of the tidal delta was measured with high resolution using a Dynavision™ SPR-2 laser with an accuracy of 0.4 mm in the x, y and z directions. The laser was mounted on an automated x-y positioning system, and made measurements overnight when the experiment was interrupted. For that purpose, water was drained slowly and carefully from the tank. After drainage, the surface was measured twice. A grid with a spacing of 2 cm was used to measure the flood-tidal delta (2.2 m wide and 1.9 m long; Fig. 5.2), followed by a measurement with a detailed grid spacing of 0.5 cm covering an area of 1 by 1 m in the back-barrier basin just behind the inlet. The laser did not reach the 5 cm next to the inlet channel.

5.2.3 Scaling of the experiment
The setup of our experiment was inspired by the Marsdiep Inlet (Fig. 5.4), located between the Dutch mainland and the island of Texel (e.g. Sha, 1989a, 1989b, 1990; Elias *et al.*, 2006), one of the inlet systems with cyclical patterns in the ebb-tidal delta behaviour described above. This inlet has a width of roughly 2.5 km, a depth up to 53 m, and it is 5 km long. It is east-west orientated, perpendicular to the south-north directed longshore tidal current. These longshore tidal currents result from the tidal wave, which in the North Sea rotates around two amphidromic points (Reineck, 1982). Near the Marsdiep Inlet, the flood wave moves from the southwest to the northeast, and the ebb wave moves into the opposite direction (Sha, 1989a). Due to tidal asymmetry, the flood currents are slightly stronger, so net sediment transport is towards the northeast (Van Straaten, 1961; Postma, 1982). The effect of the flood dominance is enhanced by the prevailing incoming waves, which most of the time come from the southwest (Sha, 1989a). The tidal range averages 1.4 m and approaches 2 m during spring tide. Tidal velocities in the inlet are between 1 and 2 m s^{-1}. Due to the large back-barrier basin, the tidal prism of the Marsdiep Inlet

is significantly larger than in other tidal inlets with a similar tidal range (Oost and de Boer, 1994). The main ebb channel of the flood-tidal delta, Texelstroom, rotated anticlockwise between 1933 and 1997 following closure of part of the back-barrier basin in 1932, the resulting increase of tidal amplitude in the back-barrier basin and the consequent increased tidal prism (Elias *et al.*, 2003).

We mimicked Marsdiep Inlet morphology in our setup, and aimed at comparable sediment mobility during the tidal flow. The initial and ultimate model characteristics and the equivalent values of the Marsdiep Inlet are shown in Table 5.1. To compare the hydrodynamic conditions of the 2 systems, we calculated Froude numbers (*Fr*), Reynolds numbers (*Re*) and Shields sediment mobility (θ) of the flow in the model and the prototype (Table 5.1, equations in Appendix). Froude number in the model is higher than in the prototype, but the model inlet had a considerably lower width-depth ratio than the Marsdiep Inlet; a higher width-depth ratio would have led to lower Froude number as the larger wetted perimeter of the inlet would produce more friction. Reynolds numbers are much lower in the model, but still above $Re = 2000$, ensuring that the flow was fully turbulent (Peakall *et al.*, 1996), in agreement with the situation in the Marsdiep Inlet. The Shields sediment mobility θ of the model shows fair agreement with the values in the Marsdiep inlet, especially during neap tide.

Other dimensionless parameters are used to compare the hydraulics between the model and the Marsdiep Inlet; the Rouse number, and the ratio between two depositional parameters γ/σ (Table 5.1, equations in Appendix). The Rouse number is the ratio between the settling velocity ω_s (calculated by the criterion derived by (Soulsby, 1997) and the depth-averaged velocity, here approximated by the flow velocity. The calculated Rouse numbers are all around 0.02, confirming that bed-load transport dominated the experiment. The value of $1/\gamma$ equals the ratio of the settling velocity ω_s and the flow depth h, giving an estimate of the time scale a particle needs to settle
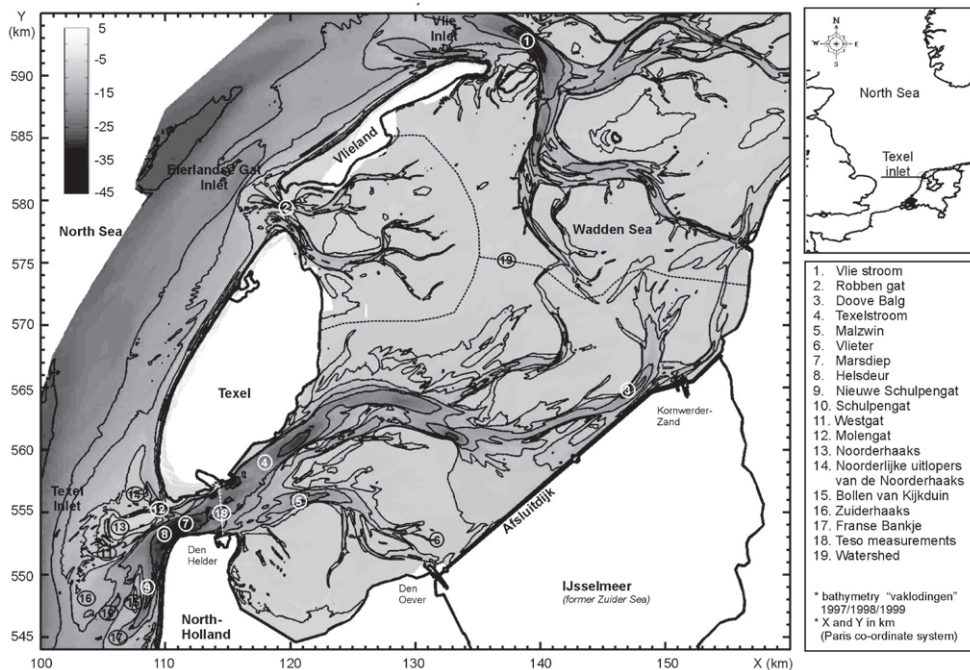

Figure 5.4 Marsdiep Inlet, modified after Elias et al. (2006).

Table 5.1 Hydraulic, physical and non-dimensional parameters for the model and the Marsdiep Inlet. For an explanation of the symbols, see the Appendix.

	Marsdiep		Experiment		
	Low tide	High tide	Before vel. set	After vel. set	Ch. grain size
D_{50} (m)	0.0002	0.0002	0.00007	0.00007	0.00014
Velocity (m/s)	1	2	0.25	0.15	0.15
ω_s (m/s)	0.023	0.023	0.0033	0.0033	0.13
Fl. Depth (m)	50	50	0.2	0.2	0.2
Fr (-)	0.05	0.09	0.18	0.11	0.11
Width (m)	2500	2500	0.04	0.04	0.04
W/D ratio (-)	50	50	0.2	0.2	0.2
Re (-)	$4.8 * 10^7$	$9.6 * 10^7$	$4.5 * 10^3$	$2.7 * 10^3$	$2.7 * 10^3$
C″ (m s$^{0.5}$)	109.4	109.4	74.5	74.5	69.0
θ (-)	0.253	2.56	0.247	0.0890	0.518
Ro (-)	0.023	0.012	0.013	0.022	0.083
γ (s^{-1})	0.00046	0.00046	0.017	0.017	0.063
σ (s^{-1})	$7.7 * 10^{-7}$	$7.7 * 10^{-7}$	0.0011	0.00087	0.00087
σ/γ (-)	0.0017	0.0017	0.067	0.052	0.014

to the channel bottom. The value of σ equals 1/tidal period. The dimensionless parameter σ/γ then expresses whether or not particles can settle over the duration of a tidal period, giving an indication of the tidal energy in the system. Table 5.1 shows that the values of σ/γ of the model and the Marsdiep Inlet agree within an order of magnitude, which is sufficiently close for this study. These values also agree with those used in a numerical model by van Leeuwen (2002) for a similar inlet of the Dutch Wadden Sea, the Frysian Inlet.

The sediment transport averaged over a tidal cycle in the experiment was aimed to be roughly comparable to the transported sediment over a full neap-spring tide cycle in the natural tidal system, justified by the comparable Shields sediment mobility as showed above. One tidal cycle in the experiment corresponds to one neap-spring tidal cycle covering 15 days. The duration of the tidal cycle in the experiment initially was 1150 seconds (19 min, 10 s), with a tidal range of 2 cm. Every 'neap-spring cycle', 0.2 litre of sediment (70 μm glass beads in the beginning, 105 μm in the end) was added to the flow in the tidal inlet. The inlet width measured 4 cm, leading to initial flow velocities up to 27 cm s^{-1} at the imposed discharge (see also Fig. 5.5). By trial and error we altered the flow velocity in the inlet to avoid the sediment being carried too far into the lagoon.

In the experiment, 0.2 l of sediment was added during every 'neap-spring tidal cycle' (see also Table 5.2). During the experiment, the supply of sediment was altered twice, first after 88 hours and later at 233 hours. The changed supply is expressed as the different 'factor' (Table 5.2). This 'factor' is the correlation between the sediment added during a tidal cycle in the experiment and the amount of time in the model prototype (Marsdiep Inlet). As the volumes were used to scale time, increased sediment supply in the experimental cycles enlarged the time represented by an individual cycle. At 88 hours the supply was tripled, similarly tripling the amount of time covered
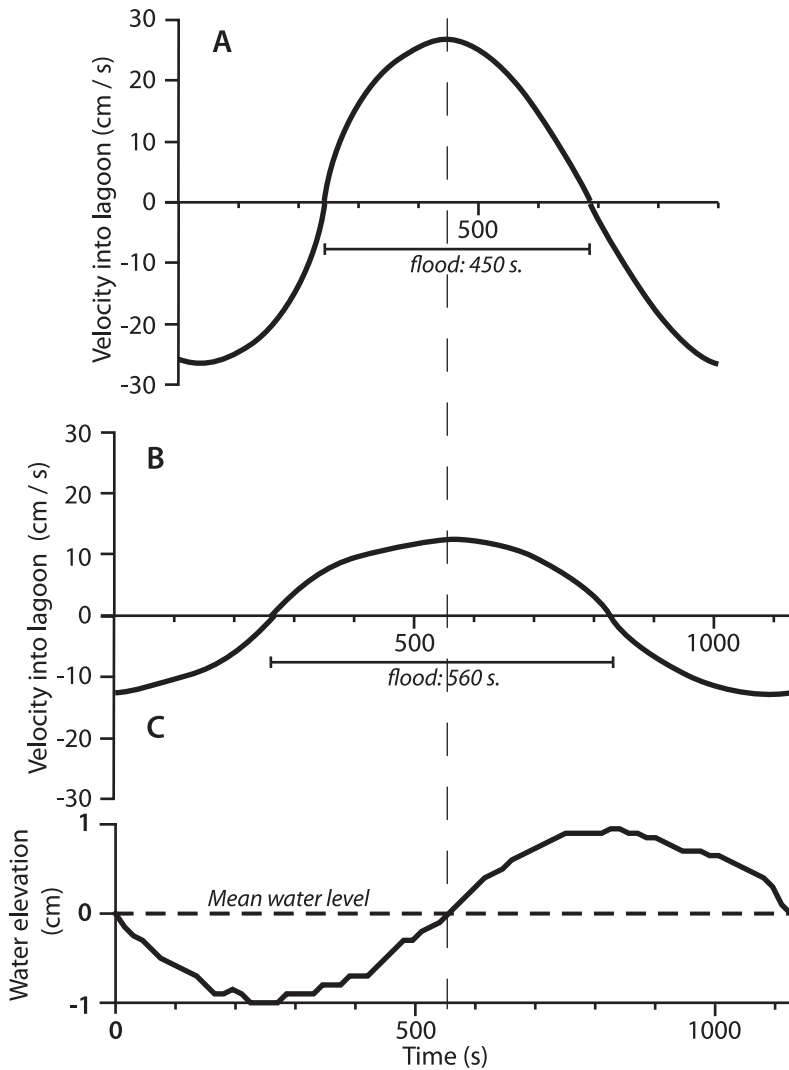
Figure 5.5 The velocities measured in the lagoon next to the inlet (yet without the presence of a delta) and water level in the lagoon during an experimental tidal cycle: A) Initial flow conditions, and B) decreased flow conditions from 20 hours onwards. Note that the scale on the y-axis differs between panel A and B, and C) water level during the tidal cycle, corresponding to the velocities measured in B.

by an experimental tidal cycle. At 233 hours, supply as lowered to twice the starting value and the amount of time was lowered correspondingly (Table 5.2).

Estimates of volumes of sand transported into the natural inlet range from 1 to 5 Mm³/year (Sha, 1989a, 1989b; Louters and Gerritsen, 1994; Dronkers, 1998; Ligtenberg, 1998; Elias *et al.*, 2003; Elias *et al.*, 2006). This corresponds with 40 to − 200 × 10³ m³ of sand passing through the Marsdiep tidal inlet over a neap–spring–neap tidal cycle. A difference between the Marsdiep and the model is that during ebb, sand leaves the lagoon (the Wadden Sea). In the model, no sediment

Table 5.2: Calibration of the evolution of the tidal delta. Time and the number of tidal cycles involved are calibrated to time in the prototype by means of the correlation 'factor', related to the sediment added to each tidal cycle.

Time (hrs)		Cycles		Factor	Cal.Cycles	Calibrated Time (years)		Remarkeble events
From	To	Number	Cumulative		Number	Number	Cumulative	
0	88.17	338	338	1	338	14.1	14.1	88.17: Supply tripled
88.17	98.33	39	377	3	117	4.9	19	98.33: Deposit influences flow
98.33	159.63	235	612	3	705	29.4	48.3	
158.63	194	132	744	3	395	16.5	64.8	164: deposit above low tide level
194	233	149	893	3	448	18.7	83.5	175: change in supplied material
233	280	180	1073	1.9	347	14.5	98.0	280: end of experiment

moved back through the inlet. In addition, the Marsdiep back-barrier system is connected to other inlet systems and part of the sand is lost to them.

5.3 Results

The modelled flood-tidal delta environment includes the inlet channel and a lagoon for flood-tidal delta formation. During rising tide, flood flow was directed into the lagoon (inward-directed flow).

5.3.2 Flood-tidal delta accumulation up to mean water level

The first 100 hours of the experiment showed aggradation and progradation of the flood-tidal delta. In the very beginning, the vertical growth rate was small as the initial flow velocity of the jet was too high and most of the particles were moved off far into the back-barrier basin (Fig. 5.5A). Minor deposition occurred on the incipient flood-tidal delta, and bedforms of 2 cm high and 6 cm wave length were formed (Fig. 5.6A).

After 22 hours the velocity was lowered from 27 to 12 cm/s, and the supplied sand was deposited close to the inlet (Figure 5.5B). The bedforms migrated forward and formed a delta just behind the inlet. The geometry of the body remained stationary and the ripple size constant. At the downstream end of the body bedform migration ceased and the sand avalanched, contributing to the outbuilding of the flood-tidal delta. The sand body grew steadily by aggradation and progradation. Only the inward-directed flow (flood) was strong enough to transport material during the initial 100 hours of the experiment. The outward flow (ebb) only got sufficient speed to erode sand at the flow confluence near the inlet. After 79 h 49 min the delta top was a linear crest (Fig. 5.7A). From 100 hours onwards, when the sand body had reached an elevation of 130 mm (Fig. 5.8), the flood-tidal delta was more than 600 mm wide (Fig. 5.7B) and had a lobate form; at T 110 h 37 min, the delta top had been flattened (Fig. 5.7B). By then it had reached a height of 6.5 cm below the low water line (Fig. 5.8).

A: 30h00

Barrier | Inlet | Barrier

B: 218h35

Tidal bar | Transect Fig. 9

C: 228h30

Deposition | Minor ch. | Dominant channel

D: 230h00

Dominant channel

E: 231h42

Dominant channel

F: 232h45

Dominant channel

→ late stage flood flow
⇢ early stage flood flow
→ ebb flow
— ripple crests
— limits of tidal bar
— limits of tidal delta

G: 233h47

H: 239h30

Dominant channel

I: 240h26

J: 242h57

Dominant channel

Dominant channel

K: 244h30

L: 266h06

Minor channel

Dominant channel

late stage flood flow

ripple crests

early stage flood flow

limits of tidal bar

ebb flow

limits of tidal delta

Figure 5.6 (continuing from previous pages) Autocyclic behaviour in plan-view images. The boards bounding the basin (mimicking barrier islands) are represented by the white lines. The size of the flood-tidal delta is specified by the black line, the dashed black line represents the previous limit of the deposit. The bar on top of the delta is indicated in red, and ripples transporting sediment in the channels are indicated in green. Blue arrows express the converging ebb flows. Dashed orange arrows indicate flow paths in the channels during early flood, orange arrows indicate the flow paths during late flood. Time of each image is indicated in the upper right. Location of the cross sections of Fig. 9 is indicated in panels B, C, G and H.

After 140 hours, the hindrance by the sand body was optimal, and the outward-directed flows circumnavigated the sand body and progressively displaced to the boarding along the inlet, where channels formed at both sides of the inlet (Figs 5.2 and 5.6B). Deposition near the inlet enhanced shallowing of the ebb flow, increasing the flow velocity sufficiently to transport minor amounts of sediment. The channels conveyed mostly ebb currents, but during the early flood also the flood current used the channels. Close to the mouth of the inlet, the two channels converged, and joined before entering the inlet. Flow velocities were observed to increase while the aggrading delta decreased the flow depth to 3 cm below the low-water line. The channels, outside the survey limits of the laser, are indicated in Figure 5.6B. At 150 hours, the rippled area started developing
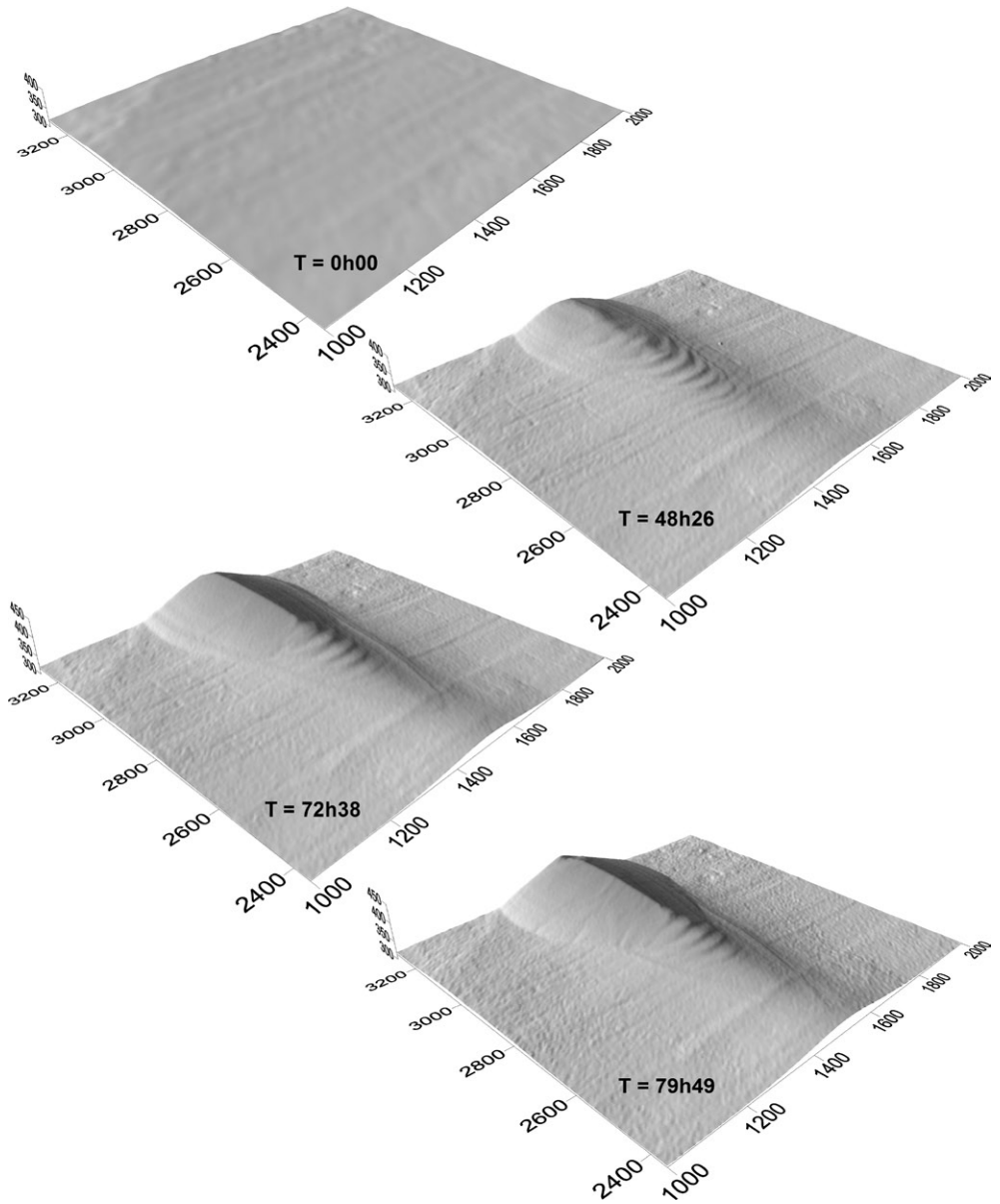
Figure 5.7A Topographical development of the flood-tidal delta in the experiment shown by shaded relief maps from the start to ~80 hours.
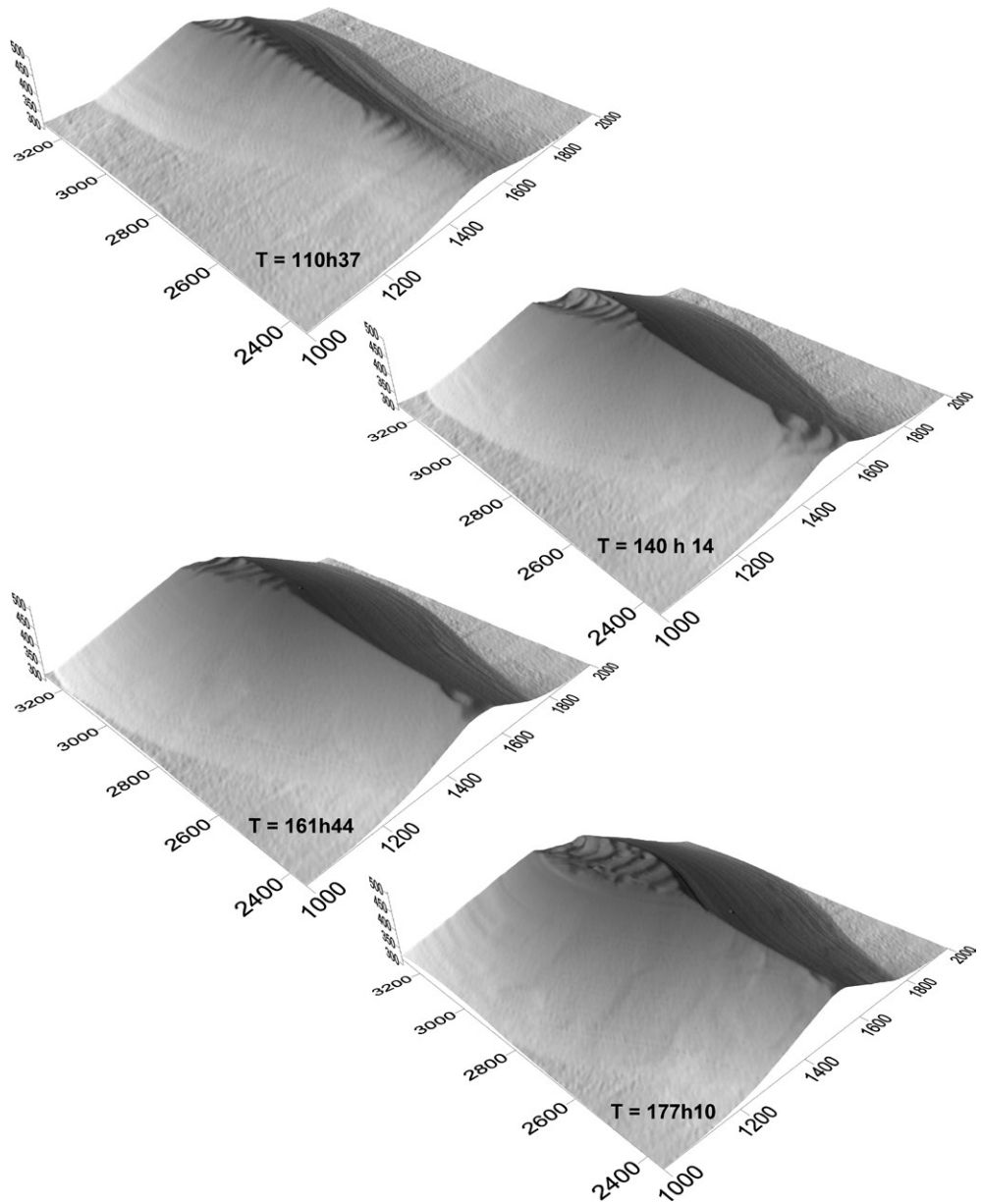
Figure 5.7B Topographical development of the flood-tidal delta in the experiment shown by shaded relief maps from ~110 to 177 hours.
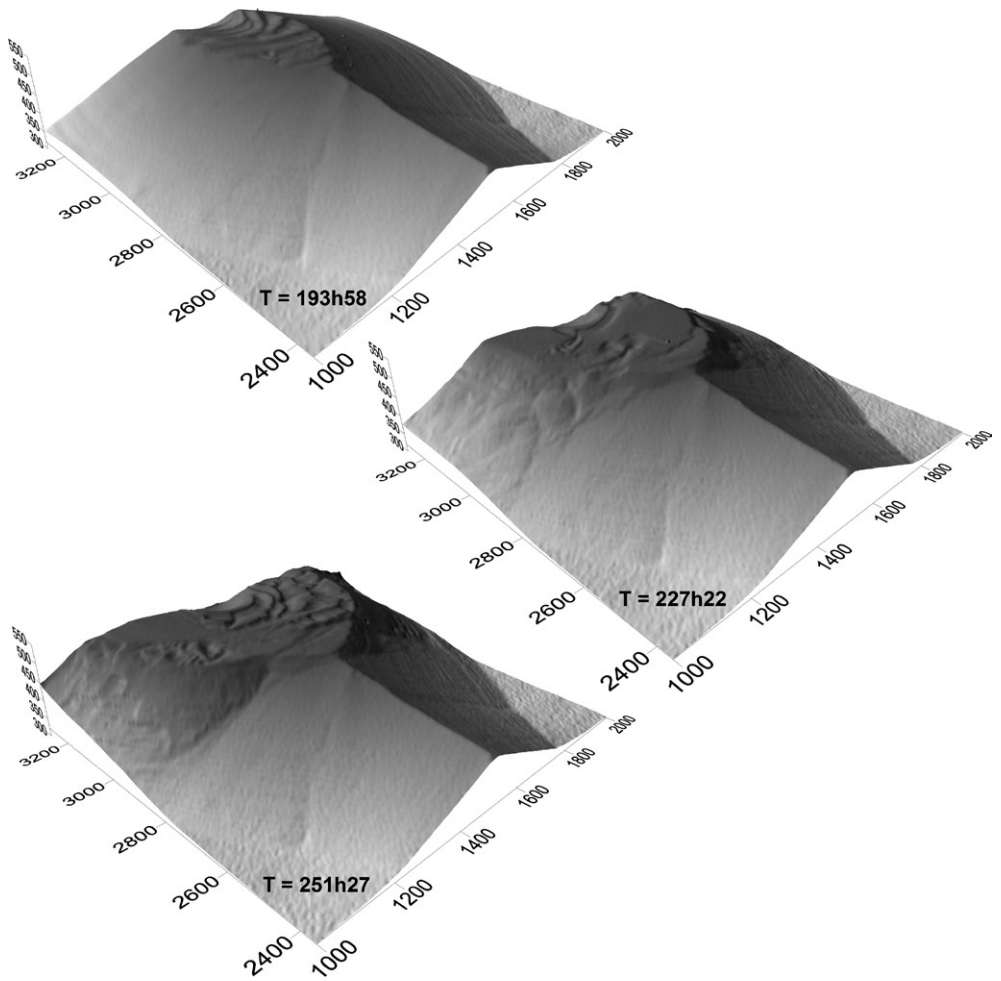
Figure 5.7C Topographical development of the flood-tidal delta in the experiment shown by shaded relief maps from ~177 to 250 hours. Note that the experiment continued, but no more topographic maps were recorded.

a cyclic pattern. The morphology alternated between: 1) several large semi-circular bedforms over the entire width of the flood delta, and 2) a mix of semi-circular bedforms spanning half the width of the delta and even less. Between 140 and 190 hours, the size of the area with bedforms grew from 10% to almost 20% of the increasing surface area of the flood-tidal delta (Fig. 5.7B). After 164 hours, the sand body partially emerged above low-tide level, as some of the bedform crests at the margin of the flood delta grew.

The supplied sediment (60 μm) ran out after 194 hours, and was replaced by coarser sediment (105 μm), which then was used until the end of the experiment. The smaller sediment mobility of the coarser sand led to deposition closer to the inlet, expressed by the intensified broadening of the delta top following the sediment change (Fig. 5.7B and C).

As the height of the delta continued to increase, the depth of the flood current traversing the delta top progressively decreased. The velocity of the flood current increased accordingly. The increased flow strength removed the bedforms from the top of the delta body, generating a smooth surface under upper-plane-bed conditions. Usually, the waning flow just before slack water caused small bedforms to re-emerge. These conditions eventually prevented further aggradation of the delta (Fig. 5.8), and delta growth continued by widening and lengthening. Delta expansion started after 190 hours and continued until the end of the experiment. At 220 hours the ebb current (from the lagoon into the inlet) became strong enough to produce bedforms in the channels.

5.3.2 Autocyclic behaviour

From 220 hours onwards, morphological changes of the sand body were restricted to the top of the delta. The delta top showed a cyclic migration of channels and associated changes in bar morphology.

Figure 5.6B illustrates the situation at the start of the first cycle. During early flood, when the water level was not yet high enough to submerge the delta, the inward-directed flow occupied the two channels. The channel on the right-hand side (seen from the inlet, see Fig. 5.6B) became slightly wider, showed an increase in flow velocity, and then quickly dominated over the other channel. The minor channel lost additional capacity as deposition occurred at the margin flanking the delta (see Fig. 5.6C). Dashed yellow arrows in Fig. 8C express the differential capacity of the channels during early flood. During mid-flood, the tidal jet, surging into the delta, locally eroded the upper 2 cm of the deposit and widened the channel (Figs 5.6C and 5.9A).

The smooth and flat delta top in Figure 5.9A is a reflection of the upper plain-bed conditions as flood submerges the delta a little later. The eroded material was transported and deposited as small bedforms. Crests of the bedforms are highlighted by a green line in Fig. 5.6D. Once the channel started to widen, erosion in the outer channel bend further intensified (Fig. 5.9B), and the flow path in the channel extension straightened, leading to anticlockwise rotation of the flow path in the channel extension (Figs 5.6D to F and 5.9B).

The material eroded from the delta top was deposited as a lobe in front of the widening channel at the delta margin (Fig. 5.6D). The lobe migrated and expanded basinward in conjunction with an anticlockwise rotating channel (Fig. 5.6E and F). Rotation of the channel shifted the flow path more across the length of the lobate delta body (Fig. 5.6E), so that the channel became longer and wider. Once the channel approached the centerline of the delta, the rate of ripple migration decreased and ripple crests merged to form a large bar that blocked part of the channel (Figs 5.6G and 5.9C), decreasing its capacity. Decreasing ripple migration continued and eventually the channel was filled (Figs 5.6H and 5.9D). The above events took place over 10 hours, involving 30

tidal cycles. The activity of the channels and bars was largest during flood. During ebb there was little activity.

Following channel filling, inward-directed flow again occupied the two ebb channels, and another 10-hour cycle of channel growth, delta-top erosion, channel extension, channel migration, filling and abandonment followed, this time showing dominance of the left-hand channel (Figs 5.6I and J). Figure 5.6K shows the return to the two-channel configuration following cycle 2, and in the succeeding cycle 3, which lasted 25 hours, the right-hand-side channel was dominant again (Figs 5.6L and M). The next cycle was preceded by another two-channel stage (Fig. 5.6N). Figures 5.6O and P display the start of the last, not-completely recorded, cycle of channel expansion and migration, with dominance of the left-hand channel. Table 5.2 summarizes the development of the tidal delta expressed in model years.
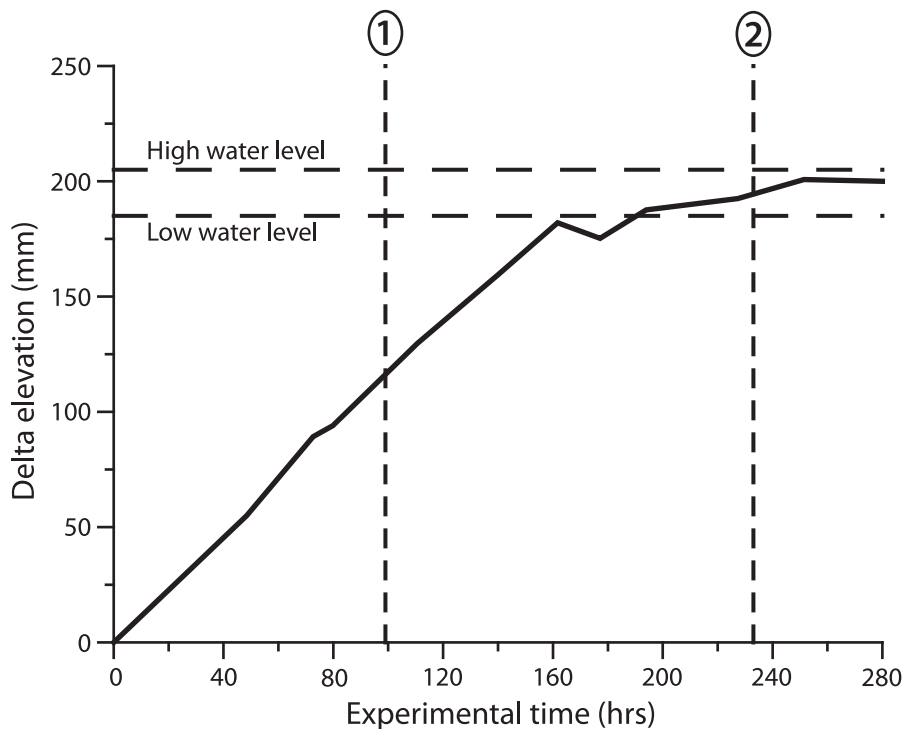

Figure 5.8 Elevation of the tidal bar on the flood-tidal delta during the experiment, including minimum and maximum water levels. Timing of (1) start of interference of the delta with the low-water level, and (2) moment when the sand body emerges above the low-water level and the subsequent equilibrium morphology are indicated.

5.4 Discussion

The evolution in the modelled flood delta showed two important stages: 1) an aggrading stage where the delta body steadily grew to the low-water level: 2) a prograding stage where the tidal channels exhibited cyclic behaviour. First we address the aggrading stage, and then we discuss the cyclical behaviour and compare that with the autocyclic behaviour found in fan-delta and alluvial-fan flume models.

5.4.1 Aggrading stage
The morphology of the flood-tidal delta remained constant during most of this stage: from the beginning of the experiment onwards the delta grew steadily higher, longer and wider (Figs 5.8 and 5.7A), and resembled the ebb-tidal delta models of van der Vegt *et al.* (2006, Fig. 5.10) Fig. 5.10), who performed an idealised physically based morphodynamic numerical modelling study on the equilibrium of ebb-tidal deltas. The resulting equilibrium morphology shows an inlet with a symmetrical ebb-tidal delta in front (Fig. 5.10a). No wave action was applied in this case, and the delta remained permanently below water. The length of the delta was less than its width, and between the delta and the inlet a scour occurred, twice as deep as the tidal delta (Fig. 5.10b). From this scour two minor channels protruded seaward, flanking the ebb-tidal delta. The similarity between the two tidal-delta models is striking. The similarity is limited to morphology (despite the absence of waves in both models), as the processes in the analogue model are not reproduced in the numerical model.

5.4.2 Prograding stage
In tidal systems, it is common to see flood currents dominating sediment transport in higher parts of the delta and ebb-flow currents dominating the channels (van Straaten, 1964; De Boer, 1998). This experiment shows the same pattern, but how can this lead to the cyclic channel migration?

   The cycle starts when one of the two channels starts to grow in favour of the other. Kleinhans *et al.* (2008) showed that river bifurcations are inherently unstable, and a dominant branch eventually forms. For the tidal channels in the experiment the same mechanism applies. Consequently, the dominant channel captures increasing discharge, and flow velocity increases. The flow velocity of the flood current is affected by two processes: 1) the varying flow velocity during the rising tide (Figure 5.5), and 2) delta height. These two factors combine to peak flow velocities in the (dominant) channel when water level approaches the elevation of the delta. Thus, peak flow velocity is concentrated on the delta top, driving local erosion, and formation and migration of the expanding and laterally migrating channel.

   Once the laterally expanding and lengthening flood channel reaches the centreline of the delta, flow deceleration eventually leads to abandonment of the channel (Fig. 5.6D-F). Flow deceleration is generated by two processes: 1) the channel widens, spreading the discharge, and 2) the flow path lengthens, and the channel has insufficient gradient to maintain flow momentum. The associated loss of flow velocity in the channel leads to deposition and ultimately the channel is filled and abandoned after 10 hours of activity. Following this first cycle, 2 more complete cycles and an incomplete one were recorded, with dominancy switching to the other side in every subsequent cycle (Fig. 5.6I-N). Dominancy in the previous cycle left behind a higher elevation at that side of the delta, promoting the other channel to become dominant and driving a switch of dominancy in each subsequent cycle.
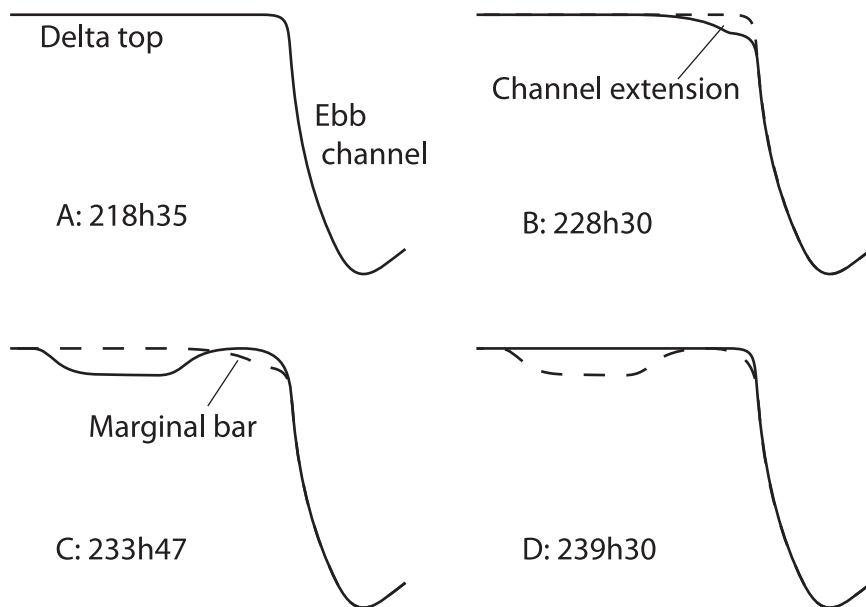
Figure 5.9 Schematic illustration of the development of the tidal channel and its extension across the delta as shown in Fig. 8. See text for detailed description.

5.4.3 Scaling of autocyclic behaviour

The duration of the cycles on the flood-tidal delta is estimated to be equivalent to 2.5 years in natural tidal systems. This age is approximated by the amount of sediment supplied to the inward-directed flow (flood). The sediment volume that was added during one model tidal cycle was scaled to represent two full neap-spring tidal cycles, so 13 model cycles roughly correspond to one year in natural systems. As sediment supply is used for scaling time in the experiment, the correlation between the experimental tidal cycles and time in the model prototype altered when sediment supply was changed (Table 5.2). The three complete cycles recorded in the final part of the experiment and described above spanned 45 hours in total, averaging 15 hours (ranging from 10 to 25 hours), which would be equivalent to an average duration of 2.5 years in nature.

The bypass-driven cycles in the ebb-tidal deltas in the Wadden Sea in The Netherlands and Germany span decades (Sha, 1989a; Oost and de Boer, 1994). The ebb-tidal delta of the Marsdiep Inlet shows channels rotating clockwise over 70 years (Sha, 1989a; Elias *et al.*, 2003, 2006). Oost (1995) describes the Pinkegat Inlet, which shows similarly rotating channels with a cycle duration of 70 years associated with alternations between a single-channel and dual-channel configuration. This is considerably longer than the inferred cycles in the experiment. However, Robinson (1975) and Oertel (1977) describe cyclic behaviour of smaller ebb-tidal deltas with a diameter of 1-2 kilometres, with comparable periods of 3-5 and 2-3 years. This involves alternations between a single channel configuration and a configuration with multiple spill-over channels diverting part of the flood flow. Fitzgerald (1984) describes Price Inlet (East Coast USA), which displays cyclical bar migration with a duration of 4-7 years. This demonstrates that the cycle observed in the experiment does have a counterpart of similar duration on ebb-tidal deltas in natural systems.

Unfortunately no hydraulic data are available for these ebb-tidal deltas, which would have given better control on scaling and comparison of the processes.

5.4.4 Morphology during autocyclic behaviour

The Hayes model (Fig. 5.1) and the experimental flood-tidal delta (Figure 5.6B) show prominent parallels, i.e., a configuration with a tidal bar in between bifurcating tidal channels. Bedforms show flow directions and the ebb flow is steered around the delta on its way out. During flood, the water level rises, and the bar is covered by water.

The morphology of the growing tidal bar remained steady before equilibrium was reached, but then it became variable. It was broadly symmetrical after 250 hours despite the small-scale variations (Fig. 5.6B), but minor variations occurred due to the rotating channels. The morphology of the bar initially was like a droplet, the tip pointing into the lagoon. At this point the channels were neither flood-dominated nor ebb-dominated. The location of the tip of the droplet-shaped bar remained fixed during the experiment (Fig. 5.6). When one of the channels became dominant over the other, the morphology of the tidal bar changed. The minor channel decreased in capacity as it was partly filled (left-hand side of Fig. 5.6C), and the dominant channel increased in width and expanded to the central part of the delta (right-hand side of Fig. 5.6C). The minor channel was ebb-dominated, while the dominant channel transported more or less equal amounts of ebb and flood waters.

During the migration of the dominant channel towards the centreline of the delta, flow velocity in the inner bend decreased as the bulk of the flow was directed along the outer bend. Some decelerating ripple crests accreted to form a marginal tidal bar (Fig. 5.6G). This bar divided the dominant flood channel in two parts. The remnant of the rotating channel traversing the delta body remained flood-dominated, but was filled soon after marginal-bar formation. The channel remnant of the expanding channel that had just been partially closed reverted back to ebb dominancy. When the rotating flood-dominant channel was abandoned after 239 hours (Fig. 5.6H), this marginal bar, still present in Figure 5.6G, reattached to the main tidal bar (Fig. 5.6H). The delta regained the symmetrical morphology it showed prior to channel expansion and abandonment at 230 hours. Like in the initial state, the two channels carried both the flood and ebb currents.

Few studies on flood-tidal deltas have been published. Nummedal and Pennland (1981) describe how the flood-tidal delta of the Norderney Inlet temporarily stores sediment bypassing the inlet. Elias *et al.* (2003) discuss the effect of the closure of the Zuiderzee on the flood-tidal delta of the Marsdiep Inlet, which lost a large part of its back-barrier basin, but due to changing resonance of the tidal wave increased its tidal prism. The increasing tidal prism led to rotation of one of the ebb-tidal channels (Texelstroom), thereby influencing the morphodynamics of the tidal inlet and also the ebb-tidal delta. Stauble *et al.* (1988) describe Sebastian Inlet in Florida, USA, and the evolution of its flood-tidal delta while it filled the back-barrier lagoon. Despite human interference by dredging and stabilisation of the inlet by 'jetties', the delta grew rapidly into the lagoon, showing many of the features found in the current experiment and in the model of Hayes (1980). The Sebastian-Inlet flood-tidal delta showed channel re-orientation and bifurcation and the formation of an ebb shield. The delta shoaled as it filled the lagoon, identical to the experiment. No cyclical behaviour is mentioned in that study. Considering the many studies on cyclic behaviour in ebb-tidal deltas (Hanisch, 1981; Nummedal and Penland, 1981; Fitzgerald et al., 1984; Sha, 1989; Oost and de Boer, 1994; Elias and Van der Spek, 2006; Elias et al., 2006), there is no reason not to expect cyclic mechanisms in flood-tidal deltas. Indeed, the experiment shows that cyclical behaviour is well possible in nature.

5.4.5 Autogenic behaviour of tidal-delta, alluvial-fan and fan-delta models compared

Certain features of the autogenic cycles on the flood-tidal delta are comparable to autogenic cycles observed in experimental fan deltas (*Chapter 2*). First we address the initiation and abandonment of the autogenically originated channels and then address the frequency of these events.

In both the fan delta and the flood-tidal delta, the behaviour focuses on the formation, maturation and eventual filling of channels. The formation of autogenic channels on the fan deltas is driven by slope, but in the tidal delta channels developed concurrently with the evolution of the flood delta and remained present following formation. One of the two channels becomes the dominant carrier of the early flood current, and shows autogenic rotation as it captures increasingly more discharge. The other remains active but marginal. The autogenic cycles in the fan deltas and the flood-tidal delta show similarities. In both deltas, channel lengthening, and subsequent loss of momentum leads to deposition and eventual filling of the channel.

Relative duration of the lengthening and filling of the channels differs between the two different delta systems, however. On the fan deltas, lengthening of the incised channels happens only in the early stage of the autogenic cycle, and filling requires most of the remainder of the cycle. For the tidal channel, in contrast, lengthening takes most of the cycle, while filling occurs only in the final stage. A more prominent difference between the two systems is the rotation of the expanding flood channel, versus the stationary upper part of the incised channel on the fan deltas. This rotation is due to the fact that the system is forced by alternating bidirectional currents. The character of the tide results in concentration of the flood current on the delta top, leading to channel expansion and migration. Note that *Chapter 2* demonstrates that the stationary incised channel is related to the small width of the feeder channel in the setup. The use of a wider feeder channel would likely have led to considerable channel migration.

Lateral channel migration does occur further downstream on the fan deltas: the two branches of the incised channel below the bifurcation point migrate laterally (*Chapter 2*). The fan-delta channels migrate away from the centreline before being abandoned, whereas the tidal channel migrates in the reverse direction, towards the centreline, prior to abandonment. The processes driving the lateral migration of the channels are also different. The lateral migration of the fan-delta channels is controlled by preceding channel lengthening and mouth-bar formation, whereas the rotation of the tidal channel is forced by the jet flowing into the lagoon during rising tide in combination with the curved path of the expanding channel. The curved path results from the bidirectional flow on the flood-tidal delta, as the interaction between the delta and the flows forces the channels to their position flanking the delta (Fig. 5.6B). When the inward-directed flow (flood) begins, the ebb channels transmit the flood current until the entire delta is submerged. In conclusion, the morphodynamics of the channels of the two systems show similarities, i.e., channel migration, lengthening and fill-up, and also differences, channel migration and fill-up occur in reversed order.

The duration of the cycles on the fan deltas is of interest over longer timescales. On the fan deltas, the autogenic cycles have a constant duration, while the duration of channelised-flow stages increases in favour of the sheet-flow stages. In the flood-tidal delta, the last of the three recorded cycles lasted 50% longer than the first two cycles. Likely, following cycles would have gradually increased if the experiment had been continued, due to the volumetric and aerial growth of the sand body. The migration of the flood channel traversing the sand body then probably would last progressively longer as well, because input conditions (tidal flows imposed by the setup and sediment supply) remain invariable while the sand body grows. For a channel to migrate from the delta margin to the centre of the delta, more sediment needs to be eroded and transported
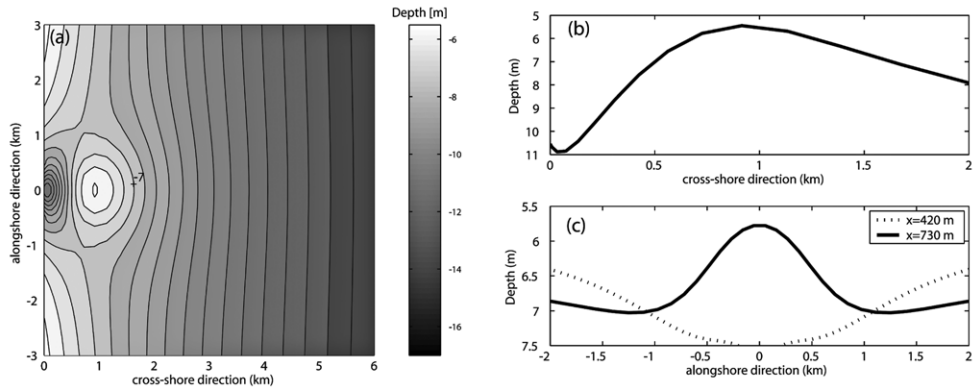
Figure 5.10 A) Equilibrium morphology of the idealised model of van der Vegt *et al.* (2005). B) Cross section through the centre of the tidal bar of panel A perpendicular to the shoreline, and C) cross sections parallel to the shoreline at 2 positions at 420 and 730 m from the shore.

when the delta becomes larger. Fan-delta growth led to progressively deeper incisions, but delta progradation associated with the incision decreased at the same rate. As a result, the volume of the incisions was more or less constant despite the increasing delta radius. No such feedback mechanism has been found in the flood-tidal delta, so we expect the cycles on the tidal deltas to lengthen as longer experimental runs are performed.

5.5 Conclusions

1. The experimental flood-tidal delta in the experiment shows autocyclical behaviour once it had grown to the mean water level.

2. Before the first cycle began, the morphology of the flood-tidal delta consisted of a central tidal bar flanked by a bifurcated channel with the branches positioned nearly perpendicular to the inlet.

3. Autocyclic behaviour began as one of the two channels became dominant over the other, capturing increasingly more discharge. The flow velocity in the flood-tidal jet peaked as the water level matched the top of the tidal bar, thus focusing its erosive momentum there. Erosion of the tidal bar led to expansion of the dominant channel and rotation towards the centre of the bar. This more central flow path increased the length of the channel, decreasing the flow momentum, which led to deposition and abandonment of the channel.

4. The autogenic cycles lasted 15 hours on average, with a tendency to longer cycles to the end of the experiment. This roughly corresponds with a duration of 2-3 years in natural systems.

5.6 Acknowledgements

5.7 Appendix

Equations used for scaling parameters:

$$Fr = \sqrt{\frac{gh}{u}}$$

$$Re = \frac{(\rho_w H u)}{\upsilon}$$

$$\theta = \frac{\tau'}{(\rho_s - \rho_w)gD_{50}}$$

$$\tau' = \rho_w g \left(\frac{u}{C''}\right)^2$$

$$C'' = 18 \log\left(\frac{12d}{2.5D_{50}}\right)$$

$$Ro = \frac{\omega_s}{\kappa u^*} \sim \frac{\omega_s}{u}$$

$$\omega_s = \frac{\upsilon}{D_{50}}\left(\sqrt{10.36^2 + 1.049D^{*3}} - 10{,}36\right)$$

$$D^* = D_{50}\sqrt[3]{\frac{\left(\frac{\rho_s - \rho_w}{\rho_w}\right)g}{\upsilon}}$$

$$\gamma = \frac{\omega_s}{h}$$

$$\sigma = \frac{1}{Tidal\ period}$$

With:
C'' = Chézy constant [ms^{½}]
D^* = dimensionless grain size [-]
g = gravitational constant 9.81 [ms^{-2}]
H = Hydraulic radius [m]
h = flow depth [m]
κ = Von Karman constant 0.4
υ = kinematic viscosity 1.2 x 10^{-6} [m^{2}s^{-1}]
ρ_s = sediment density [kgm^{-3}]
ρ_w = water density [kgm^{-3}]
τ' = bottom shear stress [Nm^{-2}]
u = velocity [ms^{-1}]
u^* = shear velocity [ms^{-1}]

Synthesis

Autogenic behaviour of several different silliciclastic sedimentary systems have been studied by means of analogue experiments; fan deltas, alluvial fans and tidal deltas. The purpose was: 1) to isolate autogenic components in the evolution of alluvial fans, fan deltas and flood-tidal deltas, 2) to establish the relative importance of intrinsic processes and externally originating variations, 3) to investigate the characteristics of autogenically and autocyclically driven deposition, 4) to compare these characteristics with those formed as the result of (allogenic) variations in boundary conditions, and 5) to investigate the effect of base level and base-level change on the autogenic evolution of these systems.

6.1 Autogenic processes

Chapter 2 and *3* demonstrate that the autogenic evolution of alluvial fans and fan deltas consists of alternating stages of sheet and channelised flow (Figs 6.1A-D, Table 6.1). Associated with these alternations, the surface gradient of the fan-shaped systems varies. During sheet flow, aggradation increases surface slope (Figs 6.1A and C). As the slope reaches a critical value, incision is initiated, followed by headward erosion connecting the incision to the feeder channel to form a fully confined channel (Figs 6.1B and D). Channelised flow diminishes the surface slope, leading to a lower gradient. Later on, this incision is filled, followed by renewed sheet flow and associated aggradation.

The incisions on the experimental fan deltas and alluvial fans have a cyclic character. The fan-delta cycles have a constant duration while the alluvial-fan cycles show increasing periodicity. An additional prominent feature in the later stage of alluvial-fan evolution is the occurrence of re-incisions; a channel still in the process of being filled is subjected to renewed incision. The incisions observed on the fan deltas (*Chapter 2*) and alluvial fans (*Chapter 3*) lead to a confinement of the flow, generating localised progradation. This leads to temporary variations in morphology. Following localised progradation, the bifurcation of the incised channel on the fan apex, causes the locality where progradation occurs to shift, levelling out the earlier variations in morphology at the end of each autogenic cycle. The morphology of the fan delta as it was prior to the incision is restored and sheet-flow dominance with it.

The flood-tidal delta (*Chapter 5*) shows a different kind of autocyclic behaviour (Figs 6.1E and 6.1F). The process begins when the tidal delta has reached a mature stage (Fig. 6.1E) and achieves full interaction with the ebb and flood. One of the two channels conveying the ebb and flood currents becomes dominant over the other, drawing increasingly more of the flow during flood tide. This expanding flow causes the dominant channel to enlarge and to migrate across the tidal delta from the flank to its centre (Fig. 6.1F). Upon reaching the centre of the delta, the channel is abandoned and filled, and the situation with two bifurcating channels is restored.

Table 6.1 summarises the morphodynamic characteristics of the autocyclic processes in the systems described in *Chapters 2* to *5*. It shows how aspects of the processes vary from system to
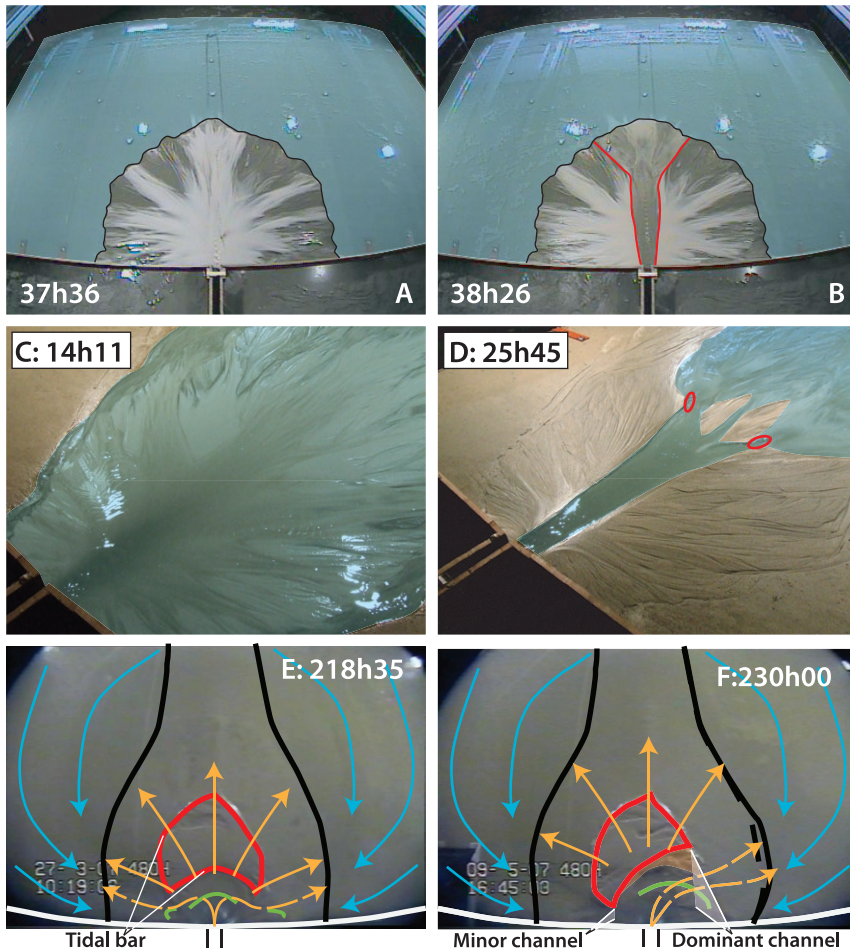
Figure 6.1 behaviour of the studied systems: A-B; sheet flow (A) and channelised flow (B) on the fan delta, C-D; sheet flow (C) and channelised flow (D) on the alluvial fan, E-F; mature stage (E) and the expanding channel (F) on the flood-tidal delta. In the panels A and B, the black line represents the shoreline and in panel B the red line bounds the incision. In the panels C and D, the red circles highlight scour holes on the fan surface. In the panels E and F the black lines indicate the margin of the tidal delta. The red line shows the margin of the delta top, and the green lines highlight the crests of bedforms. The blue arrows represent the flow directions during ebb (directed out of the basin), the orange arrows those during flood (into the basin)

system. For example, a complete autogenic cycle in the fan-delta experiments lasts up to 50 hours (*Chapter 2*), while the stepped delta in *Chapter 4* shows lobe switching associated with channel migration lasting only minutes. The position of base level is very important for the duration and frequency of the autogenic cycles, as discussed in detail in *Chapter 3*. The stepped delta of *Chapter 4* was influenced by rising base level, forcing the delta to adapt continuously. This effect was enlarged by the interaction between feeder-channel processes and mechanisms on the delta plain. The supply from the feeder channel to the delta varied because migration of the channel meanders caused the feeder channel to incise the underlying strata. Also slumping of the unstable

channel walls contributed to the pulsation of the supply. The sediment pulses typically lasted only a few seconds, but carried enough sediments to considerably enhance the effect of delta-lobe formation.

6.2 Relative importance

Autogenic processes lead to significant incisions in the modelled sedimentary systems associated with the alternations between sheet and channelised flow. Climate-related variations in precipitation can alter the upstream input of water and sediment to the system and may subsequently lead to similar incisions. *Chapter 2* demonstrates that the depth of the autogenic incisions is at least equivalent to that generated by such variations in climate conditions, which complicates determination of the source of incisions in natural systems. Thus, allogenic signals of the upstream boundary condition and autogenic signals may be of roughly equal importance.

Changes in base level (sea-level changes, tectonic movements) affect the downstream boundary condition of the systems. Thus, autogenic signals may be distorted by base-level change. Depending on the rate and magnitude of base-level change and the time scale over which they operate, the autogenic behaviour is superimposed on or interferes with the allogenic signal. *Chapter 4* nicely illustrates the superposition of the short-term autogenic processes such as delta-lobe switching and channel migration on the effects of base-level rise. In this case, shoreline migration driven by base-level rise defines the position of deposition, but autogenic processes determine the morphology of the deposit (Fig. 6.2). In addition, *Chapter 4* shows how a wider feeder channel can lead to a different morphology. In *Chapter 2* and *3*, a narrow feeder channel leads to concentration of the

Table 6.1: Summary of the autogenic processes of the studied sedimentary systems. Equivalent dimensions are indicated if relevant. Q_w and Q_s imply water and sediment discharge respectively.

	Fan delta	Alluvial fan	Stepped delta	Tidal delta
Morpho-dynamics	Alternations of sheet and channelised flow on the surface of the delta	Alternations of sheet and channelised flow on the fan surface	Channel migration and avulsions on the surface of the delta	Formation, migration and abandonment of tidal channels in the inter- and supratidal parts of the delta
Cause	Slope-driven initiation of incised channels	Slope-driven initiation of incised channels	Meander migration and slumping of cut banks in the feeder channel	Interaction between the delta obstruction and flood flow
Frequency	10-50 hours (equivalent to 100's of years)	5-25 hours (equivalent to 100's of years)	Minutes (equivalent to days to months)	10-25 hours (Equivalent to years to decades)
Size	1-3 m (equivalent to 10^2 m)	1-6 m (equivalent to $10^2 – 10^3$ m)	0.1-0.3 m (equivalent to 10^3 m)	0.5-2 m (equivalent to 10^3 m)
Frequency dependency	Delta size, Q_w/Q_s	Q_w/Q_s	Delta size	Delta size, Q_w/Q_s
Architecture	Channels depths: 5-20 mm (equivalent to 10^1 m)	Channel depths: 5-10 mm (equivalent to 10^1 m)	Delta terraces: 5-10 mm (equivalent to $10^0 – 10^1$ m)	Channel depths: 5-10 mm (equivalent to $10^0 – 10^1$ m)
Stage	Fill-up	Start-up	Start-up/Fill-up	Not relevant
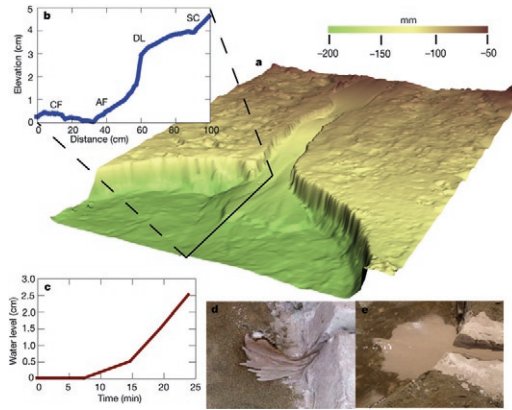
Figure 6.2 Final morphology of the delta formed in the mock-crater.

autogenic signals to the centreline of the experimental fan deltas and alluvial fans. In *Chapter 4*, a wide and unconfined feeder channel is used to supply sediment and water to the growing delta. This unconfined feeder channel enables the delta channels to migrate and avulse across the delta, distributing the sediment over the entire delta plain. Within the feeder channel, slumping and meandering generate pulsation of the supply of sediment to the delta. The interaction between the autogenic processes in the feeder channel and on the delta plain generates a complex interaction with allogenic variations in supply to generate a complex, stepped-delta morphology analogous to deltas in craters on Mars (Fig. 6.2). Here, the autogenic signals are important for the morphology of the system, while base-level rise defines where the autogenic processes can act.

6.3 Autogenic depositional architecture

The architecture of the erosional surfaces produced by autogenic incisions is described in *Chapter 2* for fan deltas and in *Chapter 3* for alluvial fans. Despite the predictable cycle durations, the preservation of material accumulated prior to incision varies in both systems, and the resultant stratigraphy shows variable thickness of the successions between erosion surfaces. On average, more sediment is preserved on alluvial fans than in fan deltas, and in alluvial fans the variation around the mean is larger.

The autogenic channel migration on the flood-tidal delta (*Chapter 5*) is hardly preserved in the deposits. The migrating channels rework the top layer of the delta, and their signals are reworked by later channels. As the dominant channel position alternates, no trace of previous cycles remains after two channels have passed in the delta stratigraphy. Of course, during base-level rise this would have been different, and the channel fills would have been preserved.

Autogenic processes can weaken external signals or distort them. The variable preservation of autogenic successions may complicate the distinction between autogenic and allogenic signals.

6.4 Effect of (changes in) base level

The effect of base level is shown best by comparing the experimental fan deltas and alluvial fans (*Chapter 2* and *3*). Postma *et al.* (2008) divide the evolution of sedimentary systems in three stages: 1) start-up stage; the initial progradation of a system to base level, 2) fill-up stage; aggradation stage showing a progressive increase in sediment bypass, and 3) keep-up stage; in which more than 90% of the supply is bypassed and less than 10% is used for aggradation. Ultimately, a system reaches equilibrium (or grade) when the conditions in the system are such that all supply bypasses. As shown in *Chapter 3*, the absence or presence of a base level places the systems in different stages of this evolutionary path; most alluvial fans are in the start-up stage; if the fans prograde and reach the shoreline they become fan deltas (by definition) and also enter the fill-up stage (Table 6.1). Consequently, fan deltas and alluvial fans show different behaviour, revealed by variations in slope, aggradation rates, sediment bypass and the duration of channelised events. When alluvial fans reach the fill-up stage, they exhibit the behaviour associated with fan deltas: frequent incisions and the corresponding generation of additional accumulation space by progradation of the shoreline.

A comparison with the principles derived by Postma *et al.* (2008), as done in *Chapter 3* for the alluvial-fan and fan-delta experiments, is of no relevance to the flood-tidal delta experiments presented here. The Postma *et al.* development of sedimentary systems is limited to fluvial systems; marine systems are not included in their model. The stepped delta (*Chapter 4*, Fig. 6.2) resides on the boundary between the start-up and fill-up stage. It continuously needs to adapt to the rising base level imposed on the delta, but the size of the delta is small enough to quickly do so. The steps characterising this system represent short periods of shoreline progradation, but the transitions from one lobe to the other are a reflection of the system being forced backwards (retrogradation), as shoreline progradation is interrupted.

When, in theory, the delta is allowed to progress even longer, an equilibrium will develop between base-level rise, sediment supply and size of the delta plain. As long as base-level rise is too large, the supply is insufficient to aggrade the entire delta plain at the same rate as the base level rises. The delta plain will decrease in size until the supply is able to keep up with the base-level rise. When supply of sediment exceeds base-level rise, the excess supply will enlarge the size of the delta plain, until again supply and delta-plain size balance the base-level rise.

To be able to extend the Postma *et al.* concepts to this small and dynamic type of sedimentary system, more experiments are needed that quantify aggradation and progradation in relation to base-level rise.

6.5 Summary

Strata formation in sedimentary systems is the result of the interplay of controls generated within (autogenic) and outside (allogenic) the system. Allogenic controls include climate, sea level and tectonics. Since the characteristics and relative importance of the autogenic processes are still poorly known and impossible to infer from natural sedimentary systems, analogue experiments have been carried out to unravel the interacting controls.

Autogenic evolution was studied separately for three different types of sedimentary systems: alluvial fans, fan deltas and a flood-tidal delta. In each experimental study the allogenic boundary conditions were held constant allowing the systems to grow and evolve in absence of externally imposed variation (base level or input of water and sediment).

Autocyclic behaviour (i.e., repetitive autogenic behaviour) of alluvial fans and fan deltas was similar, consisting of alternations of sheet and channelised flow. Channelised flow was initiated by slope-driven incision, and terminated by loss of flow momentum and subsequent channel filling. Flood-tidal delta behaviour deviated from that seen on alluvial fans and fan deltas and showed lateral migration and expansion of tidal channels followed by channel abandonment and filling.

All experiments demonstrated that autogenic processes and allogenic variations have a comparable impact on the morphodynamic evolution and, in the case of the alluvial fans and fan deltas, depositional architecture. The autogenic processes on the flood-tidal delta were limited to the intertidal part, and hardly left stratigraphic signals as the migrating tidal channels continuously reworked the remnants of previous channels.

In addition, the effect of base level was investigated by comparing the autogenic development of alluvial fans (positioned far from base level) and fan deltas (positioned at a standing body of water, so the shoreline formed its base level). With identical input of water and sediment, alluvial-fan behaviour demonstrated remarkable differences in slope and frequency of autogenic processes, until it reached base level and started acting as a fan delta, substantiating earlier flume and numerical studies.

To further apply developed concepts on autocyclic behaviour for Martian fan deltas, a series of fan deltas were formed in a mock-crater mimicking conditions similar to a specific type of deltas (stepped deltas) found on Mars. By comparing the morphology of the experimental and Martian deltas these experiments demonstrated that the Martian deltas were formed in one event of rapid water release, and the steps were generated by the interaction between the rising water level in the crater and autogenic variations in the supply related to processes in the upstream feeder channel.

References

Alexander, J. and Leeder, M.R., **1987**. Active tectonic control on alluvial architecture. In: *Recent developments in fluvial sedimentology* (Eds Ethridge, F.G., Flores, R.M. and Harvey, M.D.), *SEPM Special Publications*, **39**: pp. 243-252.

Allen, J.R.L., **1978**. Studies in fluviatile sedimentation: An exploratory quantitative model for the architecture of avulsion-controlled alluvial suites: *Sedimentary Geology*, **21**: pp. 129- 147.

Allen, J.R.L., **1979**. Studies in fluviatile sedimentation: An elementary geometrical model for the connectedness of avulsion-related channel sand bodies: *Sedimentary Geology*, **24**: pp. 253-267.

Ashworth, P.J., Best, J.L. and Jones, M., **2004**. Relationship between sediment supply and avulsion frequency in braided rivers. *Geology*, **32**: pp. 21-24.

Ashworth, P.J., Best, J.L. and Jones, M.A., **2007**. The relationship between channel avulsion, flow occupancy and aggradation in braided rivers: insights from an experimental model. *Sedimentology*, **54**: pp. 497-513.

Baas, J.H., Oost, A.P., Sztano, O.K., de Boer, P.L. and Postma, G., **1993**. Time as an independent variable for current ripples developing towards linguoid equilibrium morphology. *Terra Nova*, **5**: pp. 29-35.

Bhattacharya, J. P., Payenberg, T. H. D., Lang, S. C. and Bourke, M., **2005**. Dynamic river channels suggest a long-lived Noachian crater lake on Mars, *Geophys. Res. Lett.* **32**: pp. L10201, doi: 10.1029/2005GL022747.

Blair, T.C., **1999**. Cause of dominance by sheetflood vs. debris-flow processes on two adjoining alluvial fans, Death Valley, California. *Sedimentology*, **46**: pp. 1015-1028.

Blair, T.C., **2000**. Sedimentology and progressive tectonic unconformities of the sheetflood-dominated Hell's Gate alluvial fan, Death Valley, California. *Sedimentary Geology*, **132**: pp. 233-262.

Blair, T. C. and McPherson, J. G., **1994a**. In: *Geomorphology of Desert Environments* (eds Abrahams, A. D. & Parsons, A. J.), CRC, Boca Raton, Florida: pp. 354-402.

Blair, T.C. and McPherson, J.G., **1994b**. Alluvial Fans and Their Natural Distinction from Rivers Based on Morphology, Hydraulic Processes, Sedimentary Processes, and Facies Assemblages. *Journal of Sedimentary Research Section*, **64a**: pp. 450-489.

Blair, T.C. and McPherson, J.G., **2008**. Quaternary sedimentology of the Rose Creek fan delta, Walker Lake, Nevada, USA, and implications to fan-delta facies models. *Sedimentology*, **55**: pp. 579-615.

Brasington, J. and Smart, R.M.A., **2003**. Close range digital photogrammetric analysis of experimental drainage basin evolution. *Earth Surface Processes and Landforms*, **28**: pp. 231-247.

Blum, M.D. and Törnqvist, T.E., **2000**. Fluvial responses to climate and sea-level change: a review and look forward. *Sedimentology*, **47**: pp. 2-48.

Bridge, J.S. and Leeder, M.R., **1979**. A simulation model of alluvial stratigraphy. *Sedimentology*, **26**: pp. 617-644.

Bryant, M., Falk, P. and Paola, C., **1995**. Experimental-Study of Avulsion Frequency and Rate of Deposition. *Geology*, **23**: pp. 365-368.

Bull, W.B., **1977**. The alluvial-fan environment. *Progress in Physical Geography*, **1**: pp. 222-270.

Chandler, J.H., Shiono, K., Rameshwaren, P. and Lane, S.N., **2001**. Measuring flume surfaces for hydraulics research using a Kodak DCS460. *Photogrammetric Record*, **17**: pp. 39-61.

Clarke, L.E., Quine, T.A. and Nicholas, A.P., **2008**. An evaluation of the role of physical models in exploring form-process feedbacks in alluvial fans. In: *Sediment Dynamics in Changing Environments* (Eds Schmidt, J., Cochrane, T., Phillips, C., Elliott, S., Davies, T. and Basher, L.), Christchurch, New Zealand, IAHS publication **325**: pp. 175-183.

Clifford, S., **1993**. A model for the hydrologic and climate behavior of water on Mars, *J. Geophys. Res. E* **98**: pp. 10973-11016.

Collinson, J.D., **1988**. Foreword to: "Fan deltas; sedimentology and tectonic settings". In: *Fan Deltas; Sedimentology and Tectonic Settings* (Eds W. Nemec and R.J. Steel), Blackie and Son, Glasgow: pp. v.

DeCelles, P.G., Tolson, R.B., Graham, S.A., Smith, G.A., Ingersoll, R.V., White, J., Schmidt, C.J., Rice, R., Moxon, I., Lemke, L., Handschy, J.W., Follo, M.F., Edwards, D.P., Cavazza, W., Caldwell, M. and Bargar, E., **1987**. Laramide thrust-generated alluvial-fan sedimentation, Sphinx Conglomerate, southwestern Montana. *AAPG Bulletin*, **71**: pp. 135-155.

DeCelles, P.G., Gray, M.B., Ridgway, K.D., Cole, R.B., Pivnik, D.A., Pequera, N. and Srivastava, P., **1991**. Controls on synorogenic alluvial-fan architecture, Beartooth Conglomerate (Paleocene), Wyoming and Montana. *Sedimentology*, **38**: pp. 567-590.

De Boer, P.L., **1998**. Intertidal sediments: composition and structure. In: *Intertidal deposits: river mouths, Tidal flats, and coastal lagoons* (Ed Eisma, D.), *CRC Marine Sciences Series*: pp. 345-361.

Di Achille, G., Ori, G.G., Reiss, D., Hauber, E., Gwinner, K., Michael, G. and Neukum, G., **2006**. A steep fan at Coprates Catena, Valles Marineris, Mars, as seen by HRSC data, *Geophys. Res. Lett.* **33**: pp. L07204, doi: 10.1029/2005GL025435.

Dobrea, E. Z. N., Bell III, J. F., McConnochie, T. H. and Malin, M. C., **2006**. Analysis of a spectrally unique deposit in the dissected Noachian terrain of Mars, *J. Geophys. Res. E* **111**: pp. E06007, doi: 10.1029/2005JE002431.

Dorn, R.I., DeNiro, M.J. and Ajie, H.O., **1987**. Isotopic evidence for climatic influence on alluvial-fan development in Death Valley, California. *Geology*, **15**: pp. 108-110.

Dronkers, J., **1998**. Morphodynamics of the Dutch Delta (Eds Dronkers, J. and Scheffers, M.), *Physics of estuaries and Coastal Seas*. Balkema, The Hague.

Elias, E.P.L., Cleveringa, J., Buijsman, M.C., Roelvink, J.A. and Stive, M.J.F., **2006**. Field and model data analysis of sand transport patterns in Texel Tidal inlet (the Netherlands). *Coastal Engineering*, **53**: pp. 505-529.

Elias, E.P.L., Stive, M.J.F., Bonekamp, H. and Cleveringa, J., **2003**. Tidal inlet dynamics in response to human intervention. *Coastal Engineering Journal*, **45**: 629-658.

Elias, E.P.L. and van der Spek, A.J.F., **2006**. Long-term morphodynamic evolution of Texel Inlet and its ebb-tidal delta (The Netherlands). *Marine Geology*, **225**: pp. 5-21.

Fernandez, J., Bluck, B.J. and Viseras, C., **1993**. The effects of fluctuating base-level on the structure of alluvial-fan associated fan-delta deposits – an example from the Tertiary of the Betic Cordillera, Spain. *Sedimentology*, **40**: 879-893.

Fitzgerald, D.M., **1984**. Interactions between the ebb-tidal delta and landward shoreline: Price Inlet, South Carolina. *Journal of sedimentary petrology*, **54**: pp. 1303-1318.

Fitzgerald, D.M., Penland, S. and Nummedal, D., **1984**. Control of barrier island shape by inlet sediment bypassing: East Frisian Islands, West Germany. *Marine Geology*, **60**: pp. 355-376.

García-Mondéjar, J., **1990**. Sequence analysis of a marine Gilbert-type delta, LaMiel Albian Lunada Formation of northern Spain. In: *Coarse-Grained Deltas* (Eds A. Collela and D.B. Prior), *Int. Assoc. Sedimentol. Spec. Publ.*, **10**: pp. 255-269. Blackwell International, Oxford.

Gawthorpe, R.L. and Collela, A., **1990**. Tectonic controls on coarse-grained delta depositional systems in rift basins. In: *Coarse-Grained Deltas* (Eds A. Collela and D.B. Prior), *Int. Assoc. Sedimentol. Spec. Publ.,* **10**: pp. 113-127. Blackwell International, Oxford.

Gloppen, T.G. and Steel, R.J., **1981**. The deposits, internal structure and geometry in six alluvial-fan delta bodies (Devonian-Norway) – a study in the significance of bedding sequences in conglomorates. In: *Recent and Ancient Non-marine Depositional Environments: Models for Exploration* (Eds F.G. Ethridge and R. Flores), *Spec. Publ. Soc. Econ. Palaeontol. Mineral.,* **31**: pp. 49-69.

Hanisch, J., **1981**. Sand transport in the tidal inlet between Wangerooge and Spiekeroog. In: *Holocene Marine Sedimentation in the North Sea Basin* (Eds Nio, S.D., Shüttenhelm, R.T.E. and Van Weering, T.C.E.), *International Association of Sedimentologists Special Publication*, **5**: pp. 175-185. Blackwell, Oxford.

Harvey, A.M., **1978**. Dissected alluvial fans in southeast Spain. *Catena*, **5**: pp. 177-211.

Harvey, A.M., **2002**. The role of base-level change in the dissection of alluvial fans: case studies from southeast Spain and Nevada. *Geomorphology,* **45**: pp. 67-87.

Harvey, A.M., Foster, G., Hannam, J. and Mather, A.E., **2003**. The Tabernas alluvial fan and lake system, southeast Spain: applications of mineral magnetic and pedogenic iron oxide analyses towards clarifying the Quaternary sediment sequences. *Geomorphology*, **50**: pp. 151-171.

Hayes, M.O., **1975**. Morphology of sand accumulations in estuaries. In: *Proceedings of the 2nd International Estuaries Research Conference, Myrtle Beach, South Carolina* (Ed. Cronin, E.D.): pp. 3-22, Academic Press.

Hayes, M.O., **1980**. General morphology and sediment patterns in tidal inlets. *Sedimentary Geology*, **26**: pp. 139-156.

Hecht, M. H., **2002**. Metastability of liquid water on Mars, *Icarus,* **156,** pp. 373-386.

Hogg, S.E., **1982**. Sheetfloods, sheetwash, sheetflow, or …? *Earth-Science Rev.*, **18**: pp. 59-76.

Holbrook, J., Scott, R.W. and Oboh-Ikuenobe, F.E., **2006**. Base-Level Buffers and Buttresses: A Model for Upstream Versus Downstream Control on Fluvial Geometry and Architecture Within Sequences. *Journal of Sedimentary Research*, **76**: pp. 162-174.

Hooke, R.L., **1967**. Processes on arid-region alluvial fans. *Journal of Geology*, **75**: pp. 438-460.

Hooke, R.L. and Rohrer, W.L., **1979**. Geometry of alluvial fans; effect of discharge and sediment size. *Earth Surface Processes*, **4**: pp. 147-166.

Hooke, R.L., **1968**. Model Geology: Prototype and Laboratory Streams: Discussion. *Geological Society of America Bulletin*, **79**: pp. 391-394.

Hunt, A. G., Grant, G. E. and Gupta, V. T., **2006**. Spatio-temporal scaling of channels in braided streams, *J. Hydrol.,* **322**: pp. 192-198.

Irwin, R. P., Howard, A. D., Craddock, R. A. and Moore, J. M., **2005**. An intense terminal epoch of widespread fluvial activity on early Mars: 2. Increased runoff and paleolake development, *J. Geophys. Res.,* **110**: pp. E12S15, doi: 10.1029/2005JE002460.

Jerolmack, D. J., Mohrig, D., Zuber, M. T. and Bryne, S., **2004**. A minimum time for the formation of Holden Northeast fan, Mars. *Geophys. Res. Lett.*, **31**: pp. L21701 doi: 10.1029/2004GL021324.

Jervey, M.T., **1988**. Quantitative geological modelling of siliciclastic rock sequences and their seismic expression. In: *Sea-level changes: an integrated approach* (Eds Wilgus, C.K., Hastings,

B.S., St Kendall, C.G., Posamentier, H.W., Ross, C.A. and Van Wagoner, J.C.), *Society of Economic Paleontologists and Mineralogists Special Publication*, **42**: pp. 47-69, Tulsa.

Johnston, A. K., **2006**. Aspects of alluvial fan shape indicative of formation process: A case study in southwestern California with application to Mojave Crater fans on Mars, *Geophys. Res. Lett.,* **33**: pp. L10201, doi: 10.1029/2005GRL025618.

Kim, W. and Jerolmack, D.J., **2008**. The pulse of calm fan deltas. *Journal of Geology*, **116**: pp. 315-330.

Kim, W. and Muto, T., **2007**. Autogenic response of alluvial-bedrock transition to base-level variation: Experiment and theory. *Journal of Geophysical Research-Earth Surface*, **112**: pp. F03S14.

Kim, W. and Paola, C., **2007**. Long-period cyclic sedimentation with constant tectonic forcing in an experimental relay ramp. *Geology*, **35**: pp. 331-334.

Kim, W., Paola, C., Swenson, J.B. and Voller, V.R., **2006a** Shoreline response to autogenic processes of sediment storage and release in the fluvial system. *Journal of Geophysical Research-Earth Surface*, **111**: pp. F04013.

Kim, W., Paola, C., Voller, V.R. and Swenson, J.B., **2006b**. Experimental Measurement of the Relative Importance of Controls on Shoreline Migration. *Journal of Sedimentary Research*, **76**: pp. 270-283.

Kleinhans, M. G., **2005**. Flow discharge and sediment transport models for estimating a minimum time scale of hydrological activity and channel and delta formation on Mars, *J. Geophys. Res.,* **110**: pp. E12003, doi: 10.1029/2005JE002521.

Kleinhans, M.G., Jagers, H.R.A., Mosselman, E. and Sloff, C.J., **2008**. Bifurcation dynamics and avulsion duration in meandering rivers by one-dimensional and three-dimensional models. *Water Resources Research*, **44**: pp. W08454.

Kocurek, G., **1998** Aeolian system response to external forcing factors – a sequence stratigraphic view of the Saharan region. In: *Quaternary Deserts and Climatic Change* (Eds Alsharhan, A.S., Glennie, K., Whittle, G.L. and Kendall, C.G.S.C.): pp. 327-337. Balkema Press.

Kocurek, G. and Havholm, K.G., **1993**. Eolian sequence stratigraphy: A conceptual framework. In: *Silliciclastic Sequence Stratigraphy: Recent Developments and Applications* (Eds Weimer, P. and Posamentier, H.W.), *American Association of Petroleum Geologists Memoir*, **58**: pp. 393-410.

Leeder, M.R., **1978**. A quantitative stratigraphic model for alluvium, with special reference to channel deposit density and interconnectedness. In: *Fluvial sedimentology* (Ed Miall, A.D.), *Canadian Society of Petroleum Geologists Memoir*, **5**: pp. 587-596.

Li, Y.L., Yang, J.C., Tan, L.H. and Duan, F.J., **1999**. Impact of tectonics on alluvial landforms in the Hexi Corridor, Northwest China. *Geomorphology*, **28**: pp. 299-308.

Ligtenberg, J., **1998**. De rol van het getij bij de aanzanding van het Marsdiep, voor en na de afsluiting van de Zuider Sea (in Dutch), Report Rijkswaterstaat, RIKZ-OS-98.106x, The Hague, the Netherlands.

Louters, T. and Gerritsen, F., **1994**. The riddle of the sands, A tidal system's answer to a rising sea level, Report Rijkswaterstaat RIKZ-94.040, The Hague, the Netherlands.

Mackey, S.D. and Bridge, J.S., **1995**. Threedimensional alluvial stratigraphy: Theory and application. *Journal of Sedimentary Research*, **B65**: pp. 7-31.

Mackin, J.H., **1948**. Concept of the graded river. *Bulletin of the Geological Society of America*, **59**: pp. 463-512.

Malin, M. C. and Edgett, K. S., **2003**. Evidence for persistent flow and aqueous sedimentation on early Mars, *Science,* **302**: pp. 1931-1934.

Melosh, H. J., **1996**. Impact Cratering: A Geologic Process. Oxford Univ. Press, New York.

Milana, J.P., **1998**. Sequence stratigraphy in alluvial settings: a flume-based model with applications to outcrop and seismic data. *AAPG Bull.*, **82**: pp. 1736-1753.

Milana, J.P. and Ruzycki, L., **1999**. Alluvial-fan slope as a function of sediment transport efficiency. *J. Sed. Res.*, **69**: pp. 553-562.

Milana, J.P. and Tietze, K.W., **2002**. Three-dimensional analogue modelling of an alluvial basin margin affected by hydrological cycles: processes and resulting depositional sequences. *Basin Res.*, **14**: pp. 237-264.

Milliman, J. D. and Syvitski, P. M., **1992**. River data set, *J. Geol.,* **100**: pp. 525-544.

Moore, J. M. and Howard, A. D., **2005**. Large alluvial fans on Mars, *J. Geophys. Res.,* **110**: pp. E04005, doi: 10.1029/2004JE002352.

Moore, J. M., Howard, A. D., Dietrich, W. E. and Schenk, P. M., **2003**. Martian layered fluvial deposits: Implications for Noachian climate scenarios. *Geophys. Res. Lett.*, **30** (24): pp. 2292, doi: 10.1029/2003GRL019002.

Moscariello, A., **2005**. Exploration potential of the mature Southern North Sea basin margins: some unconventional plays based on alluvial fluvial fan sedimentation models. In: *North–West Europe and Global Perspectives – Proceedings of the 6th Petroleum Geology Conference* (Eds Doré, A.G. and Vining, B.A.): pp. 595-605. Geological Society of London.

Muto, T. and Steel, R.J., **1997**. Principles of regression and transgression: the nature of the interplay between accommodation and sediment supply. *J. Sed. Res.*, **67**: pp. 994-1000.

Muto, T. and Steel, R.J., **2000**. The accommodation concept in sequence stratigraphy: some dimensional problems and possible redefinition. *Sed. Geol.*, **130**: pp. 1-10.

Muto, T. & Steel, R. J., **2001**. Autostepping during the transgressive growth of deltas: Results from flume experiments, *Geology,* **29**: pp. 771-774.

Muto, T., Steel, R.J. and Swenson, J.B., **2007**. Autostratigraphy: a framework norm for genetic stratigraphy. *J. Sed. Res.*, **77**: pp. 2-12.

Nanninga, P. M. and Wasson, R. J., **1985**. Calculation of the volume of an alluvial fan, *Math. Geol.,* **17**: pp. 53-65.

Nemec, W. and Postma, G., **1993**. Quaternary alluvial fans in southwestern Crete: sedimentation processes and geomorphic evolution. In: *Alluvial Sedimentation* (Eds Marzo, M. and Puigdefabregas, C.), *Special Publication of the International Association of Sedimentologists*, **17**: pp. 235-276.

Nemec, W. and Steel, R.J., **1988a**. Preface to: 'Fan deltas; sedimentology and tectonic setting'. In: *Fan Deltas; Sedimentology and Tectonic* Setting (Eds W. Nemec and R.J. Steel): pp. vii-ix. Blackie and Son, Glasgow.

Nemec, W. and Steel, R.J., **1988b**. What is a fan delta and how do we recognize it? In: *Fan Deltas; Sedimentology and Tectonic Settings* (Eds W. Nemec and R.J. Steel): pp. 3-13. Blackie and Son, Glasgow.

Nicholas, A.P. and Quine, T.A., **2007**. Modeling alluvial landform change in the absence of external environmental forcing. *Geology*, **35**: pp. 527-530.

Nummedal, D. and Penland, S., **1981**. Sediment dispersal in Nordeneyer Seegat, West Germany. In: *Holocene Marine Sedimentation in the North Sea Basin* (Eds Nio, S.D., Shüttenhelm, R.T.E. and Van Weering, T.C.E.), *International Association of Sedimentologists Special Publication*, **5**: pp. 187-210. Blackwell, Oxford.

Oertel, G.F., **1977**. Geomorphic cycles in ebb deltas and related patterns of shore erosion and accretion. *Journal of Sedimentary Research*, **47**: pp. 1121-1131.

Oost, A.P., **1995**. *Dynamics and sedimentary development of the Dutch Wadden Sea with emphasis on the Frisian Inlet*. Ph.D. Thesis, Utrecht University, 455 pp.

Oost, A.P. and De Boer, P.L., **1994**. Sedimentology and development of barrier islands, ebb-tidal deltas, inlets and backbarrier areas of the Dutch Wadden Sea. *Senckenbergiana Maritima*, **24**: pp. 65-115.

Paola, C., **2000**. Quantitative models of sedimentary basin filling. *Sedimentology*, **47**: pp. 121-178.

Parker, G., Paola, C., Whipple, K.X. and Mohrig, D., **1998a**. Alluvial fans formed by channelized fluvial and sheet flow. I: Theory. *Journal of Hydraulic Engineering-Asce*, **124**: pp. 985-995.

Parker, G., Paola, C., Whipple, K.X., Mohrig, D., Toro-Escobar, C.M., Halverson, M. and Skoglund, T.W., **1998b**. Alluvial fans formed by channelized fluvial and sheet flow. II: Application. *Journal of Hydraulic Engineering-Asce*, **124**: pp. 996- 1004.

Peakall, J., Ashworth, P. J. and Best, J. L., **1996**. In: *The Scientific Nature of Geomorphology: Proceedings of the 27th Binghamton Symposium in Geomorphology* (eds Rhodes, B. L. & Thorn, C. E.), Wiley and Sons, Chichester: pp. 221-253.

Pierson, T. C. and Scott, K. M., **1985**. Downstream dilution of a lahar: Transition from debris flow to hyperconcentrated stream flow, *Wat. Resour. Res.,* **21**: pp. 1511-1524.

Posamentier, H.W. and Vail, P.R., **1988**. Eustatic controls on clastic deposition II – Sequence and Systems Tract Models. In: *Sea-level changes: an integrated approach* (Eds Wilgus, C.K., Hastings, B.S, St Kendall, C.G., Posamentier, H.W., Ross, C.A. and Van Wagoner, J.C.), *Society of Economic Paleontologists and Mineralogists Special Publication*, **42**: pp. 125-154, Tulsa.

Pope, R., Wilkinson, K., Skourtsos, E., Triantaphyllou, M. and Ferrier, G., **2008**. Clarifying stages of alluvial fan evolution along the Sfakian piedmont, southern Crete: New evidence from analysis of post-incisive soils and OSL dating. *Geomorphology*, **94**: pp. 206-225.

Postma, G., Kleinhans, M.G., Meijer, P.T. and Eggenhuijsen, J., **2008**. Sediment transport in analogue flume models compared with real world sedimentary systems: a new look at scaling sedimentary systems evolution in a flume. *Sedimentology* **55**: pp. 1541-1557.

Postma, H., **1982**. Hydrography of the Dutch Wadden Sea, Tech. Rep., Working Group Sticht. Veth Steun Waddenonderz., Leiden.

Price, W.A., **1963**. Patterns of flow and channeling in tidal inlets. *Journal of Sedimentary Research*, **33**: pp. 279-290.

Reineck, H.E., **1982**. Allgemeines Hydrografie. In: *Das Watt, Ablagerungs- und Lebensraum 3rd Edition* (Ed Reineck, H.E.): pp. 12-17. Waldemar, Frankfurt am Mainz.

Ritter, J.B., Miller, J.R., Enzel, Y. and Wells, S.G., **1995**. Reconciling the Roles of Tectonism and Climate in Quaternary Alluvial-Fan Evolution. *Geology*, **23**: pp. 245-248.

Robinson, A.H.W., **1975**. Cyclical changes in Shoreline Development at the Entrance to Teignmouth Harbour, Devon, England. In: *Nearshore sediment dynamics and sedimentation: an interdisciplinary review* (Eds Hails, J.R. and Carr, A.): pp. 181-200. John Wiley & Sons, Southampton.

Saito, K. and Oguchi, T., **2005**. Slope of alluvial fans in humid regions of Japan, Taiwan and the Philippines. *Geomorphology*, **70**: pp. 147-162.

Schumm, S.A., Mosley, P.M. and Weaver, P.H., **1987**. *Experimental Fluvial Geomorphology*. John Wiley & Sons, New York: 413 pp.

Scott, P.F. and Erskine, W.D., **1994** Geomorphic Effects of a Large Flood on Fluvial Fans. *Earth Surface Processes and Landforms*, **19**: pp. 95-108.

Sears, D. W. G. and Chittenden, J. D., **2005**. On laboratory simulation and the temperature dependence of the evaporation rate of brine on Mars, *Geophys. Res. Lett.* **32**, pp. L23203, doi: 10.1029/2005GL024154.

Sha, L.P., **1989a**. Cyclic morphological changes of the ebb-tidal delta, Texel Inlet, the Netherlands. *Geologie en Mijnbouw*, **68**: pp. 35-48.

Sha, L.P., **1989b**. Sand transport patterns in the ebb-tidal delta off Texel Inlet, Wadden Sea, the Netherlands. *Marine Geology*, **86**: pp. 137-154.

Sha, L.P., **1990**. Surface sediments and sequence models in the ebb-tidal delta of Texel Inlet, Wadden Sea, The Netherlands. *Sedimentary Geology*, **68**: pp. 125-141.

Sha, L.P. and De Boer, P.L., **1991**. Ebb-tidal delta deposits along the West Frisian Islands (The Netherlands): processes, facies, architecture and preservation. In: *Clastic tidal sedimentology* (Eds Smith, D.G., Reinson, G.E., Zaitlin, B.A. and Rahmani, R.A.), *Canadian Society of Petroleum Geologists Memoir*, **16**: pp. 199-218, Calgary.

Sheets, B.A., Hickson, T.A. and Paola, C., **2002**. Assembling the stratigraphic record: depositional patterns and timescales in an experimental alluvial basin. *Basin Res.*, **14**: pp. 287-301.

Slingerland, R. and Smith, N.D., **2004**. River avulsions and their deposits. *Annual Review of Earth and Planetary Sciences*, **32**: pp. 257-285.

Soria, J.M., Alfaro, P., Fernandez, J. and Viseras, C., **2001**. Quantitative subsidence-uplift analysis of the Bajo Segura Basin (eastern Betic Cordillera, Spain): tectonic control on the stratigraphic architecture. *Sed. Geol.*, **140**: pp. 271-289.

Soulsby, R., **1997**. *Dynamics of marine sands*. Thomas Telford, London: 215 pp.

Steel, R.J., Maehle, S., Nilsen, H., Roee, S.L. and Spinnangr, A., **1977**. Coarsening-upward cycles in the alluvium of Hornelen Basin (Devonian) Norway; sedimentary response to tectonic events. *Geol. Soc. Am. Bull.*, **88**, pp. 1124-1134.

Stokes, M. and Mather, A.E., **2000**. Response of Plio-Pleistocene alluvial systems to tectonically induced base-level changes, Vera Basin, SE Spain. *Journal of the Geological Society*, **157**: pp. 303-316.

Stauble, D.K., Da Costa, S.L., Monroe, K.L. and Bhogal, V.K., **1988**. Inlet flood-tidal deltadevelopment though sediment transport processes. In: *Hydrodynamics and sediment dynamics of tidal inlets* (Eds Aubrey, D.G. and Weishar, L.) edn, *Lecture notes on coastal and estuarine studies*, **29**: pp. 319-347. Springer-Verlag, New York.

Van den Berg van Saparoea, A.P. and Postma, G., **2008**. Control of climate change on the yield of river systems. In: *Recent Advances in Models of Siliciclastic Shallow-marine Stratigraphy* (Eds G. Hampson, R.J. Steel, P.M. Burgess and R.W. Dalrymple), *SEPM Spec. Publ.* (in press).

Van der Vegt, M., Schuttelaars, H.M. and De Swart, H.E., **2006**. Modeling the equilibrium of tide-dominated ebb-tidal deltas. *Journal of geophysical research F*, **111**: pp. F02013.

Van Heijst, M. and Postma, G., **2001**. Fluvial response to sea-level changes: a quantitative analogue, experimental approach. *Basin Res.*, **13**: pp. 269-292.

Van Heijst, M. I. W. M., Postma, G., Meijer, X. D., Snow, J. N. and Anderson, J. A., **2001**. Analogue flume-model study of the Late Quaternary Colorado/Brazos shelf, *Basin Res.* **13**: pp. 243-268.

Van Leeuwen, S.M., **2002**. *Tidal Inlet Systems*. Ph.D. Thesis, Utrecht University, 154 pp.

Van Straaten, L.M.J.U., **1961**. Directional effects of winds, waves and currents along the Dutch North Sea coast. *Geologie en Mijnbouw*, **40**: pp. 333-346 and 363-391.

van Straaten, L.M.J.U., **1964**. De bodem der Waddenzee (in Dutch). In: *Het Waddenboek*: pp. 75-151, Zutphen.

Viseras, C., Calvache, M.L., Soria, J.M. and Fernandez, J., **2003**. Differential features of alluvial fans controlled by tectonic or eustatic accommodation space. Examples from the Betic Cordillera, Spain. *Geomorphology*, **50**: pp. 181-202.

Vollmer, S. and Kleinhans, M.G., **2007**. Predicting incipient motion, including the effect of turbulent pressure fluctuations in the bed. *Water Resources Research*, **43**: pp. W05410.

Weissmann, G.S., Mount, J.F. and Fogg, G.E., **2002**. Glacially driven cycles in accumulation space and sequence stratigraphy of a stream-dominated alluvial fan, San Joaquin Valley, California, U.S.A. *J. Sed. Res.*, **72**: pp. 240-251.

Weitz, C. M., Irwin, R. P., Chuang, F. C., Bourke, M. C. and Crown, D. A., **2006**. Formation of a terraced fan deposit in Coprates Catena, Mars, *Icarus* **184** (2): pp. 436-451.

Weaver, P.H., **1984**. *Experimental Study of Alluvial Fans*. PhD thesis, Colorado State University, Fort Collins, CO.

Wells, S.G., McFadden, L.D. and Dohrenwend, J.C., **1987**. Influence of late Quaternary climatic changes on geomorphic and pedogenic processes on a desert piedmont, Eastern Mojave Desert, California. *Quaternary Research*, **27**: pp. 130-146.

Wescott, W.A. and Ethridge, F.G., **1980**. Fan-delta sedimentology and tectonic setting – Yallahs Fan Delta, Southeast Jamaica. *American Association of Petroleum Geologists Bulletin*, **64**: pp. 374-399.

Williams, R. M. E., Zimbelman, J. R. and Ori, G.G., Marinangeli, L. and Baliva, A., **2000**. Terraces and gilbert-type deltas in crater lakes in Ismenius Lacus and Memnonia (Mars), *J. Geophys. Res. E* **105** (7): pp. 17629-17642, doi: 10.1029/1999JE001219.

Wheeler, H.E., **1964**. Baselevel, Lithosphere Surface, and Time-Stratigraphy. *Geological Society of America Bulletin*, **75**: pp. 599-610.

Whipple, K.X. and Trayler, C.R., **1996**. Tectonic control of fan size: the importance of spatially variable subsidence rates. *Basin Res.*, **8**: pp. 351-366.

Whipple, K.X., Parker, G., Paola, C. and Mohrig, D., **1998**. Channel dynamics, sediment transport, and the slope of alluvial fans: Experimental study. *Journal of Geology*, **106**: pp. 677-693..

Samenvatting (summary in dutch)

8.1 Sedimentaire systemen

Silliciklastische sedimentaire systemen ontstaan waar erosieproducten beschikbaar komen voor transport, en zijn zowel transporteur als product van het sediment. Hun formaat varieert van meters (kleine puinzandwaaiers en beekjes) tot duizenden kilometers (grote rivieren en delta's). De ontwikkeling, grootte, vorm en interne architectuur van sedimentaire systemen worden bepaald door:

a. Allogene factoren, extern opgelegde randvoorwaarden:
    1. Aanvoer; het mengsel van water en sediment dat wordt aangeleverd aan de bovenstroomse zijde van het systeem en voor transport of sedimentatie beschikbaar is.
    2. Accommodatie/accumulatieruimte; ruimte beschikbaar om sediment af te zetten. Het begrip 'accommodatie' wordt meestal gebruikt in de mariene omgeving, en accumulatieruimte voor continentale milieus.

b. Autogene factoren, intern gegenereerde processen en mechanismen. Wanneer autogene processen cyclisch of (quasi-)periodiek optreden, noemen we ze autocyclisch.

Bijvoorbeeld, tijdens de zeespiegelstijging die plaatsvond tijdens het begin van het Holoceen moesten de rivieren die sediment en water naar de zee vervoerden meestijgen met de zeespiegel (aggradatie). Autogene processen van de rivieren werden beïnvloed door de zeespiegelstijging maar
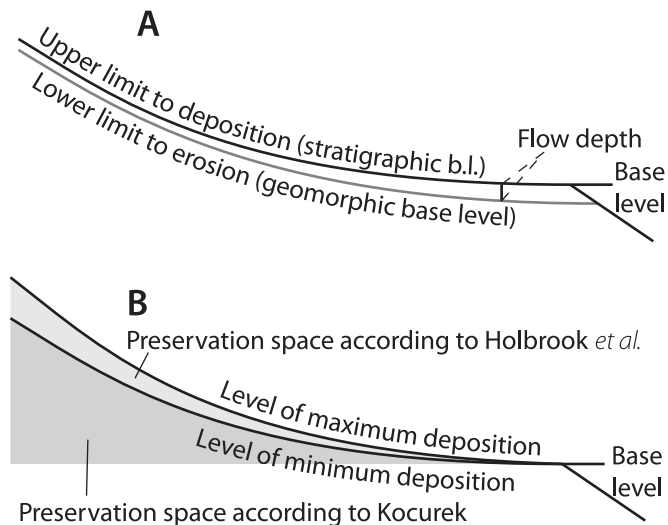

Figure 8.1 A) Verduidelijking van het principe van het basisniveau. B) De verschillende definities van 'Preservatie-ruimte'.

in sommige gevallen domineerden autogene signalen. In die gevallen is het erg lastig te achterhalen wat de oorzaak is geweest van specifieke morfodynamische gebeurtenissen. Het onderzoek voor dit proefschrift is gedaan met de volgende vraagstellingen:

1. het beschrijven en kwantificeren van autogeen en autocyclisch gedrag, en hun relatieve belang ten opzichte van allogene factoren,
2. het bepalen van de sedimentaire karakteristieken van autogene processen en hun afzettingen, en die vergelijken met afzettingen die gedomineerd worden door allogene mechanismen.

8.2 Basisniveau

De begrippen 'accommodatie' en 'accumulatieruimte' hangen samen met het basis niveau (Figuur 8.1). Voor mariene systemen gelegen *onder* het basisniveau, vormt dit de bovenste grens; het kan niet boven het basisniveau uitgroeien. Voor continentale systemen gelegen *boven* het basisniveau, bepaalt dit niveau globaal het evenwichtsprofiel van het systeem zich richt. Met andere woorden, indien een systeem zich niet op het basisniveau bevindt, zal het insnijden in zijn eigen afzettingen of er vindt ophoging plaats tot het basisniveau.

Naast het hierboven beschreven morfodynamische aspect van het basisniveau, is het ook van belang voor het definiëren van de sedimenten die bewaard kunnen blijven (preservatie). Het fluviatiele evenwichtsprofiel varieert door veranderingen in de aanvoer van water en sediment (Holbrook *et al.*, 2006). De ruimte tussen het maximum en minimum profiel definiëren Holbrook *et al.* als 'preservatieruimte'. Kocurek (1998) daarentegen definieert 'preservatieruimte' juist als de ruimte *onder* het laagste (minimum) fluviatiele profiel. Dit wordt ondersteund door een experimentele studie van Kim *et al.* (2006), die laten zien dat ook met bij constante aanvoer van water en sediment autocyclische variaties in het fluviatiele profiel kunnen ontstaan. Als het fluviatiele profiel al variaties laat zien *zonder* extern opgelegde veranderingen (aanvoer van water en sediment), dan kunnen de sedimenten in de door Holbrook *et al.* geformuleerde definitie van preservatieruimte dus opgeruimd worden zonder dat er veranderingen optreden in de aanvoer van water en sediment. Dit betekent dat sedimenten op zijn minst onder het laagste door constante aanvoer vormbare profiel moeten komen te liggen om bewaard te blijven.

8.3 Context

Zoals hierboven wordt beschreven, bepaald het basisniveau in zeer belangrijke mate het gedrag van mariene en continentale systemen, respectievelijk als bovengrens en als richtpunt voor het fluviatiele profiel. De zeespiegel wordt in het algemeen beschouwd als het basisniveau. Zeespiegelvariaties komen continu voor, en de effecten van zeespiegelveranderingen in de jongste geologische geschiedenis staan buiten kijf. Hier concentreer ik me op de effecten van veranderingen van het basisniveau (veroorzaakt door zeespiegelveranderingen) op de de ontwikkeling van sedimentaire systemen. Ik heb het gedrag van puinzandwaaier-, puinzanddelta-, en getijdedeltasystemen onderzocht door middel van analoge experimenten, waarin het basisniveau op nauwkeurige wijze kon worden gecontroleerd:

1. Autogeen gedrag van puinzandwaaiers (alluvial fans) die prograderen over een licht hellend vlak; de kustlijn (het basisniveau) is ver weg van het systeem en heeft geen invloed;

2. Autogeen gedrag van een puinzanddeltas, een puinzandwaaier die in een waterlichaam (meer, zee) uitkomt. De delta-ontwikkeling wordt beïnvloed door de kustlijn;
3. Autogeen gedrag van puinzanddelta's tijdens zeespiegelstijging;
4. Autogeen gedrag van een vloedgetijdedelta.

Nadat de intrinsieke processen en mechanismen zijn onderscheiden, is het effect van het basisniveau onderzocht door het opleggen van veranderingen van dat basisniveau met als doel:

5. inzicht te krijgen in het autogene gedrag van systemen die beïnvloed worden door een stijgend of oscillerend basisniveau.

Als laatste laat ik zien dat autogene en autocyclische processen een belangrijke invloed kunnen hebben op de morfdynamische en stratigrafische ontwikkeling van silliciklastische sedimentaire systemen. Carbonaatsystemen zijn in deze studie buiten beschouwing gelaten.

8.4 Aanpak: experimenten

Om autogene en autocyclische processen in de hierboven geïntroduceerde sedimentaire systemen te isoleren, zijn analoge experimenten ontworpen en uitgevoerd met verschillende configuraties van het basisniveau. Experimenten zijn de enige manier om sedimentaire systemen kwalitatief en kwantitatief te vergelijken. Studies van natuurlijke systemen zijn daarvoor niet bruikbaar, omdat deze altijd worden beïnvloed door allogene variaties. Daar komt bij dat de morfodynamische ontwikkeling van natuurlijke sedimentaire systemen tientallen tot duizenden jaren duurt. In
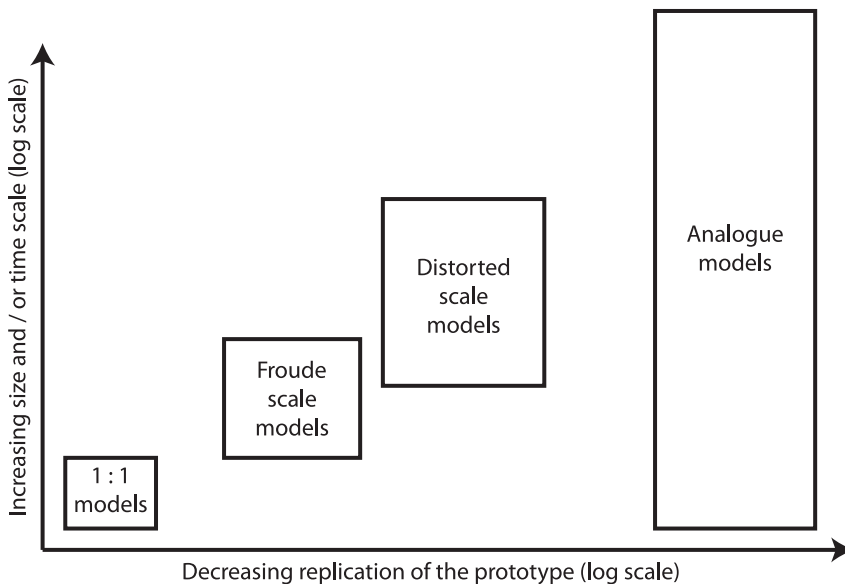

Figure 8.2 Geschematiseerde afbeelding van mate van nauwkeurigheid bij het nabootsen van het prototype en de tijd- en ruimteschaal waarvoor de modelleer-techniek geschikt is.

de geschaalde experimenten is de ontwikkeling van de systemen gelimiteerd tot uren of dagen, zodat meerdere runs per systeem uitgevoerd konden worden. De tijd- en ruimte-schalen waarop puizandwaaiers en puinzanddelta's worden gevormd, sluiten hydraulische schaling van de processen uit. Daarom is een alternatieve schalingsstrategie ontwikkeld, gebaseerd op het 'gelijkheid van processen' principe van Hooke (1968), en op het vergelijken van dimensieloze parameters die makkelijk te meten zijn in zowel de experimentele en natuurlijke systemen..

Analoge experimenten zijn slechts één voorbeeld van verschillende types experimenten. Figuur 8.2 laat schematisch een aantal verschillende typen experimenten zien, met een variërende mate van replicatie van de karakteristieken van het prototype (het natuurlijke systeem dat nagebootst wordt). Aan de ene kant van het spectrum staan 1:1 replica modellen, bijvoorbeeld gebruikt om de ontwikkeling van ribbels te bestuderen. In het midden bevinden zich Froude-geschaalde modellen en zogenaamde 'verstoorde schaalmodellen', modellen van systemen die maar ten dele worden nagebootst. Doordat maar een deel van de prototypen wordt gesimuleerd, kunnen grotere prototypes over langere periodes worden gemodelleerd. Analoge experimenten staan helemaal aan het andere kant van het spectrum van de 1:1 replica modellen, en bootsen slechts enkele aspecten na van nog grotere systemen dan 'verstoorde schaalmodellen', over nog langere tijdschalen.

Een aantal publicaties van eerder uitgevoerde experimentele studies hebben dit proefschrift flink beïnvloed. Het boek 'Experimental Fluvial Geomorphology' van Schumm *et al.* (1987) bevat vergelijkbare experimenten en behandelt onder andere delta's en puinzandwaaiers. Whipple *et al.* (1998), Parker *et al.* (1998a,b) en Clarke *et al.* (2008) hebben allerlei aspecten van vooral puinzandwaaiers beschreven en gekwantificeerd. Hoewel Nicholas en Quine (2007) geen experimentele studie deden maar een computermodel beschreven, lieten ze als eerste zien dat

Figure 8.3 Overzicht van de Eurotank. Auteur dient hier als schaal. Deze afbeelding is eigendom van Raymond Rutting, en is eerder afgedrukt in de Volkskrant in 2004.

erosie op puinzandwaaiers spontaan op kan treden. Als laatste is het werk van Kim erg belangrijk geweest. Hij en zijn co-auteurs lieten zien hoe dynamisch het intrinsieke gedrag van sedimentaire systemen kan zijn. De experimenten die uitgevoerd zijn voor dit proefschrift, waren in één opzicht anders dan de hierboven genoemde werken. De autogene en autocyclische processen zijn volledig gekwalificeerd en gekwantificeerd voordat andere externe processen zijn geïntroduceerd, waar in de genoemde werken de autogene en autocyclische processen zijn bestudeerd tijdens de aanwezigheid van externe processen.

Ik heb mijn experimenten mogen doen in de Eurotank (Figuur 8.3).Het experiment met getijdestromen is gedaan in een kleinere stroomgoot in de kelder van het Aardwetenschappen-gebouw, speciaal aangepast om de benodigde bidirectionele stromingen te produceren. De Eurotank is een 6 bij 11 meter grote stroomgoot, die als enige ter wereld tektonische (bekken) daling en opheffing kan simuleren. Ook is het mogelijk het basisniveau (de zeespiegel) en de aanvoer van water en sediment te laten fluctueren, en de opstelling kan worden aangepast aan de gewenste vorm en grootte. Er is een geavanceerd meetsysteem dat snel en met een hoge resolutie de topografie van het sedimentoppervlak kan meten, zodat de resultaten van verschillende experimenten kwantitatief met elkaar kunnen worden vergeleken.

8.5 Resultaten

In *Hoofdstuk 2* wordt beschreven hoe een serie delta's wordt gevormd bij een onveranderlijke zeespiegel en een constante aanvoer van water en sediment. De ontwikkeling van de delta's wordt enkel gestuurd door autogene (intrinsieke) processen, en laat afwisselingen tussen twee situaties zien. De stroming op de delta varieert van een ingesneden, gekanaliseerde stroming tot een breed uitwaaierende, ondiepe waterstroom die de hele delta als een film bedekt.

Tijdens het voorkomen van de breed uitwaaierende waterstromen vindt depositie plaats op de top van de delta, waardoor het profiel van de delta versteilt. Deze toename van de helling leidt tot insnijding en geulvorming, met daarin de gekanaliseerde waterstroom. Het materiaal dat geërodeerd is bij het vormen van de geul, is afgezet als een deltalob vlak voor die geul. De combinatie van erosie op de delta en depositie aan de rand van de delta leidt weer tot een afname van de steilheid van de delta. Terwijl de delta's groeien, blijft de frequentie van de insnijdingen ongeveer gelijk. De insnijdingen zijn een autocyclisch proces, waarbij de helling van de delta oscilleert.

De verschillende delta-experimenten zijn gedaan met verschillen in de wateraanvoer. Die verschillen leidden tot verschillen in de frequentie en grootte van de autocyclische insnijdingen. De diepte van de autogeen gevormde geulen is vergelijkbaar de diepte van geulen gevormd door veranderingen in de aanvoer van water en sediment, zoals klimaatveranderingen die in natuurlijke systemen kunnen veroorzaken.

In *Hoofdstuk 3* wordt de vorming van puinzandwaaiers beschreven, ook met een onveranderlijke zeespiegel en een constante aanvoer van water en sediment. Het verschil met de delta's uit *Hoofdstuk 2* is dat de puinzandwaaiers worden gevormd op een licht hellend vlak (alluviale vlakte), met het basisniveau (de zee) ver verwijderd van de waaiers. Daardoor missen de puinzandwaaiers lange tijd die invloed van het basisniveau in vergelijking met de delta's uit *Hoofdstuk 2*.

In grote lijnen is de autogene ontwikkeling van de puinzandwaaiers gelijk aan die va de delta's; er ontstaan ingesneden geulen die afwisselen met situaties waarin uitwaaierende ondiepe waterstromen domineren. Voor de puinzandwaaiers is de frequentie van de geulvorming veel hoger dan voor de delta's. Dit frequentieverschil moet het gevolg zijn van het ontbreken van een basisniveau, omdat er verder geen enkel verschil was tussen de delta- en puinzandwaaier-experimenten.

De verschillen in ontwikkeling worden verder uitgewerkt met het model van Postma *et al.* (2008). Zij laten zien dat een fluviatiel systeem een ontwikkeling doormaakt op weg naar het evenwichtsprofiel. In het begin, in het 'opstart-stadium', groeit het systeem totdat het zijn basisniveau bereikt heeft. Wanneer dat gebeurd, bereikt het systeem het 'opvul-stadium', waarin een steeds groter deel van de sedimentaanvoer wordt doorgegeven en niet wordt gebruikt om het systeem te laten groeien. In het laatste stadium, het 'doorgeef-stadium', wordt meer dan 90% van het aangevoerde sediment doorgegeven, en minder dan 10% van het sediment wordt aan het systeem toegevoegd in de vorm van hoogtegroei. Dit laatste stadium duurt in theorie oneindig lang, al valt in experimenten het verschil tussen de werkelijke en de theoretische situatie na verloop van tijd binnen de meetfout (Van den Berg van Saparoea, 2005).

De grotere frequentie van de insnijdingen die de puinzandwaaiers is een indicatie van de verschillende stadia waarin de twee systemen zijn. De delta's, die uitbouwen in het zeewater, hebben reeds het opvul-stadium bereikt. Puinzandwaaiers, daarentegen, moeten hun basisniveau nog bereiken en zijn nog in het opstart-stadium. De topografische gegevens van de puinzandwaaiers en de delta's laten zien dat de autogene hellingvariaties bij delta's ook groter is dan bij puinzandwaaiers. Dit is belangrijk, want het biedt twee criteria (helling, frequentie van autogene processen) om op basis van de morfodynamiek van systemen te bepalen in welk stadium van ontwikkeling ze verkeren.

Hoofdstuk 4 verhaalt over experimenten waarin een delta wordt gevormd in een klein kratervormig bekken waarin de waterspiegel stijgt doordat het instromende water wordt opgevangen en niet weg kan. Autogene processen op de delta en in de aanvoergeul leidden tot variaties in de aanvoerrichting van water en sediment op de zich ontwikkelende delta. In combinatie met de stijging van de waterspiegel wordt een delta gevormd die wordt gekenmerkt door een aantal trapsgewijze terrassen.

Die karakteristieke vorm is zeer goed vergelijkbaar met een aantal delta's gevonden in kraters op de planeet Mars. Gebruik makend van de vorm van de delta's en schattingen van de hoeveelheden water en sediment die betrokken waren bij hun vorming, is een nauwkeurige schatting gemaakt van de tijdsduur waarover de waterstromen op de getrapte Marsdelta actief zijn geweest. Tevens kon worden bepaald dat delta's met die karakteristieke vorm door één hydrologische gebeurtenis moeten zijn gevormd. De tijdsduur van die gebeurtenis moet in de orde van grootte van tientallen jaren zijn geweest.

Deze resultaten bewijzen dat deze specifieke getrapte delta's niet zijn gevormd door langdurige stroming van water. Daardoor dragen ze bij aan inzicht in het klimaat op Mars in de tijd dat er nog significante hoeveelheden water stroomde op het oppervlak van de planeet.

Als laatste wordt in *Hoofdstuk 5* een uniek experiment beschreven waarin een vloeddelta wordt gevormd. Vloeddelta's ontstaan aan de landwaartse kant van zeegaten die tussen twee barrière-eilanden liggen. In Nederland vinden we zulke zeegaten tussen de Waddeneilanden, de bijbehorende vloeddelta's liggen in de Waddenzee.

In het experiment werd een delta lichaam geproduceerd terwijl het waterniveau oscilleerde (getijden). De getijdenbeweging van het water werd veroorzaakt door de stroming van water in en uit de nagebootste lagune via het eveneens nagebootste zeegat. Golven speelden geen rol in het experiment.

De ontwikkeling van de delta bestond uit gelijkmatige groei in lengte, breedte en hoogte, totdat de delta zo groot was geworden dat interactie met de getijdenstromen begon. In eerste instantie vormde de delta een obstructie voor de vloedstroom die de lagune inkwam en de ebstroom die de lagune weer uit ging. Eb en vloed verlegden uiteindelijk hun loop en stroomden door geulen via een omweg van en naar het zeegat. In het laatste stadium van de ontwikkeling van de vloeddelta vormde de sterke vloedstroom een geul op de delta. Deze geul liep vanaf het zeegat met een bocht naar de zijkant van de delta, en werd onder invloed van de vloedstroom steeds rechter. Het rechter worden van de vloedgeul ging samen met geulverbreding. Dat leidde tot vertraging van de stroom in de geul, en afzetting van sediment.

Nadat de geul werd verlaten werd er een nieuwe vloedgeul gevormd, ditmaal met een bocht naar de andere zijkant van de delta. Zo vormden zich een aantal geulen op de delta, wisselend aan de ene en de andere kant van de delta. Dergelijke cyclische patronen waarmee getijdengeulen migreren en/of roteren is al lang bekend van ebdelta's (het equivalent van een vloeddelta aan de zeezijde van een zeegat), maar op natuurlijke vloeddelta's zoals in de Waddenzee zijn zulke processen nog niet geobserveerd.

Dit unieke experiment laat voor het eerst zien dat het mogelijk is om getijden beïnvloede sedimentaire systemen te modelleren in een stroomgoot. Verder toont het aan dat zulke cyclische geulprocessen ook te verwachten zijn op natuurlijke vloeddelta's, zonder de effecten van bijvoorbeeld golven.

Dankwoord – Acknowledgements

Nu mijn proefschrift bijna naar de drukker gaat, is het tijd voor een terugblik over de afgelopen 5,5 jaar. Deze periode is voor mij heel belangrijk geweest, vol mooie momenten, avonturen, ontdekkingen, veranderingen, en daarnaast momenten van twijfel en tegenslagen. Er is een leuke parallel te trekken met de manier waarop ik ruim 5 jaar lang van huis naar de universiteit geforensd heb: op de fiets. Een korte rekensom (afstand 24 km, 5 jaar, 3 dagen per week, 45 weken per jaar) leert dat ik om en nabij 32.500 kilometer heb gefietst. In zomer en winter, vaak met (zij)wind. Vooral als het ergens halverwege de rit begon te regenen, zat ik nog wel eens te foeteren en beloofde ik mezelf dat het nu toch echt tijd werd om dichterbij te gaan wonen of een tweede auto te kopen. Maar na aankomst en een douche zakte dit gevoel altijd snel en bleef vooral het vermoeide maar voldane gevoel hangen. Zo heb ik de tegenslagen in mijn promotietijd ook opgevangen; in de wetenschap dat er meestal een voldaan of in elk geval positief gevoel op volgt. Ik ben erg goed in het relativeren van mooie en minder mooie momenten, soms zelfs iets *te* goed. Ik wil daarom niet nalaten ook hier een relativerende blik terug te werken op mijn tijd als AIO (Figuur 9.1).

Dit proefschrift was er niet gekomen zonder de hulp van mijn begeleiders; Poppe de Boer, George Postma en Maarten Kleinhans. Vooral George en Maarten zijn erg direct betrokken geweest met in eerste instantie sturing en adviezen voor de experimenten en later met kritisch commentaar op mijn af en toe wat overhaaste luchtballonnetjes en manuscripten. George, vooral bedankt voor je enthousiasme, je geloof in mijn werk en je altijd positieve houding. Maarten, je niet aflatende stroom ideeën werkte voor mij erg inspirerend en ik waardeer het zeer dat je me bleef stimuleren om een breed blikveld te houden op mijn eigen resultaten. Overleg met ons drieën was voor mij altijd erg vermoeiend omdat ik bleef proberen alles wat ter tafel kwam op te nemen, en dat was meestal nogal wat. Toch wisten we altijd met een concreet resultaat weer afscheid van elkaar te nemen.

Figure 9.1 Fokke en Sukke als begeleiders. Afgedrukt met toestemming van Reid, Geleijnse & Van Tol.

Poppe, ondanks dat je mijn promotor bent, zijn we pas het laatste jaar echt intensief met elkaar bezig geweest. Dat heb ik overigens nooit als problematisch ervaren, omdat in de eerste paar jaar George en Maarten al nadrukkelijk aanwezig waren. Ik heb je (vlotte) commentaar op mijn manuscripten en presentaties altijd als erg constructief ervaren. Verder ben ik erg blij dat de vrijheid er was om het onderzoek te laten lopen zoals het gegaan is, zonder vooraf vastgestelde richting. Ik denk dat het resultaat voor zich spreekt. Ook het samen begeleiden van studenten onder andere tijdens veldwerk bij Tremp in Spanje heb ik altijd erg leuk gevonden. Ook ben ik blij dat we naar Chili konden, waar ik veel heb geleerd.

I am very grateful to Erin, who made it possible for me to go to Chile. Dear Erin, I really enjoyed our time together in the Eurotank, talking about everything between research and family life, sharing frustrations with equipment but also the joy of doing the crater-experiments and getting the results published in Nature. Many thanks for improving my awkward English grammar.

Het doen van experimenten is onmogelijk zonder de hulp van mensen met meer technische vaardigheden dan ik. Thony, Henk en Piet-Jan, bedankt voor jullie hulp bij de opstellingen, het opzetten, uitvoeren en inmeten en monitoren van de experimenten. In het vroegste stadium van mijn promotie (en ook tijdens mijn voorafgaande afstudeerproject) heeft ook Paul Anten veel geholpen. Verder bedank ik Marjan Reith en Ton Zalm voor hulp bij de korrelgrootte-analyses. Marjolein en Jaqueline, bedankt voor jullie hulp met administratieve zaken.

De leden van de leescommissie, P. Hoekstra, S.M. de Jong, S. B. Kroonenberg, A. Moscariello, en J. Reijmer bedank ik voor hun tijd en nuttige sugesties. Ook P. Ashworth en W. Kim en een aantal anonieme reviewers van reeds gepubliceerde manuscripten bedank ik voor hun constructieve commentaar. Ook bedank ik Pim Kor. Jouw rol in vooral de uitvoering van het getijde-experiment is groot geweest. Tijdens onze discussies werd ik weer op scherp gezet, en jouw data vormden een belangrijke bijdrage aan het getijde-delta hoofdstuk. Eveline heeft geholpen met HET experiment A008, dat achteraf het begin bleek van het begrip hoe autocyclisch gedrag van de delta's in elkaar steekt. Samen met Sabine en Toke heb ik een aantal experimenten gedaan die niet direct zijn gebruikt in dit proefschrift, maar die wel hebben bijgedragen aan mijn begrip van sedimentaire systemen.

Ook had ik gelukkig een flink aantal trawanten tijdens mijn werk. Aart-Peter, Quintijn en Sjoukje waren dat in de eerste paar jaar, gevolgd door Dario, Germari, João en Matthieu. Dario, we had a very nice time during our trips to Canada and Chile, and I really appreciated that I could make use of your vast bibliographic knowledge. Matthieu, ik heb altijd genoten van onze filosofische zijstappen en discussies over de columns van Rob. Germari, ik hoop dat je uit de voeten kunt met mijn experimentele tips over de Eurotank. João, ik heb altijd genoten van de vele zinnige en onzinnige discussies tijdens lunch en koffie. Onze N308 'kamercultuur' met (harde) muziek en veel koffie heeft mij altijd erg goed geholpen bij het werk. Ook Arjan, Peter en Joris deelden als studenten in die 'kamercultuur'.

Henk, ik denk nog steeds met veel plezier terug aan onze gezamenlijke autoritjes in Tremp. Op de één of andere manier zal de muziek van Coldplay die herinneringen altijd terug halen. Maar ook de koffiepauzes en gesprekken over wat maar ter tafel kwam waren belangrijk. Een aantal ideeën in dit proefschrift is daar ontstaan. Ik ben dan ook blij dat ik voor jou wat terug heb kunnen doen. Daniël en Maarten, jullie (vaak cynische) beschouwingen over een Gutenbergse cappuccino waren altijd weer lekker relativerend. Ook de andere collega's bij wie ik afleiding zocht, Hemmo, Joost, Kees, Marian, en zij die ik onbedoeld vergeten ben hier te vermelden, bedankt.

Ook wil ik mijn huidige werkgever, Tauw Utrecht, en met name Joost, bedanken voor het feit dat af en toe de ruimte kreeg om *niet* te werken. Dat maakte het doorkomen van de laatste loodjes veel eenvoudiger, omdat dan niet alles op de weekenden en avonden aankwam.

Naast het werk ben ik ook zo lang mogelijk blijven korfballen, al heb ik het wat dat betreft het afgelopen jaar begrijpelijk genoeg toch iets rustiger aan moeten doen. Toch is er bijna geen betere manier om te ontspannen dan een uur lang te proberen een bal in een gele mand te kieperen op een doordeweekse avond of zaterdag. Ook mijn familie en schoonfamilie bedank ik van harte. Met jullie vond ik ontspanning tijdens (kampeer)vakanties, sinterklaasvieringen en samenkomsten om talloze andere redenen.

Als laatste, last but not least, mijn gezin. Selle, ik hoop dat je later ooit begrijpt wat een lol ik heb beleefd aan je gespeel, geklooi en gerommel. Niets maakte het relativeren van een lange zware werkdag makkelijker dan jouw eerste geluidjes, lachjes, en stapjes. Lean, je geboorte tijdens het corrigeren van de proefdrukken maakt het één en ander een beetje ingewikkeld, maar toch ben ik erg blij dat je er bent! Menneke, ik denk dat we allebei niet precies wisten waar ik aan begon, 5,5 jaar geleden. Samen zijn we gegroeid tot wat we nu zijn, maar zonder jouw liefde en steun was het allemaal niet gelukt. Tijdens de laatste jaren hebben we een aantal hoogtepunten mogen vieren. Eerst samenwonen, dan trouwen. Onze bruiloft was een dag om nooit te vergeten, en de geboorte van Selle was op zijn minst zo onvergetelijk. Vooral de laatste 9 maanden heb ik ondanks de grote hoeveelheid werk die nog verzet moest worden een goede balans gevonden tussen werken en thuis zijn. Nu met alle drukte wacht ons nog zo'n mooie gebeurtenis met de geboorte van Lean. Je weet niet half hoe gelukkig en gezegend ik ben, en ik zie onze toekomst samen vol vertrouwen tegemoet.

Maurits

Curriculum vitae

Maurits van Dijk was born on the 12th of October 1977 in Zeist, the Netherlands. He lived with his parents, two brothers and two sisters in Doorn, on the flanks of the ice-pushed ridges of the Utrechtse Heuvelrug and close to the northern channel belts of the River Rhine. He attended the Atheneum of the Revius Lyceum, in Doorn.

Maurits started his study in Geology at Utrecht University in 1996. During his studies, he became strongly attracted to experimental research, and graduated in 2002 with Prof. dr. P.L. de Boer. His masters' research project concerned an experimental study of the flow hydraulics of water flowing over evolving bedforms.

Soon after graduating, Maurits was presented the opportunity to start a PhD project on experiments in the newly completed Eurotank Flume Facility, in the TNO building adjacent to the Department of Earth Sciences. This Thesis is the product of this project.

In Februari 2009, he started a new job at Tauw Consultants and Engineers, at the department of Hydraulic Engineering and Construction in Utrecht. Apart from his interests in (sedimentary) geology, physical geography and his recent fascination with water-regulating structures related to his new job, Maurits likes reading about history, philosophy and politics, cycling, hiking, 'korfbal' (typical Dutch game similar to basket ball) and enjoys his daily live with his wife and two children.

Maurits van Dijk is geboren op 12 oktober 1977 in het ziekenhuis te Zeist, in Nederland. Hij leefde met zijn ouders, twee broers en twee zussen in Doorn, tussen de stuwwallen van de Utrechtse Heuvelrug en de loop van de Rijn. Hij ging naar het Atheneum op het Revius Lyceum, ook in Doorn.

Maurits begon zijn studie Geologie aan de Universiteit Utrecht in 1996. Tijdens zijn studie raakte Maurits erg geïnteresseerd in het doen van experimenteel onderzoek, en studeerde in 2002 af bij Prof. dr. P.L. de Boer. Zijn afstudeeronderzoek betrof de hydraulische aspecten van water dat over een zandbed met zich ontwikkelende ribbels stroomde.

Snel na zijn afstuderen begon Maurits aan een promotieonderzoek waarvoor hij experimenten deed in de net afgebouwde Eurotank, in de kelder van het TNO gebouw (vlak naast het Aardwetenschappen-gebouw). Dit proefschrift is het resultaat van dit onderzoek.

Sinds februari 2009 werkt hij bij het Tauw Adviseurs en Ingenieurs, afdeling Waterbouw en Constructie in Utrecht. Naast zijn interesses in (sedimentaire) geologie, fysische geografie en zijn recente fascinatie voor dijken samenhangend met zijn nieuwe baan, houdt Maurits van lezen over geschiedenis, filosofie en politiek, fietsen, wandelen, korfballen, en van het gezinsleven samen met zijn vrouw en twee kinderen.